# LOCALIZATION OF THE PHOSPHATASE CheZ TO THE CHEMORECEPTOR PATCH OF *Escherichia coli*

A Dissertation

by

BRIAN JAY CANTWELL

Submitted to the Office of Graduate Studies of
Texas A&M University
in partial fulfillment of the requirements for the degree of

DOCTOR OF PHILOSOPHY

December 2006

Major Subject: Microbiology

# LOCALIZATION OF THE PHOSPHATASE CheZ TO THE CHEMORECEPTOR PATCH OF *Escherichia coli*

A Dissertation

by

BRIAN JAY CANTWELL

Submitted to the Office of Graduate Studies of
Texas A&M University
in partial fulfillment of the requirements for the degree of

DOCTOR OF PHILOSOPHY

Approved by:

| | |
|---|---|
| Chair of Committee, | Michael Manson |
| Committee Members, | Greg Reinhart |
| | Arthur Johnson |
| | Mark Zoran |
| Head of Department | Vincent Cassone |

December 2006

Major Subject: Microbiology

## ABSTRACT

Localization of the Phosphatase CheZ to the Chemoreceptor Patch of *Escherichia coli.*

(December 2006)

Brian Jay Cantwell, B.S., Texas A&M University; M.S., University of Washington

Chair of Advisory Committee: Dr. Michael Manson

Peritrichously flagellated bacteria carry out chemotaxis by modulating the frequency of switching between smooth swimming and tumbling. The tumbling frequency is controlled by a signal transduction cascade in which transmembrane receptors modulate the activity of a histidine kinase CheA that transfers phosphate to its cognate response regulator CheY. The proteins of the chemotaxis signaling cascade are localized to clusters found primarily at the poles of cells. In this work, the localization of the CheZ protein, a phosphatase that dephosphorylates CheY~P, is examined. Using a CheZ-GFP fusion protein, we show that CheZ was localized to the polar receptor patch via interaction with the short form of CheA ($CheA_S$). Aromatic residues of CheZ near one end of the elongated CheZ four-helix bundle were determined to be critical for localization. Aliphatic residues in $CheA_S$ were also determined to be critical for CheZ localization to the receptor patch and substitution of these residues conferred a tumble bias to swimming cells. A mechanism of CheZ localization is proposed in which the CheZ apical loop interacts with a binding site formed by dimerization of the P1 domain of $CheA_S$. The potential role of CheZ localization as a means of coordinating the rotation state of peritrichously distributed flagella is discussed.

## ACKNOWLEDGEMENTS

I would like to thank all of the members of the Manson lab, past and present, for their input and help on this project over the years, especially Roger "pROG" Draheim and Run-zhi "Three Book" Lai. I would like to thank my committee members; Greg Reinhart, Arthur Johnson, Larry Griffing, and Mark Zoran, for helpful guidance and constructive criticism at all stages of my stay at Texas A&M. I want to extend special thanks to my advisor, Dr. Michael Manson, who has been a friend and mentor for many years. Thanks for everything, Mike.

My family deserves a great deal of credit for my success. They have supported my desire to earn a PhD for many years. I need to thank my mom most of all. Since I was a kid, she encouraged me to read, to be curious, and to think for myself. These attributes have served me well and are critical to a successful scientist. Finally I want to thank my wife, Beth. Her patience, understanding, and gentle prodding when needed, have been my foundation.

Financial support for B.J.C. and funding for this work was provided by the Texas A&M Department of Biology, the Texas A&M Department of Chemistry, and the National Institutes of Health (Grant GM39736 to Michael D. Manson).

# NOMENCLATURE

| | |
|---|---|
| CW | Clockwise |
| CCW | Counter-clockwise |
| ATP | Adenosine triphosphate |
| GFP | Green fluorescent protein |
| MCP | Methyl-accepting chemotaxis protein |
| HAMP | Histidine kinase, adenylate cyclase, methyl-accepting chemotaxis protein, and phosphatase |
| TB | Tryptone broth |
| IPTG | Isopropyl-beta-D-thiogalactopyranoside |
| CheY~P | Phosphorylated CheY |

| | |
|---|---|
| Ala, A | Alanine |
| Arg, R | Arganine |
| Asn, N | Asparagine |
| Asp, D | Aspartate |
| Cys, C | Cysteine |
| Gln, Q | Glutamine |
| Glu, E | Glutamate |
| Gly, G | Glycine |
| His, H | Histidine |
| Ile, I | Isoleucine |

| | |
|---|---|
| Leu, L | Leucine |
| Lys, K | Lysine |
| Met, M | Methionine |
| Phe, F | Phenylalanine |
| Pro, P | Proline |
| Ser, S | Serine |
| Thr, T | Threonine |
| Trp, W | Tryptophan |
| Tyr, Y | Tyrosine |
| Val, V | Valine |

# TABLE OF CONTENTS

## LIST OF FIGURES

# LIST OF TABLES

# CHAPTER I

# INTRODUCTION

The ability of bacteria to move in response to specific conditions in their environment has been studied as long as researchers have been able to view and study microorganisms. Early microbiologists were able to demonstrate taxis by various bacteria in response to light, oxygen, and a variety of chemicals (7). Because of advances in genetics, biochemistry, and molecular biology using *Escherichia coli* as a model system, the chemotaxis pathway of *E. coli* and the closely related *Salmonella enterica* has become the behavioral system best studied and understood at the molecular level. Julius Adler provided the first proof of direct detection of attractants by chemoreceptors in the enteric bacteria *E. coli* in 1969 (1), and work in the 1970s and 1980s identified the proteins and genes required for chemotaxis and their function (26, 74, 75, 91). The components required for chemotaxis have since been very well characterized, allowing researchers today to examine complex aspects of signaling such as signal amplification and signal integration.

## Chemotaxis in *Escherichia coli*

*E. coli* moves through liquid environments propelled by 4-6 helical flagellar filaments powered by a rotary motor. These flagella are apparently randomly distributed on the cell surface, a pattern known as peritrichous flagellation. The flagella are

---

This dissertation follows the style and format of the Journal of Bacteriology.

composed primarily of the flagellin protein, FliC, which polymerizes to form a left-handed helical filament 20 nm in diameter and up to 10 μm long (44). Each filament is connected by a flexible hook to a basal body composed of several rings and a rod, which passes through the inner and outer membranes as well as the peptidoglycan cell wall (27, 28). The basal body complex operates as proton-powered rotary motor (58) capable of turning the flagellum either clockwise (CW) or counter-clockwise (CCW) (92). CCW rotation causes the flagella to coalesce into a bundle at one end of the cell (Fig. 1) and the coordinated rotation of the bundle propels the bacterium along a smooth, gently curved path (55). CW rotation induces a change in the conformation of the flagella and causes the bundle to fall apart (56). The uncoordinated movement of the unbundled flagella results in tumbling motility that randomly reorients the bacteria with little translational movement.

Chemotaxis in *E. coli* is mediated by switching between CW and CCW rotation. In the absence of a gradient of chemoaffector, cells alternate between CCW rotation, which produces periods of smooth-swimming ("runs") that last about one second, and shorter periods of CW rotation that last approximately 0.1 seconds that cause a tumble. This pattern of runs and tumbles moves the cell in a three-dimensional random walk (8). When the cell moves in a gradient of chemoeffector, the length of the runs is extended when the cell is moving in the direction of increasing concentration of an attractant or in the direction of decreasing concentration of a repellent. Extending the run length biases the cell's normal random walk and results in a net movement of the cell in the

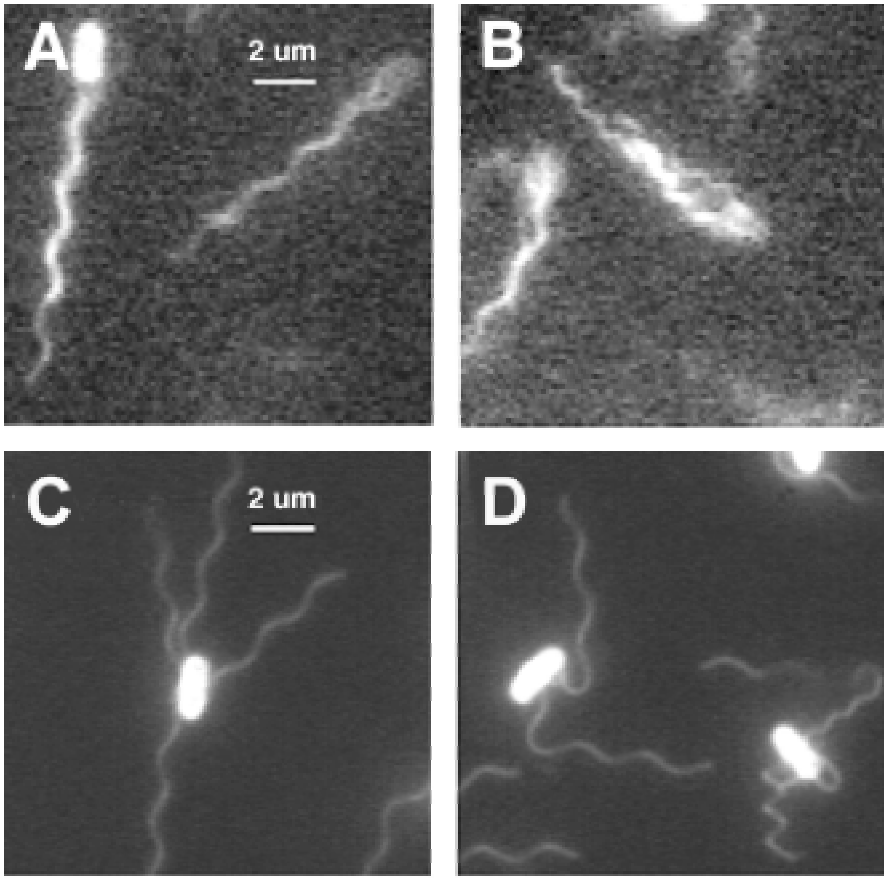


FIG. 1 Peritrichous flagella of *E. coli*. Flagella and cell bodies were stained with fluorescent dye and and the cells photographed swimming (A-B) and adhered (C-D). Propulsive bundles formed by CCW flagellar rotation can be seen in swimming cells (A-B). Peritrichious flagellation pattern and alternate waveforms induced by CW rotation can be seen in adhered cells (C-D). Images from Turner, Ryu, and Berg (112)

gradient (Fig. 2) (8). Bacterial cells monitor changes in concentration temporally, comparing the concentration of attractants or repellants in the current environment to the concentration averaged over the last few seconds and altering the pattern of flagellar rotation accordingly (85).

**Components of the *E. coli* chemotaxis signaling pathway**

The direction of flagellar rotation is controlled by a two-component signal-transduction system composed of CheA and CheY (Fig 3). CheA is a histidine protein kinase (104) that uses ATP to autophosphorylate (37) on a histidine residue (His 48) (36). The phosphate is then transferred to Asp-57 of CheY (37, 80), which is a member of the response regulator superfamily involved in signaling pathways with cognate histidine protein kinases (80). Phosphorylation of CheY induces a conformational changes that enables CheY to bind to FliM protein of the switch complex at the cytoplasmic face of the basal body (120). There are approximately 33-35 FliM molecules in the switch complex (73) and binding of a sufficient number of phosphorylated CheY (CheY~P) molecules to the basal body increases the probability of switching to CW motor rotation(83, 84). Using CheY-GFP fusion proteins to analyze the rotational bias of individual motors as a function of the concentration pf CheY~P in the cell, Cluzel, *et al.* demonstrated a steep sigmoidal relationship between CheY~P concentration and rotational bias (24). In the absence of a gradient of chemoaffector, this

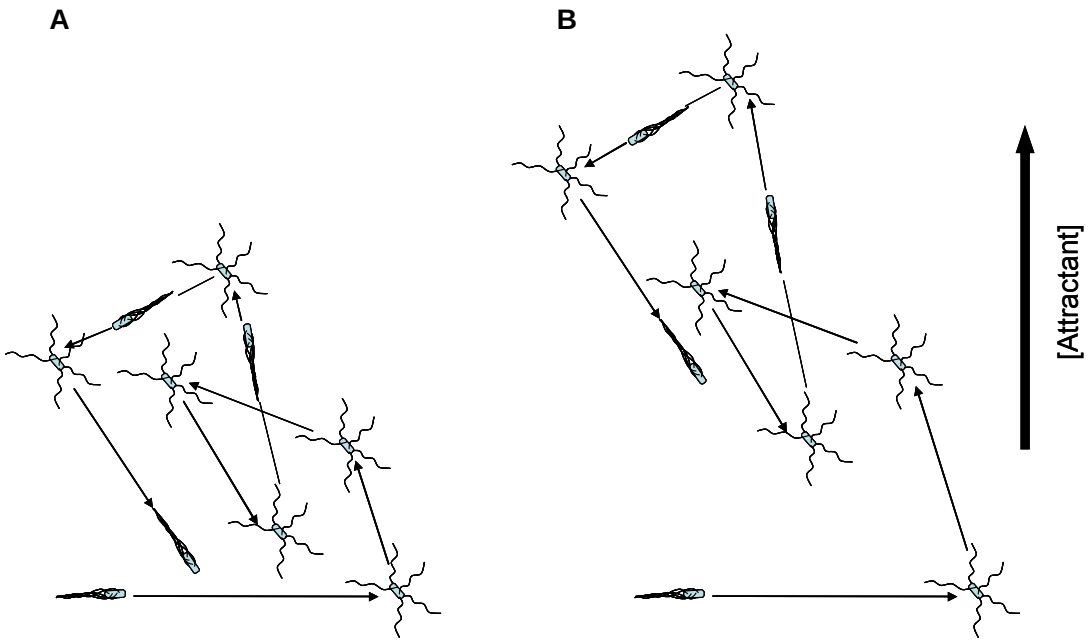


FIG. 2. Chemotaxis in *E. coli* occurs by a biased random walk. Cells alternate periods of smooth swimming ("runs") with short periods of random movement that reorient the cell ("tumbles"). In the absence of chemoaffector (A), net movement is minimal. In the presence of a gradient of chemoaffector (B), tumbles are suppressed when the cell moves in a favorable direction, biasing the random walk and creating a net movement toward an attractant or away from a repellent.

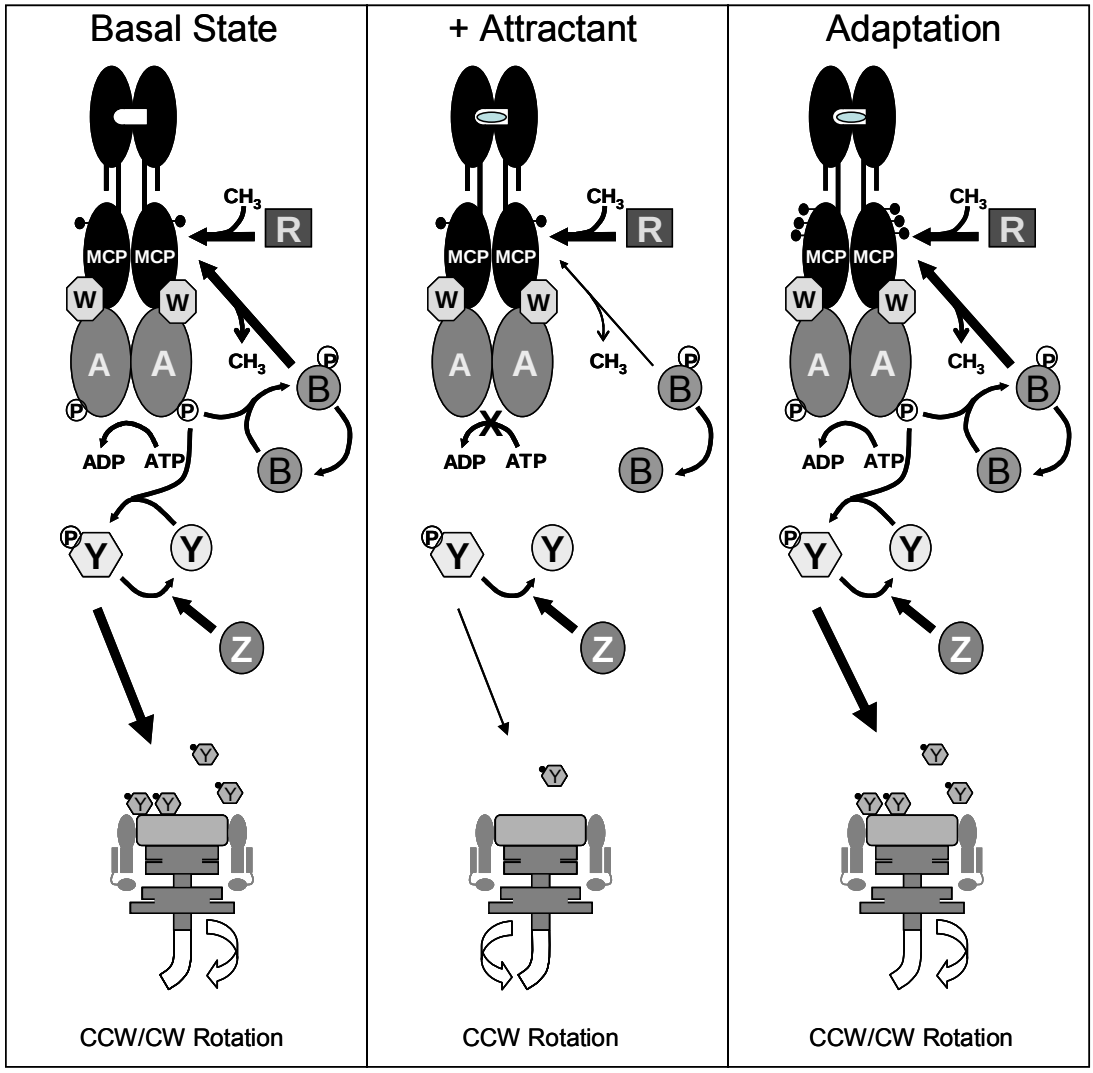


FIG. 3. Chemotactic signaling circuit of *E. coli*. In the basal signaling state, CheA kinase autophosphorylates as part of an active terinary complex with CheW and receptor (MCP). Phosphate is transferred to CheY, which binds the motor in the phosphorylated form and promotes switching to CW rotation. Phosphate groups are also transferred to the methylesterase CheB, which is thereby activated and removes methyl groups that are constitutively added to the receptor by the CheR methyltransferase. Upon ligand binding, the terinary complex is inactivated, and phosphate transfer to CheY and CheB stops. CheY~P levels deplete rapidly, resulting in CCW motor rotation and longer runs. Decreased CheB~P leads to a net increase in methylation of the receptors to effect adaptation. The methylated receptor is again able to stimulate CheA kinase activity, even in the continued presence of attractant, and cells resume periodic tumbling.

steep concentration dependence allows stochastic fluctuation of the rotational state of the motor and leads to the characteristic run-tumble behavior.

Chemoeffectors are detected by specific receptor proteins in the cytoplasmic membrane of *E. coli*. The receptors are homodimeric proteins, and each of the four principal chemoreceptors consists of a periplasmic ligand-binding domain and a cytoplasmic signaling and adaptation domain (77). Two transmembrane helices anchor the protein in the membrane, and the second transmembrane helix connects the periplasmic domain to the cytoplasmic domain via the HAMP linker (5, 121). Aspartate, serine, and presumably other amino acids interact directly with the Tar or Tsr receptor, binding in a pocket at the dimer interface (65). Other small molecules, such as ribose, galactose, or dipeptides, are sensed indirectly after first being bound to a periplasmic binding protein. The interaction of maltose-binding protein (MBP) with the Tar receptor of *E. coli* has been the best studied. MBP appears to interact with the periplasmic domain at the tip of the receptor distal to the membrane (124). The periplasmic domain of *S. typhimurium* Tar has been crystallized with and without aspartate bound (65, 123), and analysis of these structures, supplemented by cysteine cross-linking studies of the transmembrane regions (54), has indicated that ligand binding introduces small conformational changes that are transmitted to the cytoplasm through movement of the second transmembrane segment (TM2). How these subtle movements affect the cytoplasmic signaling domain is poorly understood and is an area of active research. The cytoplasmic signaling and adaptation domain of Tsr has also been crystallized and the two monomers of each homodimers form an extended four-helix coiled-coil. Three

such homodimers interacted at their distal tip, the most conserved portion of the chemoreceptor primary sequence, to form a trimer of dimers (40). Support for interaction between homodimers at the highly conserved domain *in vivo* has been by mutational analysis (2, 3, 107).

The ability of cells to sense gradients depends on adaptation by covalent modification of the chemoreceptors (Fig. 3). CheR is a methyltransferase that constitutively methylates four sites on each chemoreceptor using S-adenosyl methionine as the methyl donor (100). The action of CheR is opposed by the methylesterase CheB (106), which contains a response regulator domain (105) and like CheY, accepts a phosphoryl group from CheA (37). CheB is active only when phosphorylated (51). Shutting off CheA kinase activity by ligand binding decreases the amount of CheB~P in the cell, allowing methyl groups to accumulate on the receptor. Methylation serves to shift the receptor toward the non-ligand-bound conformation to restore CheA activation (17). This process provides the temporal component of the chemotaxis pathway that allows a cell to compare current conditions (as measured by ligand binding) to past conditions (as measured by receptor methylation).

The CheA kinase forms a ternary complex with transmembrane chemoreceptors and CheW that functions to modulate CheA activity. CheA and CheW interact with the conserved distal tip of the chemoreceptor and when in the ternary complex, the kinase activity of CheA is approximately 1000 fold higher than that of CheA in solution. The signal generated by attractant binding to the chemoreceptor is somehow communicated to CheA to shut off the kinase activity (18, 34, 70). The concentration of CheY~P

consequently falls. Since CheY~P generates CW motor rotation, cells sensing an increasing concentration of chemoattractant suppress the tumbles associated with CW motor rotation and bias the normal random walk in the up-gradient direction.

CheA contains dimerization, regulation, phosphotransfer, and CheY binding domains. The C-terminal P5 domain interacts with the adapter protein CheW and receptors to modulate CheA activity (19). The P4 domain contains the ATP-binding site and is the catalytic domain for the kinase reaction. The P3 domain is required for formation of the functional CheA dimer (19, 68). P2 is a CheY-binding domain (68), and the P1 domain contains the conserved phosphoacceptor histidine residue (36). P1 and P2 are independently folding domains separated from P3 and each other by flexible tether sequences (68). The P1 domain can be expressed as a separate polypeptide from the catalytic core (domains P3-5) and still function as a phosphoacceptor to support chemotaxis *in vivo* (109). Structures have been solved for P1 (69, 126), P2 (119), and P3-5 domains (11). Experiments combining CheA proteins with substitutions at His-48 with CheA proteins containing mutations targeting the catalytic site indicate that CheA is capable of trans-phosphorylation with the catalytic domain of one subunit transferring a phosphoryl group to His-48 of the opposite subunit (108). Phosphorylation of His-48 from ATP is the rate limiting step in the phosphotransfer pathway and CheY is thought to catalyze the rapid transfer of the phosphoryl group from CheA to CheY (102).

CheA is produced in two forms in *E. coli* cells. Initiation of translation from an alternative start site at Met 98 of full-length CheA produces an N-terminally truncated protein known as $CheA_S$ (43, 96). $CheA_S$ is present at about one half the amount of full

length $CheA_L$. $CheA_S$ lacks most of the P1 domain, including His-48, and if it is expressed alone in cells, it does not support chemotaxis, although it can trans-phosphorylate catalytically inactive $CheA_L$ (122). Mutants that do not produce $CheA_S$ do not appear to have a noticeable defect in chemotaxis in semi-soft agar (96), and the function of $CheA_S$ was unknown at the time this work was initiated.

**Chemotaxis proteins function as part of large protein complexes**

The ternary complex appears to be further organized into larger clusters. For many years, it was thought that chemoreceptors should be randomly distributed across the cell surface in order to maximize the likelihood of ligand molecules encountering receptors (9). However, in 1993 Maddock and Shapiro used immunofluorescence and immunoelectron microscopy to show that receptors, CheA, and CheW all localize in tight clusters found primarily near the cell poles (57). Some clusters were also found at positions along the lateral membrane, but these clusters were not associated with the flagellar basal bodies. Tight clustering of the chemoreceptors requires CheA and CheW to be present, and localization of CheA or CheW to the poles absolutely requires chemoreceptors to be present (57). Additional studies have shown that the high-abundance chemoreceptors Tsr and Tar can mediate clustering in the absence of other chemoreceptors, whereas the low-abundance chemoreceptors are localized to the poles but are not tightly clustered when expressed alone, even if they are expressed to levels equivalent to the full receptor complement (52). Neither CheR or CheB is required for

clustering of chemoreceptors (53), and either $CheA_L$ or $CheA_S$ can mediate clustering in the absence of the other (95).

Additional evidence of higher order interactions has been presented by several groups. The crystal structure of the cytoplasmic domain of Tsr revealed a trimer of dimers that interact at the cytoplasmic tip of the elongated four-helix bundle of each receptor dimer (40). Large complexes containing multiple chemoreceptor fragments, CheA, and CheW have been observed *in vitro* by electron microscopy. Modeling studies have postulated that clustering of receptor-CheA-CheW complexes plays an important role in chemotactic signaling and could be critical for signal integration and signal amplification. Using translational fusions to the jellyfish green fluorescent protein (GFP), Sourjik and Berg determined that CheY, CheR, CheB, and CheZ also localize to the cell pole (99).

**CheZ phosphatase**

The steady state concentration of CheY~P in *E. coli* is a function of both the rate of phosphorylation of CheY by CheA and by the rate of dephosphorylation of phospho-CheY by the CheZ phosphatase (Fig. 3). The phosphoaspartyl group of CheY is very unstable compared to other phosphorylated amino acids, and the half-life of isolated phospho-CheY is only a few seconds at physiological temperatures. However, the response time between addition of an attractant molecule and suppression of clockwise rotation is much faster, on the order of 200 msec (86). In order to overcome this limitation, *E. coli* cells produce CheZ, a phosphatase that greatly increases the rate of

CheY~P hydrolysis (37). Mutants that lack CheZ are strongly CW biased, and therefore tumbly, due to accumulation of excess CheY~P. CheZ binds to CheY~P with approximately 100-fold higher affinity compared to unphosphorylated CheY (15). CheZ binds CheY~P that is free in solution as opposed to CheY~P bound to the switch protein FliM (21), and the CheZ-binding face of CheY overlaps the FliM binding face. The extreme carboxyl-terminus of CheZ was shown to be a CheY-binding determinant. A truncated CheZ lacking residues 202-214 failed to bind CheY~P, while a peptide fragment of CheZ corresponding to amino acids 196-214 bound specifically to CheY (12). However, up until now it has not been possible to ascertain whether CheZ is actually a phosphatase or an allosteric effector of CheY that enhances its autodephosphorylation activity.

Wang and Matsumura demonstrated that CheZ associates with $CheA_S$ but not with $CheA_L$ *in vivo* by immunoprecipitation with anti-CheZ antibody. They also regenerated the $CheA_S$-CheZ complex *in vitro* under reducing conditions and estimated the molar ratio of the complex at approximately 1 $CheA_S$ : 5 CheZ. Most intriguingly, the phosphatase activity of CheZ increased upon addition of $CheA_S$, but not $CheA_L$ (117). Blat and Eisenbach reported that CheZ formed higher order oligomers, but only in the presence of CheY and the small phosphate donor acetyl phosphate, which spontaneously phosphorylates CheY (14). Mutants of CheZ with defective phosphatase activity do not appear to oligomerize in the presence of CheY~P (13). However, other researchers have examined CheZ-CheY complex formation under phosphorylated and non-

phosphorylated conditions and have observed only dimeric CheZ, without any indication of higher order complexes (94).

Mutational analysis has provided considerable information regarding the functional domains of CheZ and has identified regions responsible for loss-of-function and gain-of-function phenotypes. Loss-of-function alleles affect primarily to two areas of CheZ. Sockett *et al.* isolated CheZ missense mutants of *S. typhimurim* with CW bias and mapped the mutations to residues 110-145 (97). These mutant proteins were subsequently purified and shown to have greatly reduced phosphatase activity but normal CheY binding (13). Sanna and Simon conducted an extensive mutational analysis of CheZ using a *cheZ* gene expressed from an inducible promoter to screen for mutations that required less or more inducer to produce wild-type swarms in semi-soft agar plates. The loss-of-function mutants (*i.e.*, those requiring more inducer than wild type to produce swarms) mapped primarily to the region between residues 115 and 147 with residues 62 and 65 also giving rise to the loss-of-function phenotype. Several of these mutant proteins were purified and demonstrated decreased phosphatase activity (82). Finally, Boesch *et al.* carried out an extensive screen for CheZ-defective mutants. This screen expanded the range of residues at which loss-of-function substitutions occurred, but in general conformed to the previously identified pattern, with clusters of mutations at residues 47-76, residues 83-90, residues 110-117, and residues 124-159. In addition, a small number of loss-of-function mutations were identified between residues 186 and 206. As with previous studies, a subset of these mutated proteins were purified and demonstrated to have decreased ability to dephosphorylate CheY~P *in vitro* (16).

Gain of function mutations of CheZ were first isolated as suppressors of a CheZ-resistant mutation of CheY that substituted an Asp for the Asn at position 23 and was not able to bind CheZ. Suppressors were isolated on semi-solid agar by their ability to compensate for the CW bias of the CheY mutation. These CheZ mutations mapped in a region from residues 17-54, with additional mutations affecting residues 152, 166, 170, and 214. A subset of the mutant CheZ proteins was purified and demonstrated to restore binding of CheZ to CheY N23D. The mutations also restored the ability to dephosphorylate CheY N23D. Sanna and Simon also isolated a number of gain-of-function mutations as part of a general mutagenesis of CheZ. Gain-of-function mutations were isolated from swarms that formed with less inducer present than is required for wild-type CheZ. The sites targeted by these mutations correlated with the CheY N23D suppressors, mapping at residues 17-54 and 152-170. The phosphatase activity of several of these mutants was quantified, and the most active of these mutant proteins dephosphorylated Chey~P approximately 4.6 times better than wild-type CheZ.

An important breakthrough in understanding the CheZ protein came with the publication of a three-dimensional structure of a CheZ by Zhou *et al.* in 2002 (Fig. 4). The structure was obtained from a co-crystal of CheZ, CheY, $Mg^{2+}$, and the phosphoryl analog $BeF_3^-$. The structure revealed a dimer of CheZ arranged in an elongated four-helix bundle. Residues 35-168 of the monomer form two amphipathic helices with a single turn, and these helices assemble as a coiled-coil in the dimer to form the four-helix bundle. Residues 5-35 comprise another helix that projects away from the four-helix bundle. The crystal structure contained a third helix of CheZ, found in close

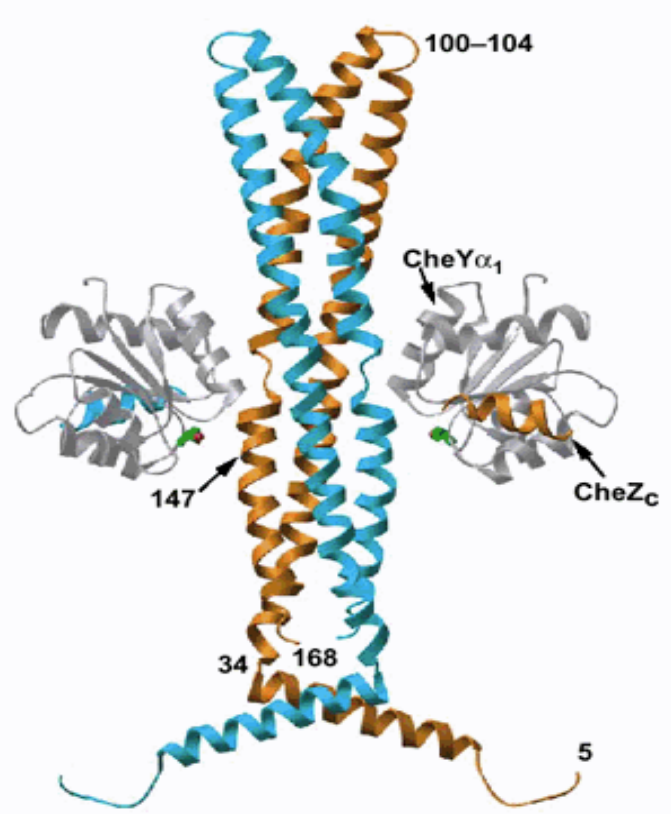


FIG. 4. Structure of the CheZ-CheY co-crystal. A ribbon diagram of the backbone structure of CheZ is presented with one monomer shown in orange and the second shown in cyan. The assignment of the c-terminal helix to each monomer is arbitrary. The CheY backbone is shown in grey. The central four-helix bundle of CheZ extends from residue 34 to 168, with the hairpin turn at residues 100-104. Location of Gln-147, predicted to participate in the dephosphorylation reaction, is shown by the arrow. Image from Zhao *et al.* (125)

contact with CheY that is believed to correspond to residues 200-213 of CheZ. The residues between the four-helix bundle and the carboxyl-terminal peptide are not resolved in the crystal structure and likely represent a disordered linker. CheY also contacts CheZ about halfway down the four-helix bundle. This face of CheY contains the active site and makes contact with residues 67-71 of one monomer of CheZ and residues 136-151 of the second monomer.

The locations of known CheZ mutations were mapped to the crystal structure and provide support that the structure reflects the *in vivo* interaction of CheY and CheZ (Fig. 5). The face of CheY that interacts with the four-helix bundle corresponds with mutations that reduce the affinity of CheY~P for CheZ. The interacting residues on CheZ correspond to two of the clusters of loss-of-function mutations previously identified. The association of the carboxyl-terminal helix with CheY is consistent with the previous binding studies using CheZ peptides corresponding to residues 196-214 as well as loss-of-function mutations at residues 204-206. Two additional clusters of previously isolated loss-of function mutations map to sites of helix-helix interaction within each monomer near the hairpin turn and likely contribute to maintaining the four-helix bundle conformation. One cluster of gain-of function mutations maps to the amino-terminal helix of CheZ (residues 5-35). The other two clusters of gain-of-function mutations (residues 40-54 and 152-170) map to a face of the four-helix bundle at the opposite end from the hairpin turn.

Finally, the co-crystal structure shed light on the mechanism by which CheZ accelerates the dephosphorylation of CheY~P. The interaction of CheY with the four-

FIG. 5. Loss-of-function and gain-of-function mutations target residues that cluster in the CheZ protein. The CheZ dimer is shown in a space-filling model with a single molecule of CheY shown in purple shown as a backbone trace. Loss of function mutations are shown in red and cluster at sites involved in CheZ-CheY interaction. Gain-of-function mutations are shown in blue and cluster in the N-terminal helix and the proximal portion of the four-helix bundle.

helix bundle of CheZ shows residues of CheZ in close proximity to the active site of CheY. Gln 147 of CheZ inserts into the CheY phosphorylation pocket and is in close proximity to the $BeF_3^-$ phosphoryl analog. This residue is highly conserved in CheZ proteins from various species, and substitution of Gln 147 with Ala completely abolished CheZ phosphatase activity, although CheY binding was retained. Comparison of the structure of CheY-BeF3- in solution (47) and bound to CheZ (125) shows that the active site residues are in nearly the same positions, indicating that CheZ binding does not act allosterically by changing the conformation of CheY. The mechanism of CheY autodephosphorylation is thought to involve an in-line attack by a water molecule, and Zhou et. al. have proposed a mechanism of CheZ action in which Gln 147 inserts into the active site and helps to properly position the water molecule to react with the phosphoryl group. This mechanism clearly involves a catalytic role for CheZ, but it sets aside the mechanism of CheY dephosphorylation by CheZ as a distinct mechanism from other phosphatases.

**Experimental rationale**

At the onset of this work, I hypothesized that CheZ would localize to the polar receptor patch and that localization would depend on an interaction with $CheA_S$, which had been shown to interact with CheZ *in vivo* and *in vitro* (117). Subcellular localization of CheZ was visualized by fusing it to GFP. I have primarily used genetic means to identify the determinants of CheZ localization, employing alleles of *cheA* to show that CheZ is localizes to the receptor patch via $CheA_S$, and using oligonucleotide-directed

mutagenesis to probe for the specific regions of CheZ and CheA that are involved in localizing CheZ. Identification of mutants defective in this interaction has allowed me and others to assess the role of CheZ localization and the $CheA_S$ protein in *E. coli* chemotaxis

# CHAPTER II

# CheZ PHOSPHATASE LOCALIZES TO CHEMORECEPTOR PATCHES VIA CheA-SHORT*

## Introduction

CheZ is a phosphatase that accelerates the removal of the intrinsically labile phosphoryl group from CheY-P (37). Zhao *et al*. (125) determined the crystal structure of the CheZ dimer complexed with two CheY monomers containing the phosphoryl analog $BeF_3^-$. CheZ can also be isolated in a complex with $CheA_S$ (117), a short form of CheA produced from an internal translation-initiation site at codon 98 of *cheA* (43). This complex was first identified in co-immunoprecipitation experiments, but it can also form with purified proteins. In experiments done *in vitro* at 4$^{o}$C to slow the spontaneous dephosphorylation of CheY-P, the CheZ/$CheA_S$ complex showed a 2.3-fold higher phosphatase activity than free CheZ (117). Binding of $CheA_S$ to CheZ may be inhibited by CheW, as indicated by the decreased level of co-immunoprecipitation when CheW is overexpressed (116). $CheA_S$ lacks the phosphoryl-accepting His-48 residue of $CheA_L$, but it is catalytically active and can phosphorylate $CheA_L$ in *trans* (122).

Using CheZ fused to yellow fluorescent protein, Sourjik and Berg (99) found that CheZ localizes to the subpolar chemoreceptor clusters identified by Maddock and Shapiro (57). We had been using CheZ fused to green fluorescent protein (GFP; (25)) to

---

*Part of this chapter is reprinted with permission from "CheZ phosphatase localizes to chemoreceptor patches via $CheA_S$" by Brian J. Cantwell et al., 2003, Journal of Bacteriology, 185: 2354-2361. Copyright 2003, American Society of Microbiology.

study the distribution of CheZ in cells and, after learning of Sourjik and Berg's work, focused our investigation on whether $CheA_S$ is needed for this localization and identifying what part of the CheZ protein is required.

## Materials and methods

**Strains and plasmids.** The strains and plasmids used in this investigation are shown in Table 1.

**Media and growth conditions.** Cells for examination of GFP fluorescence or immunoblotting were grown at 32$^{o}$C in tryptone broth (TB) (66)or H1 minimal medium (24) supplemented with 0.5% glycerol, 0.2% Casamino acids, 20 μg/ml threonine, histidine, methionine, leucine, and 1 μg/ml thiamine. Cells containing plasmid pBJC100, pBJC101, pBJC102, or pBJC104 were grown with 50 μg/ml ampicillin. Cells containing λInCh insertions of plasmid pBJC104 were grown with 25 μg/ml ampicillin.

**Construction of plasmids encoding the CheZ-GFP fusion.** The *cheZ* gene was amplified from the chromosome of wild-type strain RP437 (74) by the polymerase-chain reaction (PCR), using a primer containing a 5' BamHI site and a primer containing a 3' HindIII site. This DNA fragment was cloned into the SmaI and HindIII sites of the vector pBAD18 (15) to create plasmid pBJC100. The *cheZ-gfp* fusion was constructed by cloning overlapping PCR products. The 5' *cheZ* gene fragment was amplified from pBJC100 using a 5' primer corresponding to the pBAD promoter (primer BAD-up) and a 3' primer corresponding to the linker sequence and containing XhoI and EagI restriction

**TABLE 1. Strains and plasmids, chapter II.**

| Strain | Genotype | Comments | Reference or Source |
|---|---|---|---|
| RP437 | *thr*(Am)*1, leuB6, his-4, metF*(Am)*159, eda-50, rpsL1356, thi-1, ara-14, mtl-1, xyl-5, tonA31, tsx-78, lacY1, F⁻* | | (75) |
| AJW536 | RP437 *cheA*$_{RV}$M98L, *zig*::Tn10, *polA*(Ts) | | (64) |
| RP1616 | RP437 Δ*cheZ*6725 | | J. S. Parkinson |
| RP9535 | *RP437* ΔcheA*1643*, eda$^+$ | | (68) |
| RP1078 | RP437 Δ(*cheW-tap*)*2217* | | (75) |
| RP2867 | RP437 Δ(*tap-cheB*)*224*, eda$^+$ | | (75) |
| RP5231 | RP437 Δ(*cheY-cheZ*)*4213, eda*$^+$ | | J. S. Parkinson |
| RP1515 | RP437 *cheA169* (Am), Δ*lac*169*, eda*$^+$ | | (96) |
| RP1516 | RP437 *cheA157* (Am), Δ*lac* 169*, eda*$^+$ | | (96) |
| UU1118 | RP437 *cheA*(Δ*7-247*), *eda*$^+$ | | (33) |
| UU1121 | RP437 *cheA*(Δ*150-247*), *eda*$^+$ | | J. S. Parkinson |
| VB13 | *RP437* Δtsr7021,Δ(tar-tap)5201, trg::*Tn*10, thr$^+$, eda$^+$ | | (118) |
| DHB6521 | SM551 (λInCh1 lysogen) | | (20) |
| BC200 | RP1616 Δ(λ*att-lom*)::*bla lacI*$^q$ p*tac-cheZ-gfp* | pBJC104 into RP1616 via λInCh1 | This study |
| BC203 | VB13 Δ(λ*att-lom*)::*bla lacI*$^q$ p*tac-cheZ-gfp* | pBJC104 into VB13 via λInCh1 | This study |
| BC206 | RP9535 Δ(λ*att-lom*)::*bla lacI*$^q$ p*tac-cheZ-gfp* | pBJC104 into RP9535 via λInCh1 | This study |
| BC207 | RP1078 Δ(λ*att-lom*)::*bla lacI*$^q$ p*tac-cheZ-gfp* | pBJC104 into RP1078 via λInCh1 | This study |
| BC208 | RP5231 Δ(λ*att-lom*)::*bla lacI*$^q$ p*tac-cheZ-gfp* | pBJC104 into RP5231 via λInCh1 | This study |
| BC209 | AJW536 Δ(λ*att-lom*)::*bla lacI*$^q$ p*tac-cheZ-gfp* | pBJC104 into AJW536 via λInCh1 | This study |

**TABLE 1. Continued**

| Strain | Genotype | Comments | Reference or Source |
|---|---|---|---|
| BC210 | UU1121 Δ(λ*att-lom*)::*bla lacI*$^q$ p*tac-cheZ-gfp* | pBJC104 into UU1121 via λInCh1 | This study |
| BC211 | UU1118 Δ(λ*att-lom*)::*bla lacI*$^q$ p*tac-cheZ-gfp* | pBJC104 into UU1118 via λInCh1 | This study |
| BC212 | RP1515 Δ(λ*att-lom*)::*bla lacI*$^q$ p*tac-cheZ-gfp* | pBJC104 into RP1515 via λInCh1 | This study |
| BC213 | RP1516 Δ(λ*att-lom*)::*bla lacI*$^q$ p*tac-cheZ-gfp* | pBJC104 into RP1516 via λInCh1 | This study |
| BC214 | RP2867 Δ(λ*att-lom*)::*bla lacI*$^q$ p*tac-cheZ-gfp* | pBJC104 into RP2867 via λInCh1 | This study |

| Plasmids and Phage | Relevant Genotype | Comments | Reference or Source |
|---|---|---|---|
| pAG3 | p*tac cheA(1-149), amp*$^r$ | Expresses CheA P1 domain | (33) |
| pBAD18 | *araC*$^+$, *amp*$^{\mathbf{r}}$ | p*araBAD* expression vector | (35) |
| pCJ30 | *lacI*$^q$, *amp*$^r$ | p*tac* expression vector | (10) |
| pPM2 | *gfp mut2* | Expresses GFP Mut2 | (25) |
| pBJC100 | *cheZ, amp*$^r$ | *cheZ* in pBAD18 | This study |
| pBJC101 | p*araBAD cheZ-gfp, amp*$^r$ | *cheZ-gfp* in pBAD18 | This study |
| pBJC102 | *gfp mut2*, *amp*$^r$ | *gfp mut 2* in pBAD18 | This study |
| pBJC104 | p*tac cheZ-gfp, amp*$^r$ | *cheZ-gfp* in pCJ30 | This study |
| λInCh1 | *kan*$^r$, *cI*857 | λInCh for pBR-derived plasmids | (20) |

sites. The 3' *gfp mut2* gene fragment (25) was amplified using an upstream primer encoding the linker sequence and a downstream primer encoding a HindIII site. The PCR products were digested with XhoI and ligated. The ligated product was purified, digested with EcoRI and HindIII, and ligated into pBAD18 to create plasmid pBJC101. The fusion gene encodes full-length *cheZ* upstream of full-length *gfp mut2*. The two proteins are joined by a short, flexible linker peptide (GGSSAAG).

Plasmid pBJC102 was constructed by PCR amplification of the *gfp* gene, using a 5' primer encoding an EcoRI restriction site and the *cheZ* Shine-Dalgarno sequence immediately 5' to the *gfp* translation-start site. The 3' primer encoded a HindIII site. The PCR-amplified product was cloned into the EcoRI and HindIII sites of pBAD18. Plasmid pBJC104 was constructed by cloning the EcoRI-HindIII fragment of plasmid pBJC101 that contains *cheZ-gfp* into the EcoRI and HindIII sites of pCJ30.

All PCR reactions were performed using *Taq* polymerase (Gibco BRL). The sequence of the cloned PCR products was confirmed by dideoxynucleotide sequencing using the ABI Prism Dye-Terminator Cycle Sequencing Ready Kit and AmpliTaq DNA Polymerase (PE Applied Biosystems).

**Insertion of *cheZ-gfp* into the chromosome.** The *cheZ-gfp* gene of plasmid pBJC104 was introduced onto the chromosome utilizing the λInCh system as described (20). Briefly, pBJC104 was transformed into a strain containing λInCh1, and recombinants that contain the plasmid insert and *bla* gene were selected on ampicillin plates. A lysate of this strain was used to transduce strains of interest to ampicillin resistance. Finally, homologous recombination between a DNA sequence adjacent to the

chromosomal λ*att* site and the same sequence within λInCh1 was selected by loss of temperature-sensitive lysis. This recombination event removes much of the phage DNA and stabilizes the insertion. Strains modified in this way to carry the *cheZ-gfp* gene are listed in Table 1.

**Random mutagenesis of *cheZ***. Mutations in the *cheZ* gene of pBJC100 were created by error-prone PCR (127) using *Taq* polymerase. The PCR products were isolated by agarose-gel electrophoresis, purified using the QIAquick-gel extraction kit (Quiagen), and digested with EcoRI and HindIII. The resulting fragment was purified by agarose-gel electrophoresis and ligated into plasmid pBJC100 to replace the resident, unmutagenized *cheZ* gene. Aliquots of the ligation reaction were used to transform competent RP1616 cells, and ampicillin-resistant transformants were selected and screened for chemotactic swarming. DNA sequencing identified mutations responsible for altered chemotactic behavior. Mutations were subcloned into the *cheZ-gfp* gene of pBJC101 by replacing the EcoRI-Bsu36I fragment of plasmid pBJC101 with the same fragment from the mutated *cheZ* gene.

For direct screening of CheZ-GFP localization, the *cheZ* portion of the fusion gene was randomly mutagenized by PCR amplification of pBJC101 using a primer corresponding to a vector sequence 5' to the gene and a 3' primer corresponding to a sequence at the fusion junction. The PCR product was isolated by agarose-gel electrophoresis, purified using the QIAquick-gel extraction kit (Quiagen), and digested with EcoRI and XhoI. The resulting fragment was purified by agarose-gel electrophoresis and ligated into pBJC101 to replace the unmutagenized *cheZ* fragment.

RP1616 cells were exposed to aliquots from the ligation reaction, and $Amp^r$ transformants were selected. $Amp^r$ isolates were grown overnight in H1 medium supplemented with 0.2% Casamino acids and 0.01% arabinose and screened for defects in CheZ-GFP localization by epifluorescence microscopy (see below). Plasmids were isolated from potential mutants and used to transform strain RP1616 to confirm that mutations were plasmid-borne. Mutations were identified by sequencing the *cheZ* region of *cheZ-gfp*.

**Site-directed mutagenesis.** Specific mutations were introduced into the *cheZ-gfp* gene of pBJC101 or pBJC104 using the Quick-Change mutagenesis kit (Stratagene). Mutagenized plasmids were introduced into strain RP1616, and ampicillin-resistant transformants were screened on minimal-aspartate swarm plates containing 0.002% arabinose. Mutations were confirmed by DNA sequencing, and localization of the CheZ-GFP protein was determined (see below).

**Immunoblotting.** Cultures were grown overnight at 32$^o$C in TB containing the relevant antibiotic(s), diluted 1:50 into TB containing antibiotic(s) and arabinose or IPTG, as appropriate, and incubated at 32$^o$C with shaking. Cells from 1 ml of culture at an $OD_{590nm}$ of 0.7-0.8 were harvested by centrifugation and washed once with TE buffer (10 mM Tris [pH 8.0], 1 mM EDTA). Cells were resuspended in 100 µL of loading buffer (2% [w/v] SDS, 5% [v/v] 2-mercaptoethanol, 8.5% [v/v] glycerol, 60mM Tris [pH 6.8] and 0.0004% bromophenol blue). Extracts were prepared by three cycles of 5 min freezing at -80$^o$C and 5 min of boiling. Proteins were separated by 10% acrylamide SDS-PAGE and transferred to a nitrocellulose membrane. Anti-CheZ, anti-GFP

(Clonetech), and anti-CheA (103) polyclonal antisera were diluted 1:1000 and used to probe the membranes. Immunoreactive proteins were visualized using alkaline phosphatase-conjugated goat anti-rabbit antibody (BioRad) and SigmaFast (Sigma Chemicals) color reagent.

**Swarm assays.** Chemotaxis was assayed in semi-soft minimal swarm agar containing 100 μM L-aspartate or 50 μg/ml L-prolyl-L-leucine. The plates were incubated for 8 to 10 h at 30$^{o}$C. The swarm diameters were measured, and the sharpness of the rings was assessed. These parameters were compared to those of swarms formed by wild-type and chemotaxis-deficient control strains.

**Fluorescence microscopy.** Cells were grown overnight at 32$^{o}$C in TB media with antibiotics, diluted 1:50 into 10 ml of the same medium containing arabinose or IPTG as needed, and incubated with shaking at 32$^{o}$C. Cells from 1 ml of culture were harvested at an $OD_{590nm}$ of 0.7-0.8 by centrifugation, washed once with tethering buffer (100 mM NaCl, 10 mM KPO4 pH 7.0, 0.4% (v/v) lactic acid, 20 μM methionine, 10 μM EDTA, 22.5 μg/ml chloramphenicol), and resuspended in 1 ml of tethering buffer. The cells from 100 μl aliquots were allowed to settle for 5 min onto cover slips coated with 0.1% polylysine (Sigma). The affixed cells were then washed twice with 200 μL tethering buffer. The cover slips were inverted over a chamber containing tethering buffer, and the cells were observed at 1575X magnification using a Zeiss Axioplan 2 microscope. Light microscopy employed differential interference contrast (DIC). For epifluorescence microscopy, the excitation wavelength was 484 nm and the emission was recorded at 510-530 nm. Images were captured using a Hamamatsu C5810 CCD

camera and analyzed with the Adobe PhotoShop program.

**Protein-sequence alignment .** The amino acid sequences of CheZ from 14 species of bacteria were retrieved from the Entrez database (http://www.ncbi.nlm.nih.gov/) and aligned using the AlignX program of the Vector NTI Suite molecular biology software package.

## Results

**Construction of a CheZ-GFP chimera.** A *cheZ-gfp* gene fusion was created by PCR using primers encoding a seven amino acid flexible linker (GGSSAAG). The fusion gene was cloned into the pBAD18 vector. The resulting plasmid, pBJC101 (Table 1), enables Δ*cheZ* strain RP1616 to form wild-type chemotactic swarms in minimal semi-solid agar 100 μM aspartate and 0.002% arabinose (Fig. 6). The swarming phenotype of RP1616 is identical when complemented with either plasmid-encoded CheZ or the CheZ-GFP fusion protein. The fusion gene was subsequently cloned into the vector plasmid pCJ30 to facilitate its insertion into the chromosome using the λInCh system (20). The resulting pBJC104 plasmid was also able to restore chemotactic swarming to strain RP1616, even in the absence of the inducer IPTG. The *cheZ-gfp* gene was inserted from plasmid pBC104 into the chromosome of strain RP1616. The BC200 strain created in this way made wild-type chemotactic swarms when transcription of *cheZ-gfp* was induced with 1 mM IPTG. In the absence of IPTG, little or no swarming was observed.

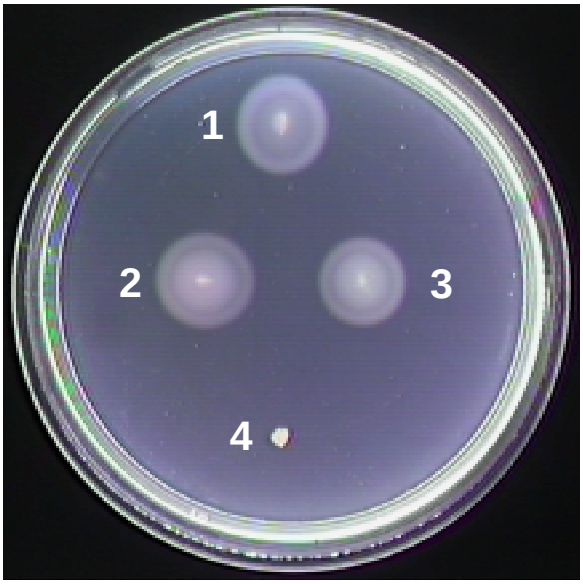


FIG. 6. CheZ-GFP restores chemotaxis to *ΔcheZ* cells. Cells were inoculated into soft-agar motility plates containing 100 μM aspartate and 0.002% arabinose and incubated at 30º C. RP437 (1) is wild type, while RP1616 (4) has a *cheZ* deletion and does not support chemotaxis, but arabinose induced expression of CheZ from plasmid pBJC100 (3) restores chemotaxis. Arabinose-induced expression of CheZ-GFP from plasmid pBJC101 (2) restores chemotaxis as effectively as CheZ.

Extracts from cells containing plasmid or chromosomal copies of *cheZ-gfp* were analyzed by SDS-PAGE and western blotting (Fig. 7). Cells expressing CheZ-GFP from plasmids pBJC101, pBJC104, or from the chromosome (strain BC200) contained a protein of the size expected (~54kD) for CheZ-GFP, detectable whether the immunoblots were developed with anti-CheZ or anti-GFP antibody. Only a small amount of normal-length CheZ was detected, indicating that the fusion protein does not undergo substantial proteolysis. Since the amounts of CheZ and CheZ-GFP, estimated from immunoblots, appeared to be about the same under the same induction conditions, we concluded that CheZ-GFP is functional and responsible for the observed complementation of Δ*cheZ* (Fig. 6).

**Subcellular localization of CheZ-GFP.** Subcellular localization of GFP fluorescence was examined in strains containing the *cheZ-gfp* gene in single copy on the chromosome. In strain BC200 (Δ*cheZ*), CheZ-GFP localized to patches, as was previously observed by Sourjik and Berg (99) for plasmid-encoded CheZ-YFP. All cells exhibited diffuse cytoplasmic fluorescence, but bright, localized patches of fluorescence were seen in 85% of the cells, primarily near the poles but also laterally in 15 to 20% of the cells (Fig. 8A). This pattern was similar to that seen by immunofluorescence using antibody to CheA or Tsr (57). Thus, these patches are likely to represent CheZ-GFP associated with clusters containing chemoreceptors, CheA, and CheW. Similar patterns fluorescence were observed in cells of strain RP1616 carrying plasmid pBJC101 or plasmid pBJC104.

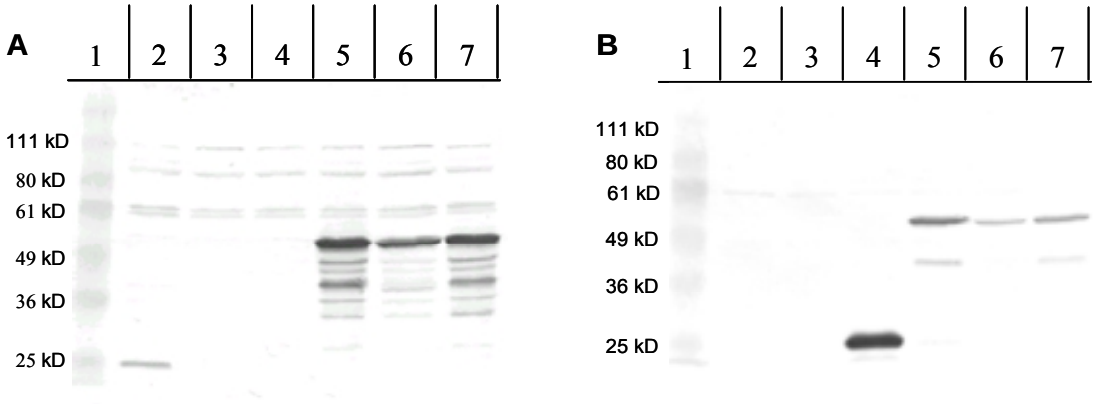


FIG. 7. The *cheZ-gfp* gene directs production of a full-length CheZ-GFP fusion protein. Protein extracts were prepared from each of the strains indicated below and separated by electrophoresis on 10% SDS-polyacrylamide cels. Expression of GFP or CheZ-GFP from p*araBAD* in plasmids pBJC102 and pBJC101, respectively, was induced by addition of 0.002% arabinose (lanes 4 and 5), and expression of chromomosomally encoded CheZ-GFP from p*tac* was induced by addition of 1 mM IPTG (lane 7). Expression of CheZ-GFP from p*tac* plasmid pBJC104 (lane 6) is in the absence of inducer. Lane 1, molecular weight standards; lane 2, RP437 (pBAD18); lane 3, RP1616 (pBAD18); lane 4, RP1616 (pBJC102); lane 5 RP1616 (pBJC101); lane 6, RP1616 (pBJC104); lane 7, BC200. (A) Immunoblot developed with CheZ antiserum. (B) Immunoblot developed with GFP antiserum.

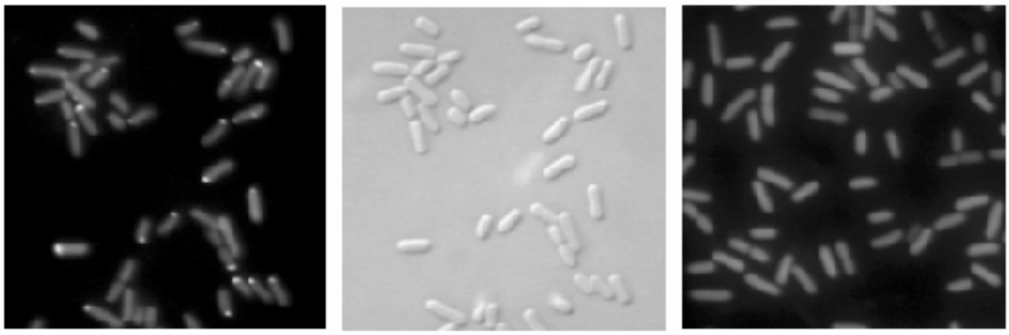

FIG. 8. CheZ-GFP localizes to patches. (A) Representative fluorescence micrograph of cells of strain BC200 grown to late-exponential-phase in the presence of 1mM IPTG. Cells exhibit uniform fluorescence and localized patches of brighter fluorescence can be seen in almost all cells. (B) DIC photomicrograph of the same field of cells as in A. Comparison of the pictures in A and B indicates that nearly all of the cells fluoresce at the same intensity. (C) Representative fluorescent micrograph of cells of strain BC206 (*ΔcheA*) grown to late-exponential-phase in the presence of 1 mM IPTG. Note that the level of background fluorescence is the same as in A but that no intense patches of brighter fluorescence are visible

An essentially identical number and distribution of patches of fluorescence were seen cells of strain BC214 (Δ*tap-cheB*) and BC208 (Δ*cheY-cheZ*), but no patches were detectable in cells of strain BC206 (Δ*cheA*) (Fig. 8C), strain BC207 (Δ*cheW-tap*) or strain BC203 (Δ*tar-tap* Δ*tsr trg*::Tn10). These results mirror the strain-dependence for formation of receptor clusters (53, 57). Immunogold labeling of thin sections of cells, carried out with anti-CheZ antibody, indicated that the wild-type CheZ protein also localizes in clusters near the cell poles (J. R. Maddock, personal communication).

**Localization of CheZ-GFP to receptor patches requires $CheA_S$ but not $CheA_L$.** We next examined the dependence of CheZ-GFP patching on $CheA_S$ and $CheA_L$. Strain BC209 produces only $CheA_L$ because ATG codon 98 of *cheA*, the $CheA_S$ start codon (43), has been changed to CTG. The M98L version of $CheA_L$ has about 70% of the kinase activity of wild-type CheA, and a strain producing M98L $CheA_L$ makes swarms with 70% the diameter of wild-type swarms (95). Strains BC212 and BC213 contain amber mutations in the *cheA* sequence between the start codon of $CheA_L$ and codon 98, so that both strains produce only $CheA_S$. A schematic of the CheA polypeptides produced by these strains is shown in Figure 9A. The ratio of the intensities of bands of $CheA_L$ versus $CheA_S$ detected on immunoblots prepared with our CheA antiserum (103) is about 2:1 in extracts from strain BC200 (Fig. 9B). The ratio of the intensities of the $CheA_L$ band in extracts of strain BC209, and of the $CheA_S$ band in extracts from strains BC212 and BC213, is also about 2:1. Thus, each form of CheA exists in a normal amount in the absence of the other.

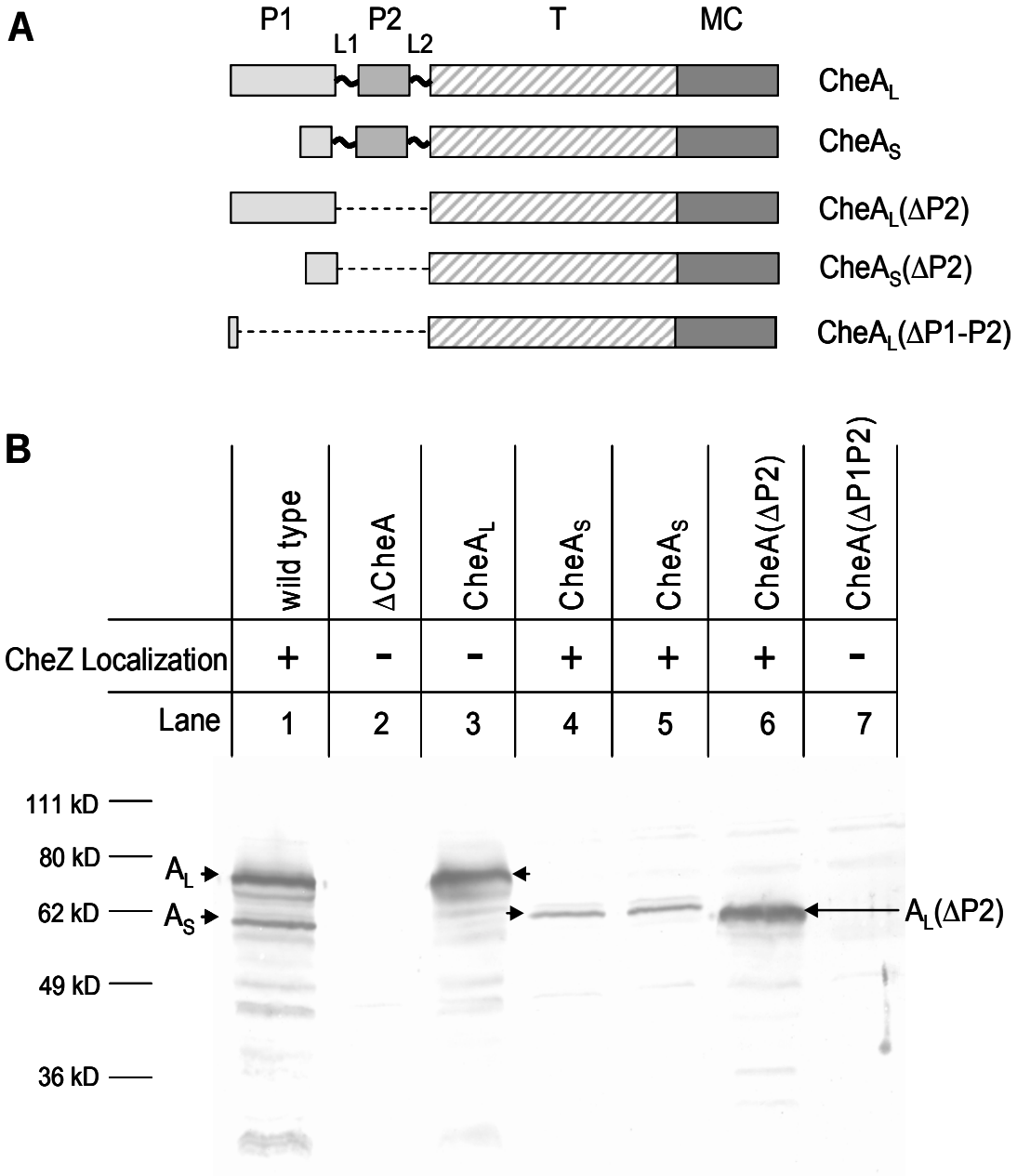


FIG. 9. Cellular levels of various forms of the *E. coli* CheA protein.. (A) Schematic representation of $CheA_L$, $CheA_S$, $CheA_L(\Delta P2)$, $CheA_S(\Delta P2)$, and CheA(ΔP1-P2). P1, P2, T, and MC represent the phosphorylation domain, the CheY-binding domain, the dimerization and catalytic domain, and the CheW/receptor input domain, respectively. (B) Immunoblot with polyclonal CheA antiserum. Proteins in extracts were separated by SDS-PAGE on 10% acrylamide gel. Lanes: (1) RP437; (2) RP9535; (3) AJW536; (4) RP1515; (5) RP1516; (6) UU1121; (7) UU1118; (8) MW standards. The type of CheA protein produced by each strain is indicated above the relevant lane.

Cells of strain BC209 contained no detectable bright patches and showed only the diffuse cytoplasmic fluorescence found in cells of strain BC206 (Δ*cheA*) (Fig. 10A-B). Cells of the $CheA_S$-only strains BC212 and BC213 (Fig. 10C) localized CheZ-GFP to patches just like strain BC200. These data suggest that CheZ interacts with $CheA_S$ at the patch *in vivo* and is required for the pattern of CheZ localization observed in wild-type cells. It has previously been shown that $CheA_L$-only and $CheA_S$-only cells form receptor patches with equal facility (95).

**The N-terminal region of $CheA_S$ may bind CheZ.** Strain BC210 (*cheA*ΔP2) expresses a CheA protein missing the P2 domain, which binds CheY (68, 109). Its swarming ability is only slightly decreased from that of its wild-type parental strain RP437. Strain BC211 (*cheA*Δ[P1-P2]) expresses a CheA protein in which a *cheA*-internal deletion removes most of the P1 and P2 domain, and it does not form chemotactic swarms. Chromosomally encoded CheZ-GFP had the wild-type distribution in cells of strain BC210 (Fig. 9D) but not in cells of strain BC211 (data not shown). Expression of the P1 domain (109) from plasmid pAG3 enabled strain BC211 to form chemotactic swarms with about half the diameter of those made by strain RP437 but did not restore CheZ-GFP localization in cells of this strain. Although our polyclonal CheA antiserum did not visualize the CheAΔ(P1-P2) protein in immunoblots, it must be present at some level for complementation to occur. A protein of the size expected for $CheA_L$(ΔP2) was detected with this antiserum in an extract from strain BC210 (Fig. 9B), but no band was seen at the position expected for $CheA_S$ΔP2.

The inability to detect CheA(ΔP1-P2) and $CheA_S$(ΔP2) with our polyclonal

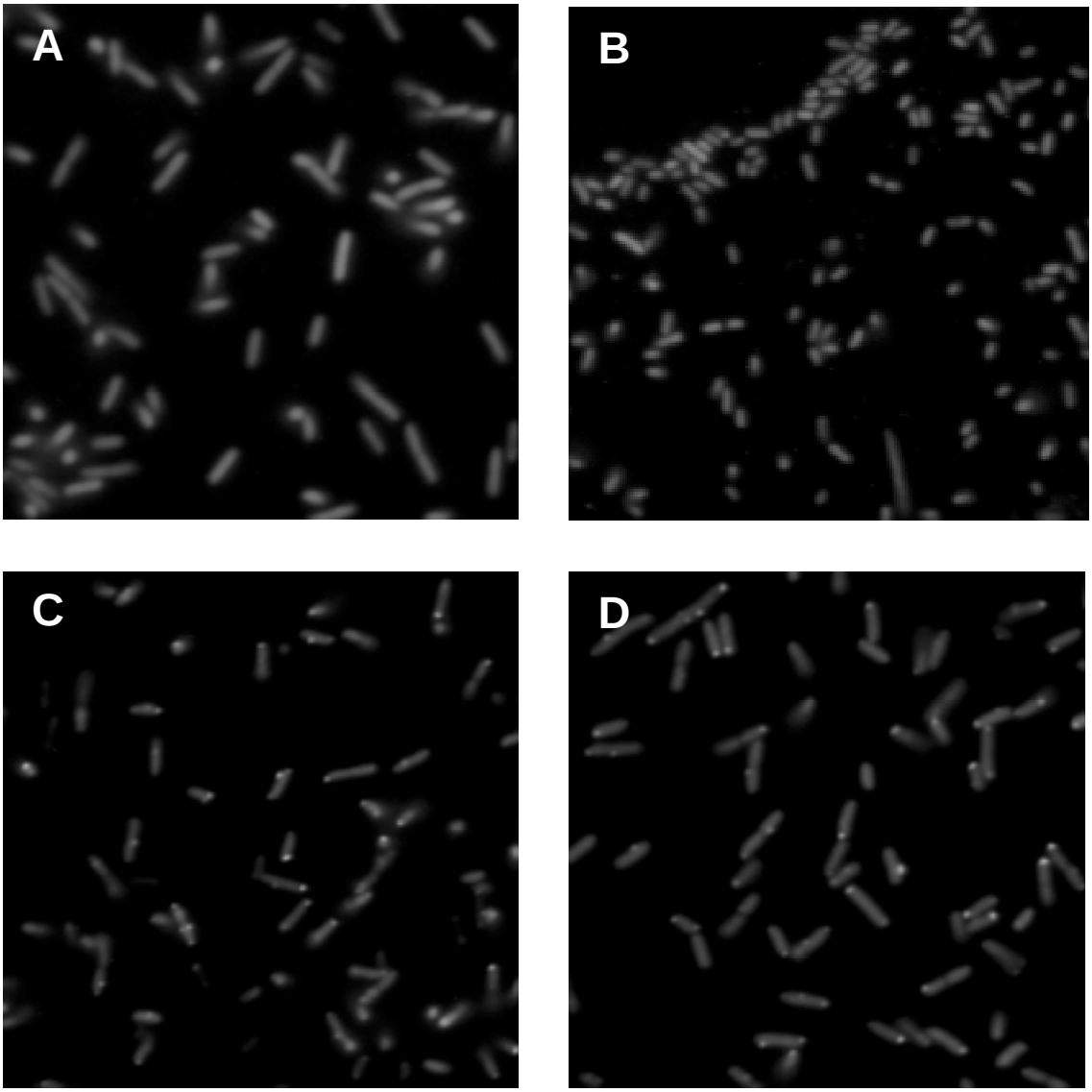


FIG. 10. Localization of CheZ-GFP requires $CheA_S$. Representative fluorescence micrographs of late-exponential-phase cells grown in the presence of 1 mM IPTG. (A) BC206 (*ΔcheA*); (B) BC209 ($CheA_L$-only); (C) BC212 ($CheA_S$-only); (D) BC210 (*cheAΔP2*)

antiserum may represent the absence of epitopes recognized by the antiserum, since 23 of 27 monoclonal antibodies raised against full-length CheA target P1 and P2 (J. S. Parkinson, personal communication). This result suggests that P1 and P2 are the most antigenic portions of CheA. When probed with monoclonal antibody to the CheA P3 domain, the expected products are seen in CheA(ΔP1-P2) and $CheA_S$(ΔP2) strains (data not shown).

**Mutations within a specific region of *cheZ* eliminate polar localization of CheZ-GFP.** To identify which part(s) of CheZ are responsible for localization, we introduced a selection of previously identified *cheZ* missense mutations (13, 16, 81, 82) scattered throughout the gene into plasmid pBJC101. Of these 17 mutations, the ones causing the L90S and F117S substitutions completely eliminated polar localization of CheZ-GFP, and cells expressing these proteins failed to form patches, looking identical to cells of the Δ*cheA* strain BC206 (Fig. 8C). Error-prone PCR mutagenesis (127) generated a mutant CheZ-GFP protein containing the W94R substitution that also did not localize to receptor patches.

A summary of the swarming behavior and localization patterns supported by these mutant proteins is given in Table 2. Note that the T25P, L28P, A87V and A87G mutant proteins showed an intermediate level of patch formation; many cells lacked visible patches, but a significant minority of cells showed essentially normal patterns of CheZ-GFP localization. Except for A87V, which completely eliminated swarming, these substitutions caused partial defects in chemotactic swarm formation. Immunoblot analyses with anti-CheZ antibody indicated that most of the mutant CheZ-GFP proteins

**TABLE 2. Effect of *cheZ* mutations on CheZ-GFP localization and chemotactic swarming.**

| Strain | Localization[a] | Swarm phenotype[b] | Reference |
|---|---|---|---|
| **A. Mutation from random mutagenesis** | | | |
| W94R | - | - | This study |
| **B. Published mutations** | | | |
| T25P | + | + | (81) |
| L28P | + | + | (81) |
| D50G | ++ | + | (81) |
| A65V | ++ | - | (16) |
| M83T | ++ | - | (16) |
| A87G | + | + | (16) |
| A87V | + | - | (16) |
| L90S | - | - | (16) |
| F117S | - | - | (16) |
| F141I | ++ | - | (13) |
| D143G | ++ | - | (16) |
| T145M | ++ | - | (13) |
| I149T | ++ | - | (81) |
| E158G | ++ | + | (81) |
| N182Y | ++ | - | (81) |
| G188E | ++ | - | (16) |
| V205E | ++ | - | (16) |
| **C. Mutations from site-directed mutagenesis of amphipathic helices** | | | |
| W94S | - | - | This study |
| W97S | - | + | This study |
| F98S | - | ++ | This study |
| I102S | ++ | ++ | This study |
| L104S | ++ | ++ | This study |
| A107S | ++ | + | This study |
| L110S | - | - | This study |
| V111S | - | - | This study |
| T114A | - | - | This study |
| L118S | - | - | This study |
| V121S | - | - | This study |

replacement imposed the same Che$^-$ Loc$^-$ phenotype as W94R. Cells expressing the W97S or F98S version of CheZ-GFP had a Che$^+$ Loc$^-$ phenotype, implying that the overall conformation and function of these mutant proteins were not significantly compromised. In the absence of the inducer IPTG, each mutant protein was produced at approximately physiologically normal amounts.

**Proposed CheA$_S$/CheZ interaction sites are conserved in enteric bacteria.** The deduced amino acid sequences corresponding to the predicted helix-turn-helix hairpin of *E. coli* CheZ were compared for the fourteen Gram-negative proteobacteria for which CheZ sequences were available in the Entrez database. Figure 11A presents the alignment of nine of these sequences, selected to avoid redundancy and to represent at least one member of each genus. Residues 95-98 are conserved as $D^D/_E$WF in all of the enteric species, which are the only bacteria known to express CheA$_S$ (12). Non-enteric γ-proteobacteria, including *Vibrio* and *Pseudomonas*, do not display this motif. However, there is substantial sequence conservation at other positions in this region, with the notable exception of CheZ from the two *Xanthomonas* species, which lack the entire region encompassing the apical helix-turn-helix hairpin. When the sequences of CheA from these same species are compared (Fig. 11B), it is clear that sequences corresponding to the putative N-terminus of CheA$_S$ are also conserved in the enteric bacteria.

**A**

```
Enteric species                                    ****
E. coli CheZ (78)          PHQ DQMEKSAKAL TQRWDDWFAD PIDLADAREL VTDTRQFLPDV
S. enterica CheZ (78)      PHQ DAMEKEAKAL TQRWDEWFDN PIELSDAREL VTDTRQFLRDV
E. cloacae CheZ (79)       PHQ DAMEKGAKAL SKRWDEWFEN PIELADAREL VTDTRQYLGDV
Y. pestis CheZ (78)        PRQ NELESSAKAL KIRWDEWFAN PIELSDARSL VTDTREYLAVV

Non-enteric species
V. cholera CheZ (99)       PIA DKLHESLLLI RPEWNGLMNG RIELMHFKSL CHRIDDLLSQV
P. aeruginosa CheZ (78)    PLV NQLGDDSREL HQEWQRFMRR EIDADGFREL AKRIEQFLVRS
P. putida CheZ (112)       PVL NDLASEAKAL STDWQRFMRR EVAAPEFRDL VKRVDSFLTHS
R. solanacearum CheZ (86)  PVQ DQLEGEAEEL VTRWQSWMDR QLGDDEIRSL VEITNGFLRSV
X. campestri CheZ (106)    LLA NQLR------ -----D--G- ---------- -----GLNQDQ
```

**B**

```
Enteric species                                        ↓    ↓   ↓
E. coli CheA (98)          M QEQLDAYKQS QEPDAASFDY ICQALRQLAL EAKGETPSAV TRLSV
S. enterica CheA (98)      M QEQLDAYKNS EEPDAASFEY ICNALRQLAL EAKGETTPAV VETAA
Y. pestis CheA (98)        M QEQLDAYKTS QEPHSESFEY ICQALRQLAL DALDQPTTED QPTTE

Non-enteric species
V. cholera CheA (99)       V NEQFRAVQER EPLQPADPEL LDELHRLSKP --------AS EDEDE
P. aeruginosa CheA (99)    V NAMFDQVREQ SEPTPATPEL LAALARLAEP EGAEPAEPVQ APPAA
P. putida CheA (99)        V NSMFGQVRER ADVTPATPQL LAALSRLAEP ---GGAEAAE APAPA
R. solanacearum CheA (98)  L KSQLEAYRHE HPIDTATLEY MVAKLNSLTA EDGAPATAAA PAAAA
X. campestri CheA (99)     I HALVETAADP SHADPAALAA EAEPLLAQLQ TYLQGSVCGA TVSDA
```

FIG. 11. Alignment of amino acid sequences of the CheZ apical loop and the C-terminal portion of the P1 domain of CheA. (A) Alignment of CheZ sequences from representatives of a number of bacterial genera for which a putative *cheZ* gene has been sequenced. Asterisks indicated the conserved $D^D/_E$WF motif at residues 95-98 of E. coli CheZ. The number in paraentheses indicates the residue number for the first position in the sequence shown. Residues highlighted in dark greyare identical in all sequences except X. campestri. Residues highlighted in light gray are identical within the enteric or non-enteric groups, again except X. campestri. Residues in bold-face type type indicate positions at which residues are chemically conserved. The sequences listed as Salmonella enterica is for serovar Typhimurium. In addition to the species and serovars shown, comparisons were made with the CheZ sequences from Salmonella enterica serovar Typhi, Yersinia enterocolitica, Vibrio parahaemolyticus, Pseudomonas syringae, and Xanthomonas axonopodis. Those sequences did not differ significantly from their congeners. (B) Alignment of sequences from the C-terminal portion of the P1 domain for the same species whose CheZ sequences are shown in (A). Residues shown correspond to the P1 residues in E. coli CheAS. Arrows indicate conserved aliphatic residues exposed in CheAS.

**Discussion**

The results presented here establish that CheZ localizes to the receptor patch only when $CheA_S$ is present. The two residues of CheZ most clearly implicated in interaction with $CheA_S$ are Phe-97 and Trp-98. These two aromatic residues, especially Phe-97, are solvent exposed in the apical hairpin loop of the CheZ crystal structure (Fig. 12A) and might be expected have an energetically favorable interaction with a hydrophobic partner. Mutations causing a $Che^-$ $Loc^-$ phenotype replace hydrophobic residues at the interhelix packing surface of the hairpin (Fig. 12A) or residues located at the subunit interface of the CheZ homodimer (125). These substitutions may destabilize the hairpin or interfere with CheZ dimerization, respectively.

The N-terminal sequence of $CheA_S$ corresponds to the C-terminal portion of the P1 domain. The crystal structure of the *Salmonella* P1 domain (15) is shown in Figure 12B. It comprises 5 α-helices, with Met-98, the first residue of $CheA_S$, residing in the middle of the fourth helix, which extends to Lys-106. Residues Ala-113 through Ala-130 constitute the fifth helix. Based on this structure, the N-terminus of $CheA_S$ is predicted to be an amphipathic helix of eight residues followed by a turn and an amphipathic helix of eighteen residues. In $CheA_S$, the hydrophobic residues Leu-123 and Leu-126 should be exposed to solvent and available to interact with CheZ. Furthermore, isothermal calorimetry (R. M. Weis, personal communication) and surface plasmon resonance (C. O'Connor and P. Matsumura, personal communication) data indicate that CheZ binds to N-terminal fragments of $CheA_S$ consisting exclusively of the C-terminal remnant of P1

FIG. 12. Stereo views of the crystal structure for the apical loop region of CheZ and the P1 domain of CheA. (A) Apical loop of CheZ (125) Residues 83-121 are shown. Substitutions at residues colored in blue displayed a chemotaxis (-), localization (+) phenotype. Substitutions at residues colored in red displayed a chemotaxis (-), localization (_) phenotype. Substitutions at residues colored in yellow displayed a chemotaxis (+), localization (-) phenotype. Green residues were not affected (chemotaxis (+), localization (+)) by Ser substitution. (B) CheA P1 domain (69) Residues in dark blue are those found in $CheA_S$. Residues in cyan form hydrophobic interactions with residues in blue in full length P1. The site of phosphorylation (His-48) is indicated in red. (C) Residues of CheA P1 domain found in $CheA_S$. Residues indicated in yellow are conserved in enteric species but not in non-enteric species. Those indicated in gray are chemically conserved in the eneteric species.

A

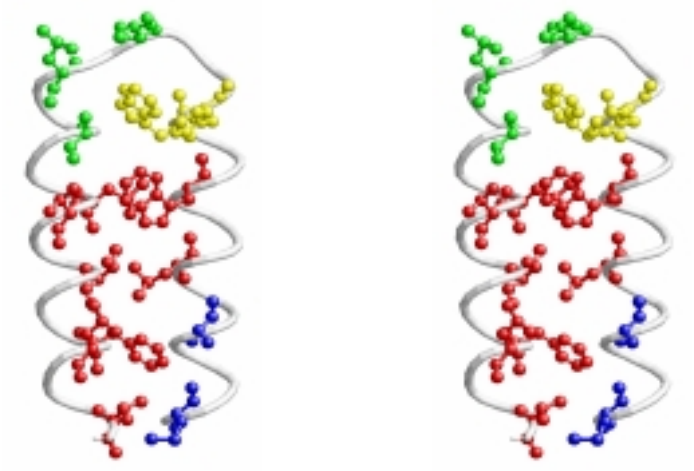

B

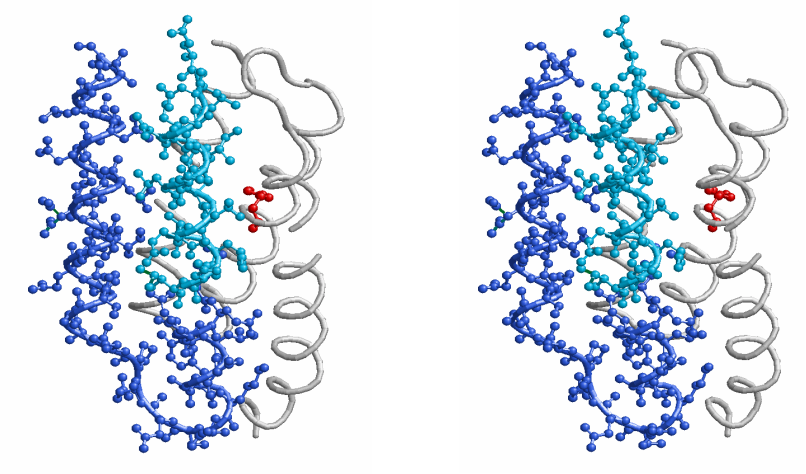

C

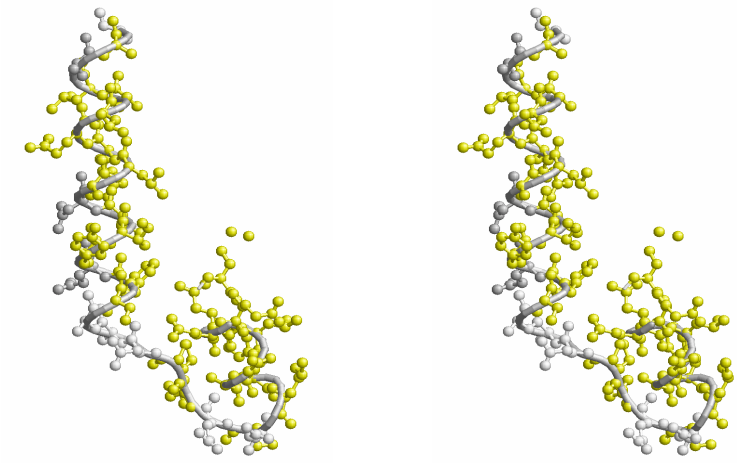

and a portion of the linker between the P1 and P2 domains.

Absence of $CheA_S$ does not diminish chemotaxis in the assays that have been employed (79). However, the specificity of the $CheA_S$/CheZ interaction and the co-occurrence of $CheA_S$ and CheZ in the enteric bacteria (64) suggest that recruitment of CheZ to the receptor patch may be important. Critical residues in the apical hairpin loop of CheZ from enteric bacteria are conserved (Fig. 11A), and sequences of the C-terminal region of the P1 domain corresponding to the N-terminus of $CheA_S$ are also conserved (Fig. 11B). Although these similarities may be coincidental or maintained by structural constraints unrelated to the CheZ/$CheA_S$ interaction, an equally plausible scenario is that localization of CheZ to the receptor patch confers a significant selective advantage to enteric bacteria under some environmental conditions they encounter.

# CHAPTER III

# CONSERVED HYDROPHOBIC RESIDUES OF CheA-SHORT ARE REQUIRED FOR CheZ LOCALIZATION AND NORMAL CHEMOTAXIS

## Introduction

The CheZ phosphatase of *Escherichia coli* catalyzes the rapid turnover of the phophorylated form of the chemotaxis response regulator CheY (37). Along with most of the component of the chemotaxis signaling pathway, CheZ is found in localized to clusters found primarily at the cell poles (22, 57, 99). The clusters are thought to be large arrays composed of chemoreceptors, CheA, and CheW (31, 89), with the other chemotaxis proteins recruited there by their interaction with CheA or chemoreceptors (6, 99).

The structure of CheZ has been solved in complex with a $BeF_3^-$ derivative of CheY (125). The CheZ dimer is composed primarily of an extended four-helix bundle composed of two helices from each monomer. An N-terminal helix of approximately 30 residues precedes the core, and an unresolved region following the core is believed to form a flexible linker that connects the core region to a short C-terminal CheY-binding helix. The catalytic site for dephosporylation of CheY is located about halfway along the four-helix bundle. Residue substitutions near the helical turn at the distal tip of the four-helix bundle disrupted localization of a CheZ-GFP fusion protein to the receptor patch and the F98S substitution specifically did so without noticeable effects on

chemotaxis in soft agar plates. Substitutions in other regions of the protein had no effect on localization of the fusion protein (22).

CheZ localizes to the receptor patches through an interaction with $CheA_S$, an N-terminally truncated form of CheA. $CheA_S$, but not full length $CheA_L$, is precipitated from cell lysates by anti-CheZ antibody, and formation of a CheZ-$CheA_S$ complex could be demonstrated *in vitro* (117). Using *E. coli* strains expressing various internally deleted CheA proteins demonstrated that $CheA_S$ is required to localize CheZ to the receptor patch (22). Based on the structure of the CheA P1 domain (69), hydrophobic residues on the fifth helix of CheA P1 should be exposed in $CheA_S$ and could serve as binding site for CheZ (22).

In this study, the localization domain of CheZ was characterized using deletions of CheZ-GFP to identify the minimal fragment of CheZ required for localization to the receptor patch. It was also demonstrated that hydrophobic residues of $CheA_S$ predicted to be required for CheZ localization are required for effective localization of CheZ-GFP. However, mutations at these residues and the previously identified F98S mutation of CheZ behave differently in measurement of swimming behavior in single cells, indicating that these sites are not likely to directly interact with CheZ-GFP. Deletions of CheZ-GFP were used to explore the roles of the N-terminal and C-terminal segments of the protein in regulation of phosphatase activity.

## Materials and methods

**Strains and plasmids.** The strains and plasmids used in this investigation are shown

in Table 3.

**Media and growth conditions.** Cells were grown with shaking at 30$^{o}$C in tryptone broth (TB) (66) following dilution from overnight cultures. Ampicilin was added to the media at a final concentration of 50 μg/ml for growth of cells harboring pBJC104, pBJC100, or derivatives. Chloramphenicol was added to the media at a final concentration of 30μg/mL for cells harboring pBJC200 or their derivatives. IPTG was added to the growth media at the concentrations listed to induce expression of CheZ-GFP. Sodium salicylate was added to the media at a final concentration of 100 μM to induce expression of CheA from pBJC200. CheZ-GFP encoded by a chromosomal gene in single copy was induced by addition of 1mM IPTG to the medium.

**Construction of plasmids.** The *cheA* gene was amplified from the chromosome of RP437 using an upstream primer homologous to the region upstream of the *cheA* ribosome-binding site and a downstream primer homologous to the 3' end of the *cheA* coding sequence. Each primer encoded a BamHI restriction site 5' of the *cheA* sequence. The *cheA* gene was amplified using standard PCR and PFU Turbo polymerase (Stratagene). The PCR product was gel-purified, digested with BamH for 2 h at 37º C and inserted into the BamHI site of pLC112 using T4 DNA ligase (NEB). The products were introduced into strain RP9535 by calcium-chloride transformation, and chloramphenicol resistant clones were screened for restoration of swarming in soft-agar motility plates containing sodium salicylate. Insertion and orientation of the *cheA* gene was confirmed by sequencing. Plasmids pBJC140 and pBJC141 were constructed

**TABLE 3. Strains and plasmids, chapter III.**

| Strain | Genotype | Comments | Reference or Source |
|---|---|---|---|
| RP437 | *thr*(Am)*1, leuB6, his-4, metF*(Am)*159, eda-50, rpsL1356, thi-1, ara-14, mtl-1, xyl-5, tonA31, tsx-78, lacY1, F⁻* | | (75) |
| RP1616 | RP437 Δ*cheZ*6725 | | J. S. Parkinson |
| RP9535 | *RP437* ΔcheA*1643*, eda$^+$ | | (68) |
| BC206 | RP9535 Δ(λ*att-lom*)::*bla lacI$^q$* p*tac-cheZ-gfp* | pBJC104 into RP9535 via λInCh1 | (22) |
| **Plasmids** | **Relevant Genotype** | **Comments** | **Reference or Source** |
| pLC112 | | | (3) |
| pKG110 | | | (3) |
| pBJC100 | | | (22) |
| pBJC104 | p*tac cheZ-gfp, amp*$^r$ | *cheZ-gfp* in pCJ30 | (22) |
| pBJC120 | p*tac cheZ*$_{31-214}$*-gfp, amp*$^r$ | | This study |
| pBJC121 | p*tac cheZ*$_{1-200}$*-gfp, amp*$^r$ | | This study |
| pBJC122 | p*tac cheZ*$_{1-166}$*-gfp, amp*$^r$ | | This study |
| pBJC123 | p*tac cheZ*$_{31-166}$*-gfp, amp*$^r$ | | This study |
| pBJC124 | p*tac cheZ*$_{50-152}$*-gfp, amp*$^r$ | | This study |
| pBJC125 | p*tac cheZ*$_{70-133}$*-gfp, amp*$^r$ | | This study |
| pBJC126 | p*tac cheZ*$_{81-121}$*-gfp, amp*$^r$ | | This study |
| pBJC200 | p*nahG cheA, cm*$^r$ | *cheA* in pLC112 | This study |
| pPA113 | p*nahG cheA, cm*$^r$ | *cheA* in pKG110 | J.S. Parkinson |
| pOC407 | p*nahG cheA*$^{L126A}$*, cm*$^r$ | *cheA*$^{L126A}$ in pKG110 | (71) |
| pBJC140 | p*nahG cheZ, cm*$^r$ | *cheZ* in pKG110 | This study |
| pBJC141 | p*nahG cheZ*$^{F98S}$*, cm*$^r$ | *cheZ*$^{F98S}$ in pKG110 | This study |

by inserting the ~700 base pair BamHI-HindIII fragment of pBJC100 and pBJC106, respectively, into the BamHI and HindIII sites of pKG110. Correct insertion was confirmed by sequencing.

**Construction of CheZ-GFP deletions**. Deletions of the *cheZ-gfp* gene on plasmid pBJC104 were constructed by oligonucleotide-directed mutagenesis using the QuickChange mutagenesis method (Stratagene), with modifications. Primer pairs used were homologous to the upstream and downstream ends of the deletion site. Primers were phosphorylated with T4 polynucleotide kinase (NEB), amplification was carried out using PFU Turbo, and DpnI was obtained from New England Biolabs. The amplification products were precipitated and ligated overnight at room temperature using T4 DNA ligase (NEB). The ligated products were introduced into strain RP1616 by calcium-chloride transformation and ampicillin-resistant transformants were identified by sequencing.

**Oligonucleotide-directed mutagenesis.** Point mutations of *cheZ-gfp* in pBJC104, *cheZ* in pBJC100, or *cheA* in pBJC200 were created by oligonucleotide-directed mutagenesis using the QuickChange protocol (Stratagene) with modifications. Primers were phosphorylated using T4 polynucleotide kinase (NEB) and template DNA amplified by PCR using 2x PFU Turbo Master Mix (Stratagene). Amplified products were treated with DpnI (NEB) for 2 h at 37º C to remove template DNA then precipitated. DNA was resuspended in appropriate buffer and ligated overnight at room temperature using T4 DNA ligase (NEB). The ligated products were introduced into strain RP1616 for *cheZ-gfp* mutations or strain RP9535 for *cheA* mutations by calcium-

chloride transformation. DNA from antibiotic-resistant transformants was screened by sequencing to identify mutagenized clones and DNA from positive clones was used to transform appropriate deletion strains of *E. coli* for phenotypic analysis.

**Swarm assays.** Chemotaxis was assayed in semi-soft TB swarm plates containing 0.35 g/L Difco BactoAgar. Swarm plates were inoculated from single colonies grown overnight on Luria broth plates (66) and incubated for 8 to 10 h at 30°C. Swarm diameters were measured and compared to those of swarms formed by wild-type and chemotaxis-deficient control strains on the same plate. IPTG was added to the plates at the concentrations indicated in each experiment.

**Observation of swimming cells.** Five mL cultures of cells were grown with shaking in TB at 30º C as above. Approximately 10 μL of cells in late exponential phase ($OD_{595}$ ~0.8 - 1.0) were placed on slides inside vacuum grease rings and sealed with a coverslip. Cells were observed at 400X magnification using phase contrast microscopy on an Olympus BH-2 microscope. Five to ten fields of cells were observed for approximately 30 sec each and the smooth swimming and tumbling behavior was qualitatively compared to wild-type and smooth- or tumble-biased mutant cells. At least two independent cultures of each strain were examined.

**Fluorescence microscopy.** Cells were grown overnight at 32°C in TB with appropriate antibiotics, diluted 1:50 into 10 ml of the same medium containing arabinose or IPTG, as needed, and incubated with shaking at 32°C. Cells from 1 ml of culture were harvested at an $OD_{590nm}$ of 0.7-0.8 by centrifugation, washed once with tethering buffer (100 mM NaCl, 10 mM KPO4 pH 7.0, 0.4% (v/v) lactic acid, 20 μM methionine,

10 μM EDTA, 22.5 μg/ml chloramphenicol), and resuspended in 1 ml of tethering buffer. The cells from 100 μL aliquots were allowed to settle for 5 min onto cover slips coated with 0.1% polylysine (Sigma). The affixed cells were then washed twice with 1 mL tethering buffer. The cover slips were placed on slides and sealed with clear enamel, then viewed at 1000X magnification using a Olympus IX inverted microscope. For epifluorescent microscopy, the excitation filter wavelength was 484 nm and the emission wavelength was set at 510-530 nm. Images were captured using a Hamamatsu Orca ER CCD camera and the Simple PCI software package. Images were processed using Adobe Photoshop to enhance of brightness and contrast.

**Computer-assisted motion analysis.** Cells were grown to mid-exponential phase (OD600 ~0.5) after which 4 μM or 0.33 μM sodium salicylate was added to induce CheA or CheZ synthesis, respectively. Cells were grown in the presence of inducer for an additional 1.5 h, then diluted 1:4 with isotropic media prepared by centrifugation of a sample of the culture being assayed. The rate of change of direction (RCD) was measured using a computer-assisted motion analysis system (MotionAnalysis Inc.) as previously described (4, 78).

## Results

**Localization determinants of CheZ-GFP are restricted to residues 70-134 of CheZ.** Certain residue substitutions near the hairpin turn at the apex of the elongated four helix bundle of CheZ (125) specifically abolish localization to the polar receptor patch, whereas substitutions in other areas of the protein do not affect CheZ-GFP

localization (22). To determine if the region identified by mutagenesis is sufficient for localization of CheZ to the polar receptor patch, CheZ proteins with increasingly large deletions from the amino-terminal and carboxyl-terminal ends were fused to GFP. Each fusion protein was expressed from a plasmid using IPTG at a concentration (10 μM) that allows normal swarming when used to express full length CheZ-GFP. The pattern of localization of each was observed by fluorescence microscopy. The results are presented in Figure 13. A region of 64 residues (70-133) around the hairpin turn (residues 100-104) is required for normal localization of CheZ-GFP. A smaller protein of approximately 41 residues (81-121) is not localized (Fig. 13 A). Residues 70-83 and 121-134 are at the top of the four-helix bundle that forms the core of the CheZ structure and may provide critical contacts required for dimerization of CheZ dimer (Fig 13 B-C). These data indicate that the localization domain is restricted to the area previously identified by mutagenesis.

**The amino-terminal helix of CheZ is a negative regulatory element.** A number of point mutations isolated as gain-of-function mutants (81) affect residues at the amino-terminal helix of CheZ (125). Residues 2-30 of CheZ were deleted from the version of CheZ-GFP encoded by plasmid pBJC120, and the effects of this deletion on chemotaxis were measured in motility agar (Figure 14) and by observing swimming cells in liquid media (Table 4). The swarm diameter for cells expressing full-length CheZ GFP was maximal at 10 μM IPTG and became smaller as the inducer concentration increased. Complementation of Δ*cheZ* with pBJC120 expressing $CheZ_{31-214}$-GFP produced smaller

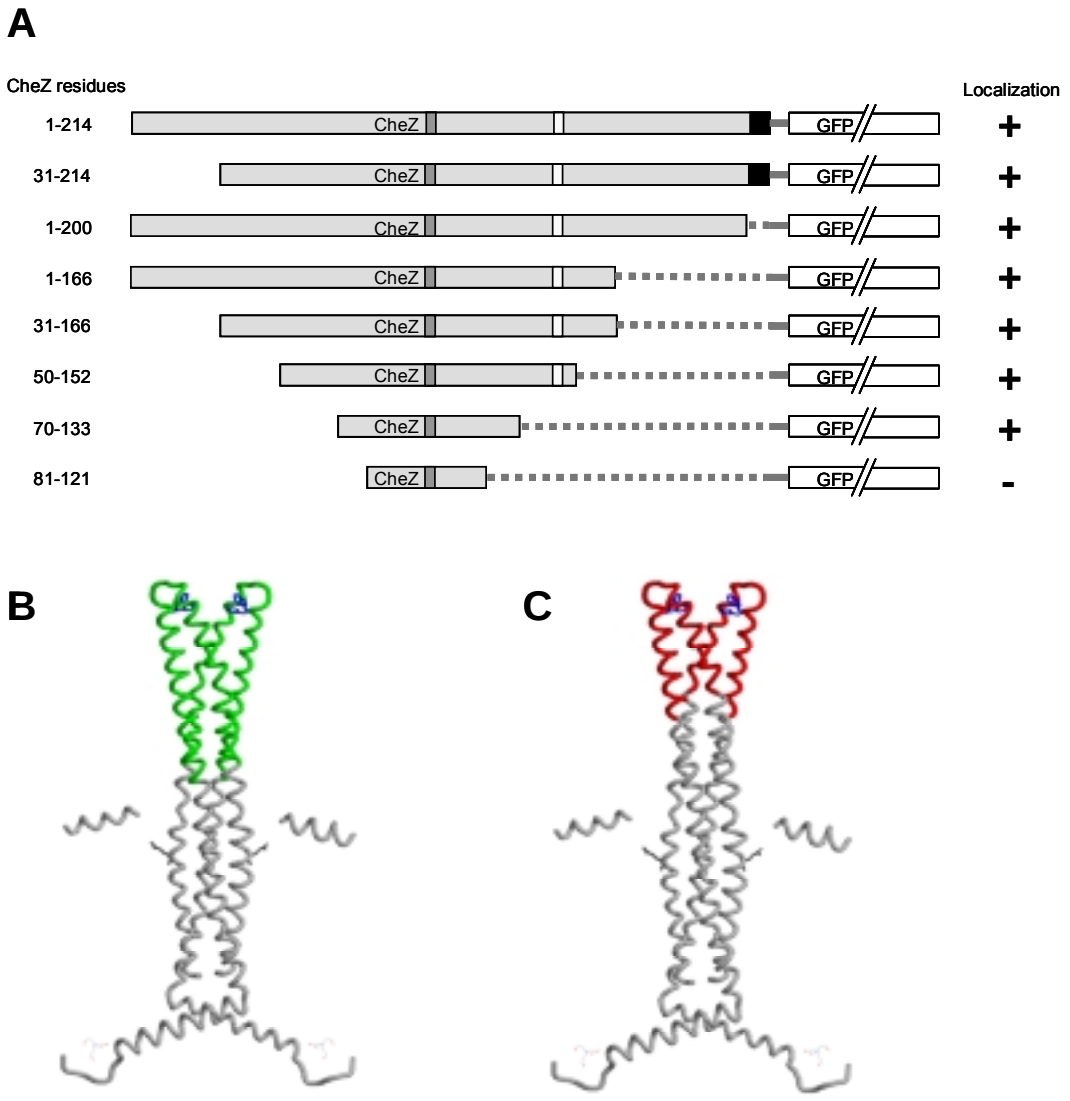


FIG. 13. Determinants of CheZ localization lie entirely within hairpin regionof CheZ. (A) Systematic deletion of CheZ-GFP showing the extent of CheZ coding sequence and localization phenotype. Localization designated as + was indistinguishable from that of full-length CheZ-GFP. The dark grey box denotes site of non-localizing mutations, and the white box denotes phosphatase active site residues. The black box indicates the CheY-binding peptide. (B-C) Backbone structure of the CheZ dimer showing the minimal localization fragment (B, green) and a non-localizing fragment (C, red). Side chain atoms of Trp-97 and Phe-98 are shown in blue and those of Gln-147 are shown in grey.

swarm rings at 10 μM IPTG, and the swarm diameter decreased with increasing IPTG concentrations (Fig. 14).

The swimming behavior of a strain RP1616 complemented with either pBJC104 or pBJC120 was observed by dark field microscopy. Cells were visually compared to wild-type cells, a smooth-swimming mutant, or a tumbly mutant and their smooth-tumble bias estimated qualitatively. Cells expressing full-length CheZ-GFP (pBJC104) were tumbly in the absence of inducer, exhibited mix of running and tumbling at 10 μM IPTG, and became progressively more smooth swimming as the inducer concentration, and presumably the CheZ levels in the cell, increased. Cells containing pBJC120 were smooth biased and showed limited tumbling even in the absence of inducer, then became completely smooth swimming with increasing IPTG (Table 4). The level of $CheZ_{31-214}$-GFP produced at 10 μM IPTG appeared identical to that of full length CheZ-GFP (data not shown). These data indicate that the amino-terminal helix plays a negative regulatory role in controlling the activity of CheZ.

**The CheY-binding peptide is not strictly required for CheZ activity.** The structure of the CheZ-CheY co-crystal indicated that two regions of CheZ interacted with CheY, the catalytic site in the central core and an alpha-helix at the extreme carboxyl-terminus (125). Plasmid pBJC121 expresses CheZ-GFP with the CheY-binding peptide (residues 201-214) deleted, and pBJC122 expresses a CheZ-GFP with the CheY-binding peptide and proposed flexible linker (residues 167-214) deleted. These proteins were expressed in strain RP1616, and the effects on chemotaxis were measured in soft-agar motility plates (Fig. 14) and by observing free-swimming cells

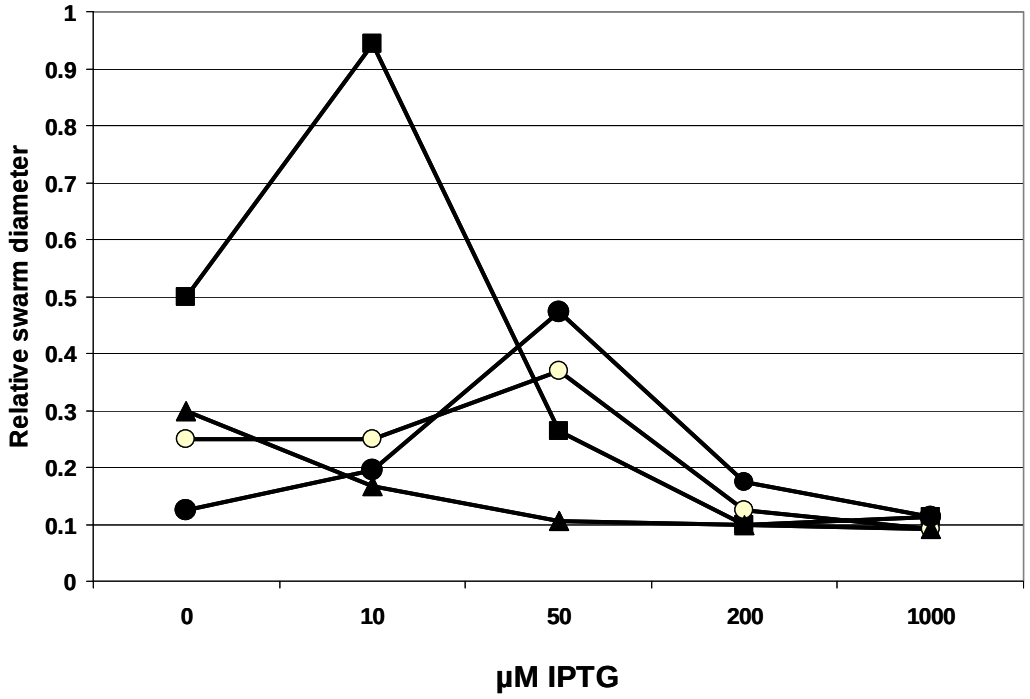


FIG. 14. Effects of CheZ-GFP deletions on chemotactic swarm . Strain RP16161 (Δ*cheZ*) carrying plasmids expressing full-length CheZ-GFP (■, pBJC104), $CheZ_{31\text{-}214}$-GFP (▲, pBJC120), $CheZ_{1\text{-}200}$-GFP (●, pBJC121), and $CheZ_{1\text{-}166}$-GFP (○, pBJC122) were inoculated into soft agar motility plates containing the indicated concentrations of IPTG and incubated at 30º C. Swarm diameter was expressed as the ratio of the diameter of reference swarms of wild-type E. coli strain RP437, which was not affected by IPTG.

**TABLE 4. Swimming behavior of cells expressing CheZ-GFP deletion mutants.**

| Plasmid | CheZ residues | IPTG concentration (uM) 0 | 10 | 50 | 200 | 1000 |
|---|---|---|---|---|---|---|
| pBJC104 | 1-214 | Tumble bias | Smooth / Tumble | Smooth | Smooth | Smooth |
| pBJC120 | 31-214 | Smooth Bias | Smooth | Smooth | Smooth | Smooth |
| pBJC 121 | 1-200 | Tumble | Tumble | Tumble Bias | Smooth / Tumble | Smooth / Tumble |
| pBJC122 | 1-166 | Tumble | Tumble Bias | Smooth / Tumble | Smooth | Smooth |

Tumble - cells exhibit continuous tumbling.
Smooth – cells exhibit continuous smooth swimming.
Smooth / Tumble – cells exhibit periods of smooth swimming with periodic tumbling.
Smooth or Tumble Bias – cells exhibit primarily smooth or tumbling behavior with infrequent periods of tumbling or smooth-swimming behavior, respectively.

(Table 4), as above. As expected, $CheZ^{1-200}$-GFP and $CheZ_1^{-166}$-GFP produced significantly smaller swarm diameter than wild type CheZ-GFP at 10 μM IPTG and were also tumble-biased in their swimming behavior. However, at higher concentrations of IPTG, the swarm diameter increased, and some smooth swimming was observed. These data indicate that the effects of the deletion can be overcome by increasing the intracellular protein level and that binding to the carboxyl-terminal helix is not required for dephosphorylation of CheY~P.

**Conserved charged residues are not required for CheZ-GFP localization.** Alignment of CheZ sequences from a number of enteric and non-enteric bacterial species revealed several charged residues near the hairpin turn that are conserved in the enteric bacteria but not in non-enteric species (Fig. 15 A) in the immediate vicinity of Trp-97 and Phe-98. Since the enterics are the only bacteria known to produce $CheA_S$ (64), these residues could be involved in binding CheZ to $CheA_S$ at the receptor patch. Asp residues at positions 95, 96, and 100 of *E. coli* CheZ were mutagenized to Ala in plasmid pBJC104 and the ability of the mutant CheZ-GFP proteins to localize to the receptor patch was examined. In each case the pattern of localization was indistinguishable from that of wild-type CheZ-GFP (data not shown). The D95A/D96A double mutant was also constructed, and it also showed wild-type localization.

Examination of the CheZ structure shows that Arg-108 of *E. coli* CheZ is exposed and in close proximity to Trp-97 and Phe-98 (Fig 15 B). Arg or Lys is conserved at this position in the CheZ protein from many species. However, R108A replacement had no affect on localization of CheZ-GFP to the receptor patch (data not shown).

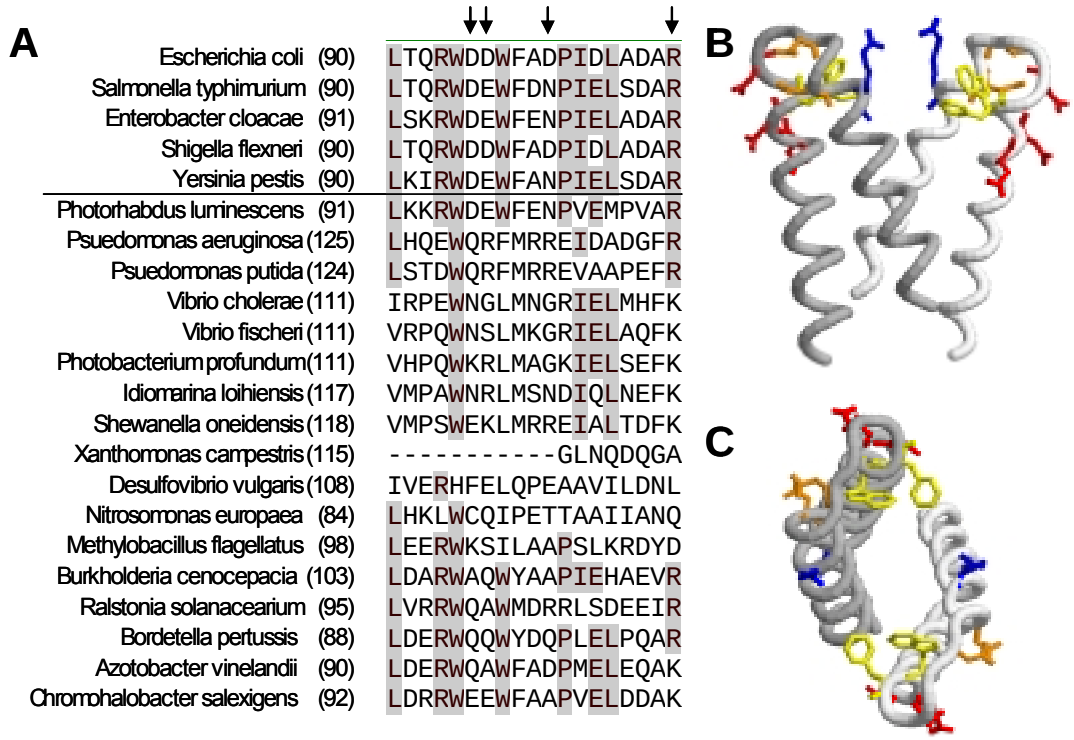


FIG. 15. Charged residues near site of non-localizing CheZ mutations are conserved. (A) Alignment of CheZ sequences showing the region around the site of non-localizing mutations of *E. coli* CheZ. Sequences above the line are enteric species. Arrows indicate charged residues substituted with Ala. (B-C) Structure of CheZ localization domain showing positions of mutated Asp (red) and Arg (blue) residues. Try-97 and Phe-98 are shown in yellow. Additional conserved Asp residues (positions 103 and 106 of *E. coli* CheZ) are shown in orange. (C) Top down view of same region.

**Hydrophobic residues in the $CheA_S$ P1 domain are required for localization of CheZ-GFP.** The crystal structure of the isolated CheA P1 domain shows that it comprises a four-helix bundle plus on additional amphipathic helix that lies adjacent and anti-parallel to the fourth helix. The starting methionine of $CheA_S$ is located near the carboxyl-terminal end of the fourth helix, leaving the hydrophobic face of helix five exposed. This face is a good candidate for interaction with CheZ. The aliphatic and aromatic residues of helix five were substituted to Ala or Ser by oligonucleotide-directed mutagenesis of the *cheA* gene on plasmid pBJC200. The correctly mutagenized plasmids were identified by sequencing and introduced into strain BC206, a Δ*cheA* strain that expresses CheZ-GFP from the *λatt* chromosomal locus. Cells were grown to late-exponential phase in TB broth with 100 μM sodium salicylate present to induce CheA expression and 1mM IPTG present to induce CheZ-GFP expression. Fluorescent images of cells expressing different CheA proteins were captured digitally, and the effects of each mutation quantified by counting the number of cells with one, two, or three or more receptor patches (Fig. 16). Expression of wild-type CheA enabled receptor patches to be visualized in approximately 75-80% of the cells. The L123A, L123S, and L126A (Fig. 17 C) substitutions dramatically reduced CheZ-GFP localization, with receptor patches visible in less than 20% of the cells. Substitution of Ser for Ile-119 produced moderate effects, as did the Y118S and R124E replacements. However, CheZ-GFP with Ala substitutions at these two positions resulted in wild-type localization. Substitutions at Phe-116 or Leu-128 also had no significant effect on CheZ-GFP localization. The amount of each mutant CheA protein produced, as

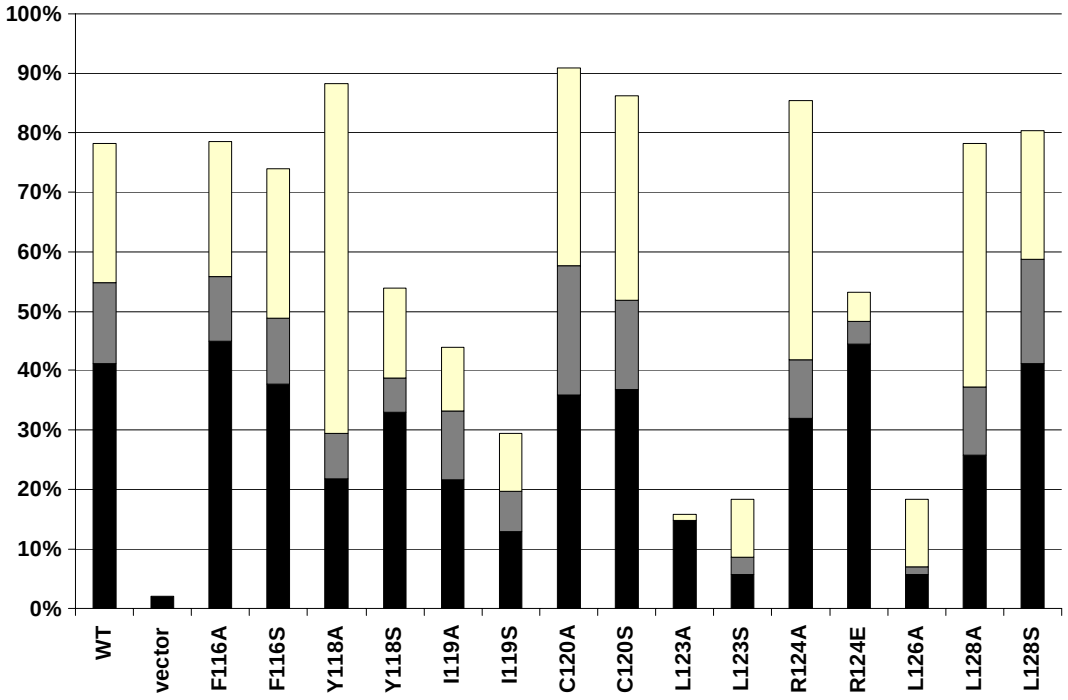


FIG. 16. Hydrophobic residues in the fifth helix of the CheA P1 domain are required for effective localization of CheZ-GFP. RP 9353 cells (Δ*cheA*) were transformed with derivatives of pBJC200 expressing various residue-substituted forms of CheA. The ability of each CheA species to mediate localization of CheZ-GFP to the receptor patch was quantified by determining the percentage of cells with one (black), two (gray), or more (white) visible receptor patches. Substitutions at positions 119, 123, and 126, which lie on the same face of the amphipathic fifth helix, severely inhibited localization of CheZ-GFP to receptor patches.

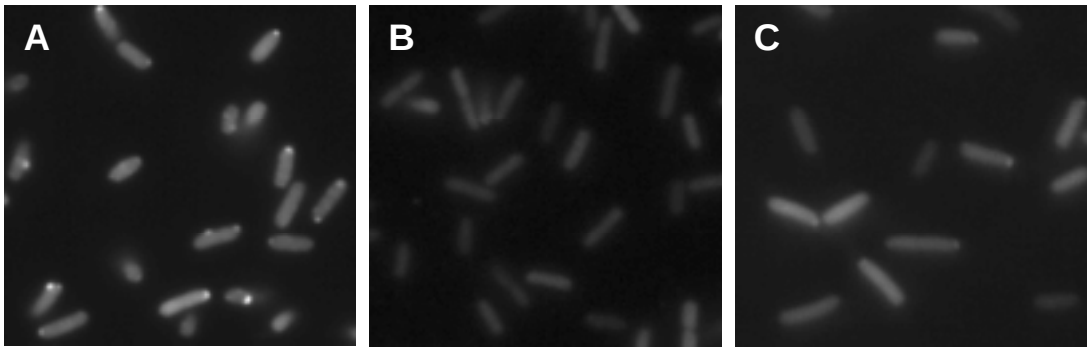


FIG. 16. Fluorescent micrographs of *E. coli* cells expressing different *cheA* alleles. RP9535 cells transformed with (A) pBJC200 expressing wild type CheA, (B) the pLC112 vector control, and (C) a pBJC200 derivative expressing $CheA_{L126A}$. Cells were grown with 100 μM sodium salicylate to induce CheA expression and 1 mM IPTG to induce CheZ-GFP expression. 1000X magnification

determined by SDS-PAGE and western analysis using anti-CheA antibody, was similar for each mutant CheA protein as was the ratio of $CheA_L$ to $CheA_S$ (data not shown).

**Cells expressing a form of CheA defective for CheZ-GFP localization are tumble biased.** Both the F98S substitution in CheZ and the L126A substitution in CheA block efficient localization of CheZ-GFP to receptor patches. However, neither of these mutations affects swarming in motility agar. Recent FRET studies have indicated that CheZ F98S alters the intracellular distribution of CheY~P (113), which could affect chemotaxis. In order to measure the effects of these mutations more sensitively, the swimming behavior of individual cells was monitored using computer-assisted motion analysis, which measures the rate of change of direction (RCD) of individual swimming cells (78). Cells were grown to mid-exponential phase ($OD_{600}$ ~ 0.5) followed by 1.5 h of additional growth in the presence of inducer. Cells were then diluted three-fold with isotrophic media and RCD values calculated. Under these conditions, RP 9535 (Δ*cheA*) cells complemented with $cheA^+$ behaved like the wild-type strain RP437. RP9535 cells transformed with the vector control were smooth swimming, as expected, having a lower RCD value than wild-type cells. The RCD value of RP9535 cells complemented with $cheA_{L126A}$ was considerably higher than it was when complemented with wild-type *cheA* (Fig. 18 A). It should be noted that $CheA^{L126A}$ appears to have kinase activity and mediate responses to attractant stimuli very much like wild type CheA (71). Strain RP1616 (Δ*cheZ*) was strongly tumble biased and had very high RCD values. Complementation of RP1616 with $cheZ^+$ restored smooth swimming. Unlike the non-localizing *cheA* allele, RP1616 cells complemented with $cheZ^{F98S}$ were

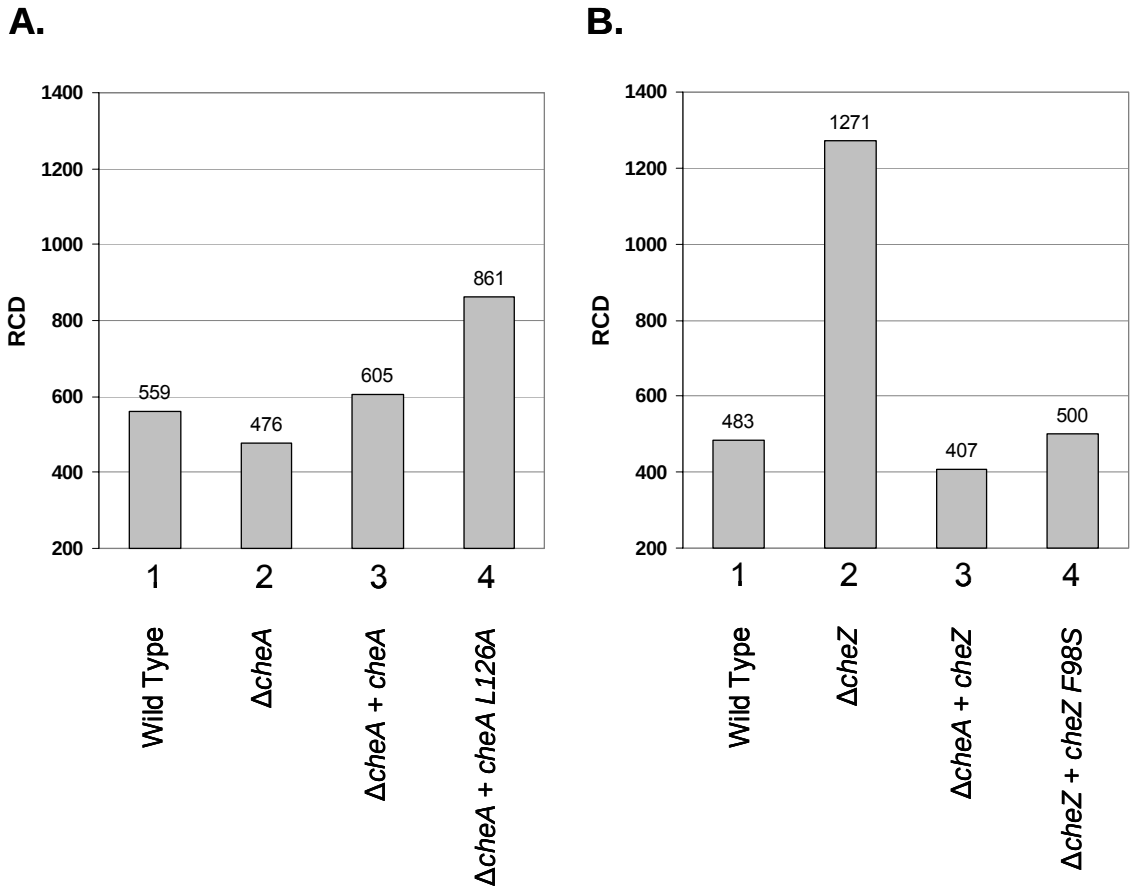


FIG. 18. Residue substitutions in CheA that reduce localization of CheZ-GFP cause a tumble bias. The rate of change of direction (RCD) of swimming cells was measured. (A) Lane 1, strain RP437; Lane 2, strain RP9535 (*ΔcheA*); Lane 3, RP9535 + pPA113; Lane 4, RP9535 + pOC407. (B) Lane 1, RP437; Lane 2, strain RP1616 (*ΔcheZ)*; Lane 3, RP1616 + pBJC140; Lane 4, RP1616 + pBJC141.

essentially identical to cells complemented with wild-type *cheZ* (Fig. 18 B). These data indicate that although these two mutations both cause deficiencies in localization of CheZ to the receptor patch, they do not have the same effect on swimming behavior.

**Discussion**

The initial screen for *cheZ* mutations that disrupt localization of CheZ-GFP to the polar receptor patch identified residue substitutions between 90 and 121 of CheZ that abolish localization of CheZ to polar receptor patches. The majority of those substitutions also abolish chemotaxis, but the W97S and F98S replacements prevent localization while having minimal impact on chemotactic ability. Point mutations targeting other regions of the protein did not abolish localization of CheZ-GFP, although Pro substitutions near the N-terminus did decrease localization but also decreased protein levels (22).

To ensure that residues required for localization in other parts of the protein was not missed by the scan using point mutations, a series of deleted forms of CheZ were fused to GFP. Removal of the N-terminal helix or of the entire unstructured C-terminal region and the C-terminal CheY-binding peptide did not affect localization. Using the crystal structure (125) as a guide, further deletions were constructed that progressively shortened the core four-helix bundle of CheZ. A protein product containing amino acids 70-134 of CheZ still localized GFP fluorescence to the receptor patch. Further deletion that left only residues 80-121 of CheZ did abolish GFP localization.

Residues 70-79 and 122-134 are part of the four-helix bundle of CheZ. The bundle splays apart between residues 80 and 121 (Fig. 13 B & C). It seems likely that the stability of CheZ, binding at the receptor patch, or both, requires the localization domain to be a dimer. In this view, the residues at the top of the four-helix bundle provide a minimal interaction that allows $CheZ_{70\text{-}121}$-GFP to dimerize whereas $CheZ_8^{0\text{-}121}$-GFP lacks sufficient contacts to form a functional dimer. No mutations in residues 70-79 or 122-134 were examined in the initial screen, and thus it is not entirely possible to rule out that amino acids in this region play a direct role in binding to $CheA_S$.

The minimal localizing fragment of CheZ does not contain catalytic or CheY~P-binding sites. Thus the $CheZ^{70\text{-}134}$-GFP fragment can be expressed in cells as a marker to visualize receptor patches without altering the stoichiometry of the normal protein complement of the chemotaxis pathway.

The crystal structure of CheZ revealed a short helix at the N-terminus that projects away from the core four-helix bundle. Some *cheZ* mutations that result in a gain of function target to this helix or the adjacent portion of the core bundle, leading Zhao *et al.* to predict that this region might be regulatory. Expression of CheZ-GFP deleted for residues 2-30 resulted in cells that were strongly smooth biased when concentrations of inducer were used that produced normal run- gain-of-function phenotype associated with a hyperactive CheZ phosphatase. Several gain-of-function mutations isolated in this regulatory helix by Sanna and Simon (82), including the strongest one found (L24P), were Pro substitutions, which are likely to disrupt the helix.

The extreme C-terminus of CheZ has been identified as a CheY~P-binding domain (12, 63), and a 14-amino acid peptide corresponding to the C-terminus was resolved in the CheZ-CheY co-crystal (Fig. 4). The region of the protein between the C-terminal peptide and the core bundle of CheZ was unresolved in the crystal structure. $CheZ^{1-181}$ (125) and $CheZ^{1-201}$ (12) have no measurable CheY~P-binding activity *in vitro*, although there is considerable contact between the core four-helix bundle of CheZ and CheY in the co-crystal structure (125). Fluorescence anisotropy measurements indicate that the C-terminal helix and linker region are highly mobile and move independent of the core bundle, a feature that may serve to increase the effective radius of potential CheZ-CheY~P interactions (93). Expression of the $CheZ^{1-200}$-GFP or $CheZ^{1-166}$-GFP proteins from plasmids using high levels of inducer indicated that both of these proteins could restore some smooth swimming *in vivo*, demonstrating that binding and dephosphorylation of CheY~P does occur in the absence of the carboxyl-terminal peptide. These data suggest that the role of the carboxyl-terminal linker and CheY-binding helix is to increase the local concentration of CheY~P, and possibly to position it properly relative to the catalytic site. Expression of high levels of CheZ, combined with localization to receptor patches where CheY~P is being produced, appears to partially bypass this through a residual low-affinity interaction of CheY~P with the core of CheZ. This hypothesis can be tested by introducing the F98S substitution into $CheZ^{1-166}$-GFP. Failure to localize CheZ-GFP would prevent the formation of the very high local concentration of CheZ-GFP needed for the proposed low affinity interaction of CheY~P and the CheZ core.

The crystal structure of the CheA phosphotransfer domain shows a four-helix bundle with a fifth helix at the carboxyl-terminal end of the domain. The conserved His at position 48 that serves as the site of phosphorylation is located on the second helix. The fifth helix has hydrophobic contacts with helix four and translation from Met 98 produces the $CheA_S$ protein that has unpaired hydrophobic residues on what would be helix 5 of full-length P1 (69). We previously proposed these hydrophobic residues as a site of interaction between $CheA_S$ and CheZ (22). O'Connor and Matsumura demonstrated that a fragment of $CheA_S$ P1 domain corresponding to amino acids 98-139 of the full length CheA protein was able to bind to CheZ and enhance the phosphatase activity (72), as had been previously shown for full length $CheA_S$ (117). This activity depends on $CheA_S$ being reduced, as had been previously shown for the CheZ-$CheA_S$ interaction. $CheA_S$ P1 fragments also form dimers under oxidizing conditions (45, 72).

CheA contains a Cys residue at position 120, and addition of bulky sulfhydryl modifying reagents such as fluorescein 5-maleimide also inhibited CheZ binding (72). In order to determine whether the hydrophobic amino acids exposed in $CheA_S$ P1 are required for CheZ interaction, these were substituted with Ala or Ser residues, and the ability of the resulting mutant proteins to localize GFP to the receptor patch was determined. The Leu-123 and Leu-126 residues were determined to be most important for proper localization of CheZ-GFP, whereas substitution Ile-119 had an intermediate effect. These three hydrophobic residues are on the same face of helix 5 of CheA P1. Ala substitutions at Cys-120 or Leu-128 had no effect on localization.

Since the two non-localizing mutants of CheZ replaced aromatic residues, the two aromatic residues at the base of helix 5 of CheA P1 were also replaced. The Y118S substitution had intermediate effects, and the Y118A, F116A, and F116S substitutions had no effect on localization. Thus, we have no evidence that formation of an aromatic "sandwich" between Trp-97 and Phe-98 of CheZ and aromatic residues of CheA P1 helix 5 is key to the CheZ-$CheA_S$ interaction.

Researchers in the laboratory of Philip Matsumura concurrently tested the effect of a similar set of substitutions on the ability of the $CheA^{98-139}$ fragment to bind CheZ *in vitro*. Their results correspond closely to the *in vivo* results (Fig. 19). Thus these hydrophobic residues clearly play an important role in binding of $CheA_S$ to CheZ.

Both CheZ F98S and CheA L126A disrupt localization of CheZ-GFP to the receptor patch, but neither causes a substantial chemotaxis defect in soft-agar motility plates (22, 71). In order to better analyze the swimming behavior of these mutants, we collaborated with the Matsumura laboratory to analyze the swimming of individual cells using computer-assisted motion tracking. Expression of $CheA^{L126A}$ resulted in an increase in the tumble bias compared to $CheA^{wt}$ cells, but expression of $CheZ^{F98S}$ produced no different result than wild type CheZ. Vaknin and Berg observed a 10% defect in the rate of migration of the serine swarm ring in tryptone soft agar for cells expressing $CheZ^{F98S}$ compared to cells expressing wild-type CheZ (113).

These data indicate that the two residue substitutions may act in different ways to perturb CheZ-GFP localization, although both mutant proteins appear to have normal baseline activity (22, 71). Kott *et al*. concluded, based on sedimentation equilibrium

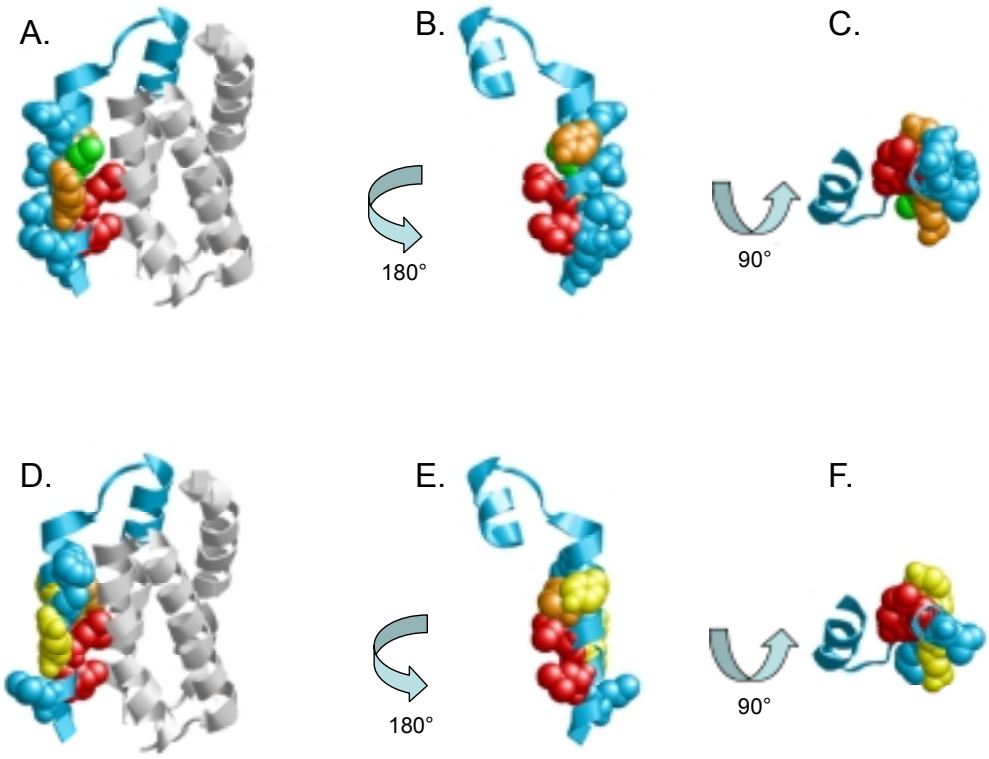


FIG. 19**.** Mapping the cysteine scanning results on the P1 structure. Residues mutated and tested for the effects on CheZ binding *in vitro* (A-C) or CheZ-GFP localization in vivo (D-F) are indicated by space-filling residues in the model of CheA P1 (accession number, 1I5N). (A-C) When mutated to cysteine, the cyan residues still bind CheZ in the presence of fluroscein-5-maleimide (5-FM). The green residue is Cys-120, which was previously shown as capable of binding CheZ when mutated to serine. When Cys-120 is labeled with 5-FM, CheZ binding is lost. The residues colored in orange represent Y118 and R124, which have partial CheZ-binding defects. The residues in red (L123 and L126) are the cysteine mutants that are unable to interact with CheZ *in vitro* (71). (D-E) When mutated to alanine or serine, the cyan residues localized CheZ-GFP to the polar receptor patch as wild-type. The yellow residues (L118, R124) showed reduced localization when substituted with serine. The orange residue (I119) showed reduced localization when substituted with alanine and negligible localization when substituted with serine. The red residues (L123, L126) showed negligible localization with either substitution. Only the portion of the P1 domain found in $CheA_S$ is shown in the reverse (B, E) and bottom (C, F) views.

studies, that the P1 domain of $CheA_S$ contributes significantly to the stability of $CheA_S$ homodimers (45). Transphosphorylation between heterodimers of $CheA_S$ and $CheA_L$ has been demonstrated (48, 122), but it is not known what proportion of the $CheA_S$ and $CheA_L$ in a cell normally exists as homodimers or heterodimers.

The differential effects of the *cheA* and *cheZ* mutations on motility can be explained by a model in which $CheA_S$ P1 domains are dimerized through interaction of the hydrophobic face buried by interaction with helix four in $CheA_L$ P1 (Fig. 20). Since a $CheA_S$/$CheA_S$ homodimer has no phosphoacceptor His-48, it is catalytically inactive. Following Kott *et al*., disruption of hydrophobic face by the L126A mutation may allow formation of a higher percentage of catalytically active $CheA_L$/$CheA_S$ heterodimers, possibly changing the balance of CheY~P generated in the cell. For example, if CheAL and CheAS are present at a 2:1 ratio, as in Figure 9B, the ratio of active to inactive CheA dimers could go from 2:1 with wild-type $CheA_S$ with all homo dimers to 8:1 if association is random. That would represent s potential increase of 33% in active CheA dimers, which could lead to an increase in CheY~P levels. In this model, the binding site for CheZ is formed by the dimerized $CheA_S$ P1 domains, and mutations that disrupt dimerization decrease formation of the CheZ-binding site, by two-thirds in the example just given. In keeping with this idea, the L126A/S and L126A substitutions in CheA do not fully abolish localization, while the W97S and F98S substitutions in CheZ do. Immunoprecipitation using CheZ antibodies recovered only $CheA_S$ and no $CheA_L$ (117). Using CheZ immobilized to a column, $CheA_L$ can be recovered using low salt wash, while a high salt wash recovers only $CheA_S$ (Philip Matsumura, personal

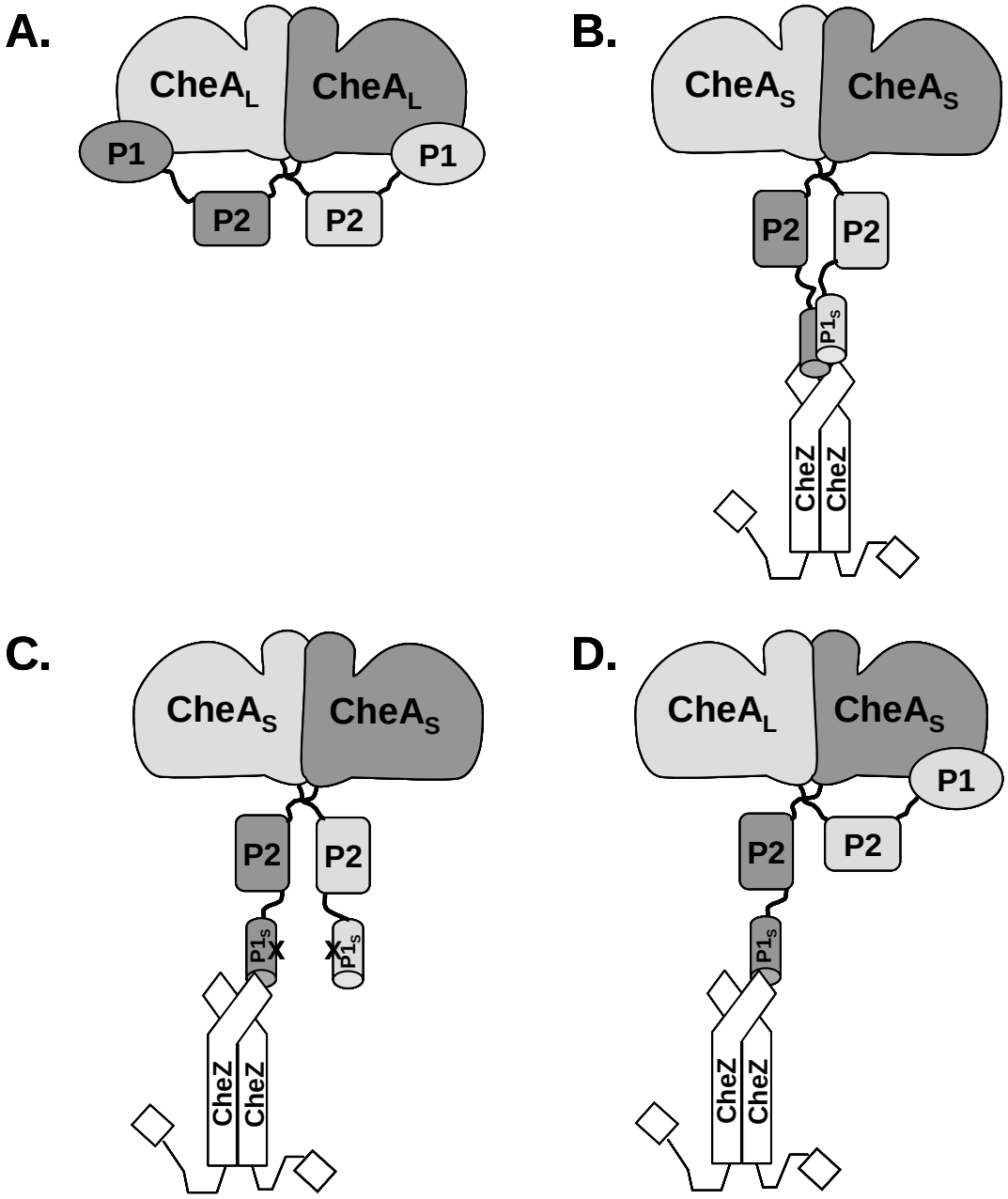


FIG. 20. Model for CheZ-CheA interactions. CheA in wild type cells forms primarily homodimers of (A) $CheA_L$ and (B) $CheA_S$ driven by interactions between P1 domains as described by Kott et.al. (45). CheZ interacts strongly with the dimerized $P1_S$ domain. CheZ interacts weakly with $P1_S$ monomers formed by (C) mutation of the $P1_S$ interaction face or by formation of (D) $CheA_L/CheA_S$ heterodimers.

communication). These data could be interpreted in two ways: i) some weak interaction exists between $CheA_L$ and CheZ or ii) some weak interaction exists between monomeric $CheA_S$ P1 domain and CheZ, allowing $CheA_S$/$CheA_L$ heterodimers to bind CheZ under less stringent conditions. This model then predicts that in wild-type cells most of the $CheA_S$ is confined to a catalytically inactive homodimer whose primary function is to localize of CheZ to the receptor patch.

# CHAPTER IV

# OVEREXPRESSION OF CheA INCREASES FORMATION OF CHEMORECEPTOR PATCHES IN THE LATERAL MEMBRANE

## Introduction

Chemotaxis in *Escherichia coli* is mediated by a signal transduction pathway that controls the activity of the histidine protein kinase CheA. When in association with transmembrane receptors and CheW, CheA autophosphorylates and transfers phosphate to the response regulator CheY, which binds to flagellar motors in its phosphorylated form and mediates clockwise rotation. The central components of this pathway, as well as other associated factors, are clustered into patches localized primarily to the cell poles. Formation this receptor patch requires CheA, CheW and receptors(57, 99).

The crystal structure of the cytoplasmic domain of the serine receptor Tsr showed a trimer-of-dimers structure (40), and this structure formed the basis of a molecular model proposing that the receptor patch is composed of a lattice of receptor trimers-of-dimers interconnected by CheA dimers (89). Electron microscopic studies of purified protein complexes also showed higher order organization of CheA, CheW, and receptors (30, 31), and *in vivo* electron microscopy analysis of *E. coli* membranes overproducing receptors show defined lattice patterns (61, 62). The mechanism by which receptors localize to receptor patches have been poorly understood. Electron microscopy of

immunogold labeled cells indicated that receptors localize to poles and in the absence of CheA but that optimal clustering requires functional CheA protein (95).

Recent advances have shown that cell shape and polarity are determined largely through bacterial actin homologues which polymerize into helical filaments (reviewed in (23, 67, 101). Actin-like filaments are also involved in other cellular activities, such as chromosome segregation (60). *E. coli mreB* mutants form spherical cells in which normally polar proteins such as Tar or the *Shigella* IscA actin-binding protein are randomly distributed (87).

Shiomi *et al.* utilized a Tar-GFP fusion protein to analyze the formation of polar receptor complexes. They determined that chemoreceptors are inserted into the membrane at random locations and subsequently localize to the poles. Tar-GFP in the lateral membranes was found in helical patterns associated with elements of the Sec translocon.

In this study, I show that overexpression of CheA leads to a major increase in the number of lateral receptor patches. In many of these cells, the lateral patches form clear bands or helical coils with widely varying helical pitch.

## Materials and methods

**Strains and plasmids.** The strains and plasmids used in this investigation are shown in Table 5.

**Media and growth conditions.** Cells were grown at 30$^{o}$C in tryptone broth (TB) following dilution from overnight cultures. Chloramphenicol was added to the media at

**TABLE 5. Strains and plasmids, chapter IV.**

| Strain | Genotype | Comments | Reference or Source |
|---|---|---|---|
| RP437 | *thr*(Am)*1, leuB6, his-4, metF*(Am)*159, eda-50, rpsL1356, thi-1, ara-14, mtl-1, xyl-5, tonA31, tsx-78, lacY1, F⁻* | | (75) |
| MM509 | *RP437*□tar-tap)5201, *eda*$^{+}$ | | (32) |
| DHB6521 | SM551 (λInCh1 lysogen) | | (20) |
| BC201 | RP437 Δ(λ*att-lom*)::*bla lacI*$^{q}$ p*tac-cheZ-gfp* | pBJC104 into RP437 via λInCh1 | This study |
| BC202 | MM509 Δ(λ*att-lom*)::*bla lacI*$^{q}$ p*tac-cheZ-gfp* | pBJC104 into MM509 via λInCh1 | This study |
| BC203 | VB13 Δ(λ*att-lom*)::*bla lacI*$^{q}$ p*tac-cheZ-gfp* | pBJC104 into VB13 via λInCh1 | (22) |
| BC206 | RP9535 Δ(λ*att-lom*)::*bla lacI*$^{q}$ p*tac-cheZ-gfp* | pBJC104 into RP9535 via λInCh1 | (22) |
| BC214 | RP2867 Δ(λ*att-lom*)::*bla lacI*$^{q}$ p*tac-cheZ-gfp* | pBJC104 into RP2867 via λInCh1 | (22) |
| **Plasmids and Phage** | **Relevant Genotype** | **Comments** | **Reference or Source** |
| pBJC104 | p*tac cheZ-gfp, amp*$^{r}$ | *cheZ-gfp* in pCJ30 | (22) |
| pBJC200 | p*nahG cheA, cm*$^{r}$ | *cheA* in pLC112 | C. O'Connor |
| λInCh1 | *kan*$^{r}$*, cI*857 | λInCh for pBR-derived plasmids | (20) |

a final concentration of 30μg/mL for cells harboring pBJC200. Sodium salicylate was added to the media at a final concentration of 100μM to induce expression of CheA from pBJC200. CheZ-GFP carried in the chromosome was induced by addition of 1 mM IPTG to the growth media.

**Insertion of *cheZ-gfp* into the chromosome.** The *cheZ-gfp* gene of plasmid pBJC104 was introduced onto the chromosome utilizing the λInCh system as described (20). Briefly, pBJC104 was transformed into a strain containing λInCh1, and recombinants that contain the plasmid insert and *bla* gene were selected on ampicillin plates. A lysate of this strain was used to transduce strains of interest to ampicillin resistance. Finally, homologous recombination between a DNA sequence adjacent to the chromosomal *attλ* site and the same sequence within λInCh1 was selected by loss of temperature-sensitive lysis. This recombination event removes much of the phage DNA and stabilizes the insertion. Strains modified in this way to carry the *cheZ-gfp* gene are shown in Table 5.

**Fluorescence microscopy**. Cells were grown overnight at 30$^{o}$C in TB media with antibiotics, diluted 1:100 into 5 ml of the same medium containing sodium salicylate or IPTG as needed, and incubated with shaking at 30$^{o}$C. A 100 μL aliquot of cells in late exponential phase (~$OD_{590nm}$ of 0.8 - 1.0) were mixed with 300 μL of tethering buffer (100 mM NaCl, 10 mM KPO4 pH 7.0, 0.4% (v/v) lactic acid, 20 μM methionine, 10 μM EDTA), placed onto cover slips coated with 0.1% polylysine (Sigma), and allowed to settle for 5 min. The affixed cells were then washed twice with 1 mL tethering buffer. The cover slips were placed on slides and sealed with clear enamel, then viewed at

1000X magnification using a Olympus IX inverted microscope. For epifluorescent microscopy, the excitation filter wavelength was 484 nm and the emission filter wavelength was set at 510-530 nm. Images were captured using a Hamamatsu Orca ER CCD camera and the Simple PCI software package. Images were processed to enhance of brightness and contrast using Adobe Photoshop.

**Measurement of helical pitch of fluorescent patches.** To measure the helical pitch of bands of fluorescent patches, images of 100 individual cells were taken from photomicrographs and enlarged using Adobe Photoshop. Cells chosen for analysis had two or more parallel bands of receptor patches or an arrangement of three or more patches in line. Using the ImageJ software package, a line was drawn through the long axis of each cell and a line drawn through the band (Fig. 21). The acute angle between the two lines was measured using ImageJ.

## Results

**Multiple receptor patches per cell are visualized when CheA is overexpressed in the presence of CheZ-GFP**. In otherwise wild-type cells expressing CheZ-GFP from a chromosomal locus, a single polar receptor patch is observed in the majority of cells, with a subset of cells possessing a second polar receptor patch or a lateral receptor patch ((22); (Fig 22 A). However, when CheA was overexpressed in cells expressing CheZ-GFP, cells with large numbers of lateral patches of localized fluorescence, or with multiple polar fluorescence patches at the same pole, were seen (Fig 22 B-C). Multiple patches of localized CheZ-GFP fluorescence were not seen in cells that overexpress

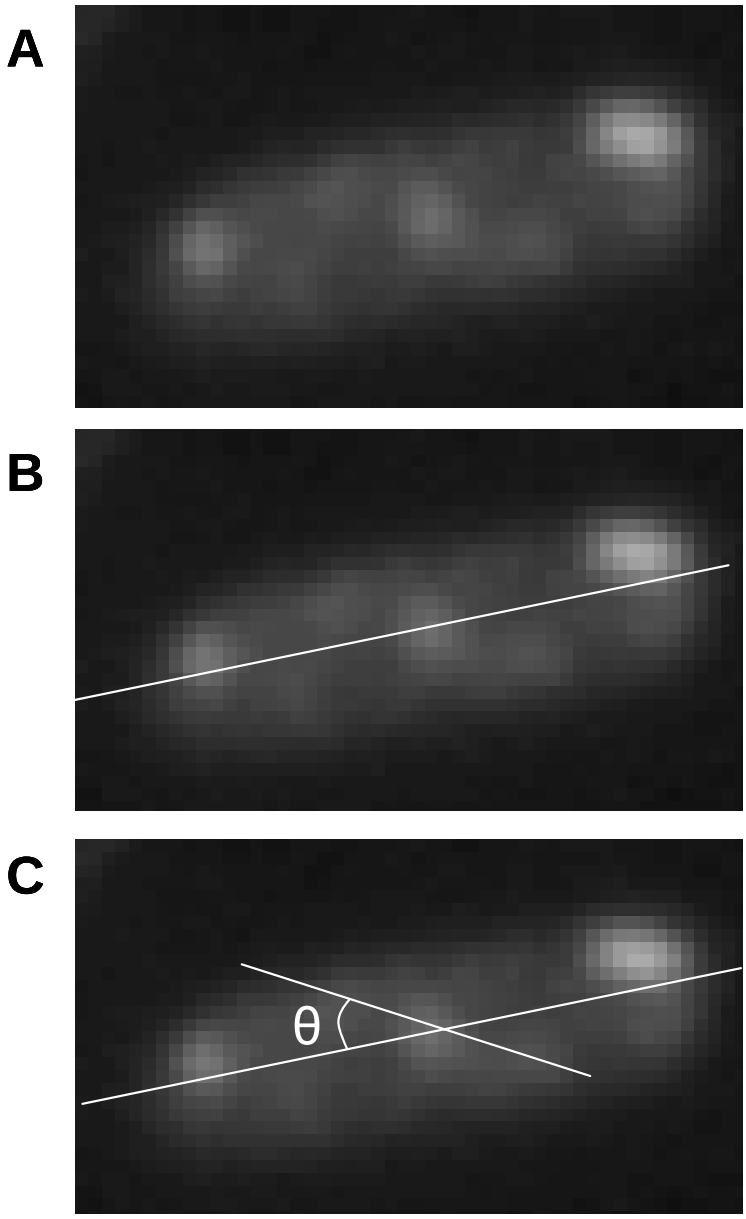


FIG. 21. Determining the helical pitch of receptor arrays. (A) individual cells were selected from photomicrographs and enlarged. (B) A line was drawn through the long axis of each cell, (C) a second line was drawn through the band of fluorescent patches, and the acute angle (θ) formed by the two lines was measured.

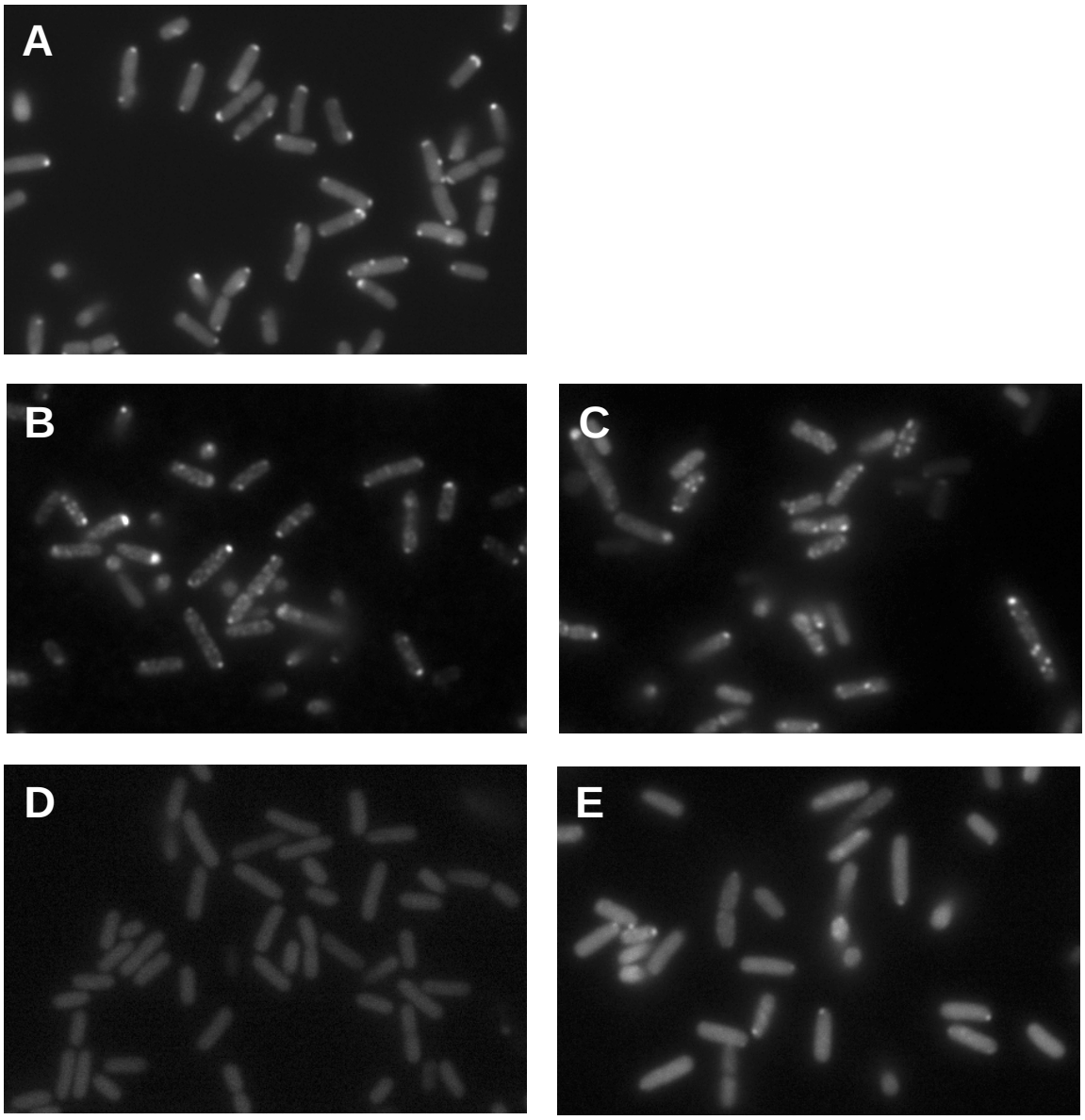


FIG. 22. Multiple receptor patches are visualized when CheA is overexpressed in cells also expressing CheZ-GFP. (A) BC201 cells expressing CheA from the normal chromosomal locus generally have at most 3 receptor patches per cell. (B-C) BC206 cells with CheA expression from pBJC200 induced with 100 μM sodium salicylate. Numerous cells with >3 receptor patches are seen. Even when CheA expression is induced, localized fluorescence is lost in BC203 cells (D), which do not express chemoreceptors, and reduced in BC202 cells (E), which express only Tsr and Trg.

CheA but do not express chemoreceptors (Fig. 22 D), so the lateral spots of fluorescence represent receptor patches and not artifacts of CheA overexpression. Expression of a full set of chemoreceptors enhanced formation of multiple receptor patches, since cells expressing only the Tsr and Trg receptors formed fewer receptor patches that were largely restricted to the cell poles (Fig. 22 E).

**Multiple receptor patches are arranged in helical arrays of varying helical pitch.** In many of the cells overexpressing CheA, the lateral receptor patches clearly formed helical or banding patterns. Cells with identifiable helical arrays of receptor patches were analyzed to determine the pitch of the helical or repeating array (Fig. 23). There was no significant correlation between cell length and helical pitch in the cells examined (data not shown). Using the ImageJ software package, the acute angle of the helical arrays relative to the long axis of the cell was determined for 100 cells. Figure 24 shows the distribution of helical pitch angles for those cells. A wide distribution of angles was observed, with the mean angle being 56º ± 21º.

## Discussion

In this study, the CheA protein was overexpressed from a plasmid and CheZ-GFP used as a marker. The formation of a large number of lateral patches of localized fluorescence was observed along the entire length of the cells. Overexpression of CheA in the absence of receptors did not lead to CheZ-GFP localization, indicating that the patches contain the CheA/CheW/receptor complex and are not simply an artifact of increased CheA levels in these cells.

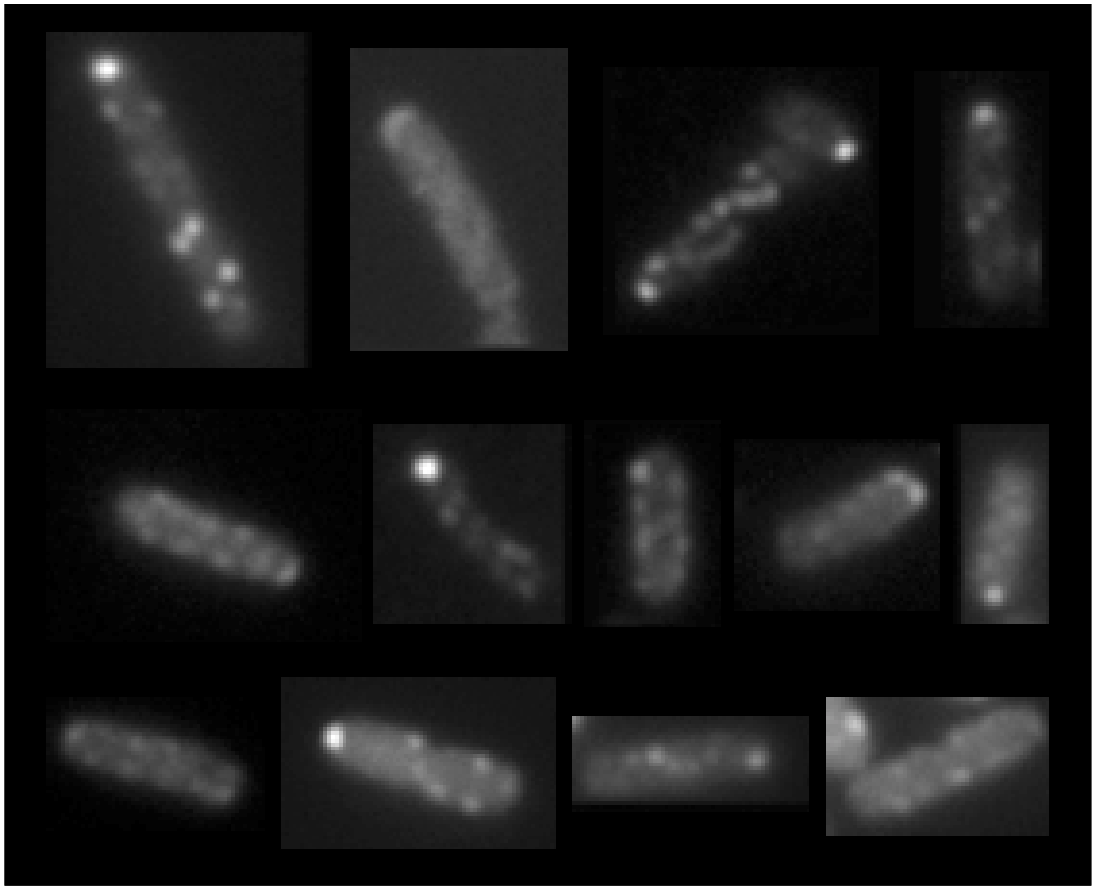

FIG. 23. Helical patterns of CheZ-GFP localization. High-level expression of plasmid-encoded CheA was induced in cells expressing CheZ-GFP, allowing visualization of multiple receptor patches in each cell. Representative cells with helical arrangements of receptor patches with various pitches are shown. All cells are shown at the same magnification (1000X).

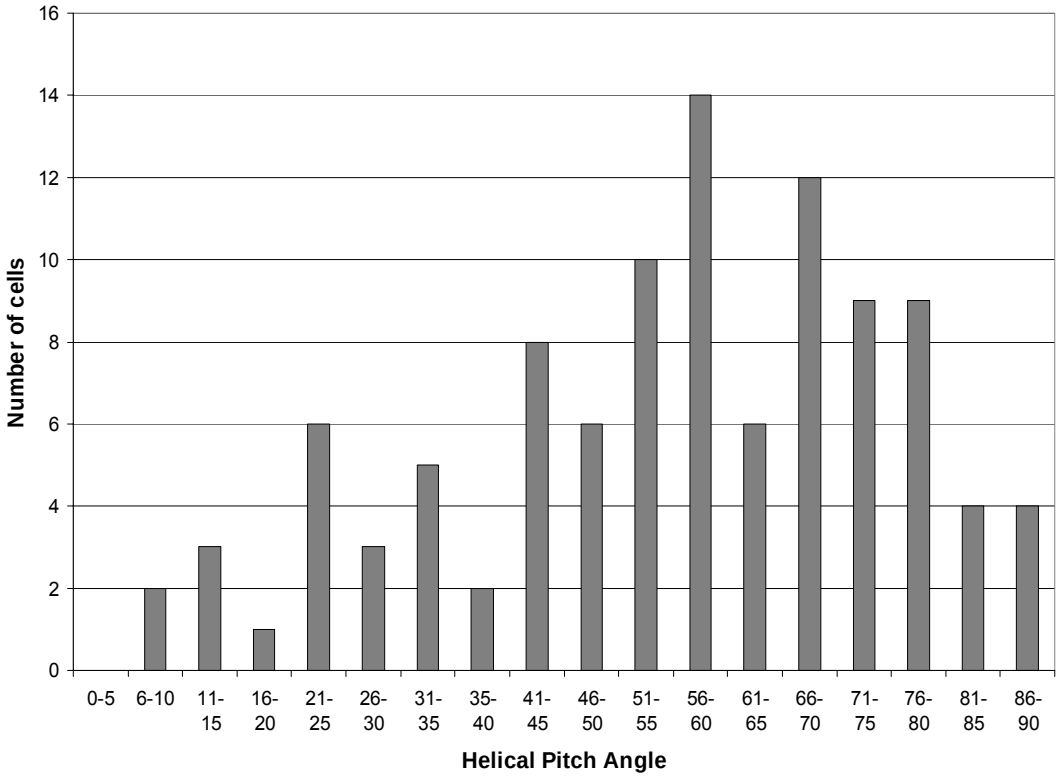


FIG. 24 Helical pitch of receptor patch arrays is highly variable. Histogram of helical pitch angles measured for 100 cells.

Lateral receptor patches have been seen in some cells using CheZ-GFP (22, 99), but normally only a single lateral patch is seen. In addition, helical arrangements of receptor patches were seen in some cells. The helical pitch of the patches in 100 cells was measured and found to be widely distributed.

In recent years, a number of actin homologs have been identified in bacteria. These proteins have limited sequence homology with eukaryotic actin, but when the crystal structure of two of these proteins was determined, their folds were found to have strong similarity to the fold of eukaryotic actin (114, 115). These actin-like molecules in bacteria form helical filaments positioned adjacent to the cell membrane (38, 88). Multiple, independent helical filaments have been identified simultaneously in *Bacillus subtillus* (38) and *Caulobacter* (29), and MreB has been shown to form spiral structures of varying pitch in *E. coli* (88).

Shiomi *et al.* reported that Tar-YFP associated with the Sec machinery forms coiled structures that are distinct from coils formed by MreB-CFP. The MreB-CFP coils were reported to have a tighter pitch than the Tar-YFP coils, although the images did not provide convincing proof that the two proteins were on separate helical coils (90). The wide variety of helical pitch angles observed in the helical arrays of receptor patches could be the result of interaction with different helical filaments or with a single type of helical filament with variable pitch. The images obtained in this study support the latter model in *E. coli*, since the coils observed were generally parallel and when two different helices were seen in a cell, they generally did not overlap.

The appearance of multiple lateral receptor patches upon CheA overexpression supports the idea that chemoreceptors move to the poles through random diffusion rather than by an active mechanism. MreB actively polymerizes and depolymerizes, with single molecules of MreB moving down the length of a filament as a result (41). Tar-GFP associated with Sec machinery was localized to spiral structures (90), leading to the possibility that Tar inserts along such cytoskeletal structures and is actively transported to the cell poles. However, such a model would prohibit formation of receptor clusters except at poles, since the majority of the receptors would be expected to be associated with filaments.

In contrast, appearance of lateral receptor patches along helical filaments would be expected to occur if receptors were inserted into the membrane and were free to diffuse. If the helical filaments are in close contact with the cytoplasmic face of the inner membrane, any membrane protein with a substantial cytoplasmic domain will be unable to diffuse through a filament. Chemoreceptors could accumulate along these filaments, and then associate into stabile receptor patches by interaction with CheA and CheW.

Recent evidence suggests that receptors may form clusters in the absence of CheA or CheW through contacts in their cytoplasmic domains (39). CheA and CheW would then bind to and stabilize clusters of chemoreceptors. Previous models of cluster formation depended on CheW, which is normally present in approximately equal copy to CheA (49). Thus overexpression of CheA in the absence of overexpression of CheW would be predicted to have limited effects. The model proposed by Kentner *et al.,* however, postulates that CheA is able to interact with and stabilize receptor clusters in

the absence of CheW. Appearance of multiple lateral receptor patches when CheA is overexpressed supports this latter model. The requirement for CheW in cluster formation can be explored further by overexpressing CheW alone or in the presence of excess CheA and looking for the appearance of multiple lateral receptor patches.

Overexpression of CheA in a strain producing a normal complement of chemoreceptors resulted in abundant lateral receptor patch formation, but the same result was not seen in a Δ*tar-tap* deletion strain. As Tsr is present in approximately a 2:1 ratio with Tar and the low abundance receptors Tap and Trg are present in ~10 fold fewer copies than Tar and Tsr, this strain should produce approximately 65% of the amount of receptor as wild-type. Mixed chemoreceptor units have been demonstrated to have higher activity *in vitro* (46) and *in vivo* (3, 98), and these data may indicate that mixed populations of chemoreceptors may more readily form receptor patches. However, since the total amount of chemoreceptor protein was lower in the Δ*tar-tap* strain, a threshold amount of receptor required for lateral patch formation could also explain the result. Overexpression of CheA in cells expressing Tsr or Tar to levels equivalent to those attained by the combined proteins in wild-type cells could determine whether mixed receptor populations form patches more readily than single receptor populations.

# CHAPTER V

# SUMMARY AND CONCLUSIONS

## Summary of results

In this study I utilized a fusion of the green fluorescent protein (GFP) to the chemotaxis phosphatase CheZ to define the localization of the phosphatase to the polar receptor patch. I also elucidated the determinants required for localization. The CheZ dimer forms an elongated four-helix bundle formed from two helices of each monomer(125). Deletions of CheZ fused to GFP define the region required to localize CheZ-GFP to the receptor patch as the region between amino acids 70 and 134 of CheZ. This region encompasses the turn between the two long helices of each monomer and extends to the top of the four-helix bundle. A number of residue substitutions within this region of the protein that substitute for hydrophobic amino acids with Ser were also found to abolish localization of CheZ-GFP to receptor patches. Most of these mutations also disrupted chemotaxis and were identified in the crystal structure of CheZ as having side chains that participate in interactions between the two helices of a monomer or interactions between the two monomers of the dimer. Substitutions at two residues, Trp-97 and Phe-98, abolished localization but still complemented a *cheZ* deletion to support chemotaxis. These two aromatic residues are exposed and could form the site of interaction of CheZ with its cognate binding partner in the receptor patch. Substitutions of a number of conserved, exposed charged residues in the vicinity of the two aromatic residues were tested and determined to have no effect on CheZ localization.

Deletion constructs were used to examine the role of the amino-terminal and carboxyl-terminal regions of CheZ in its function. The first 30 residues of CheZ comprise a helix that projects away from the core four-helix bundle (125). A number of gain-of-function mutations of CheZ (81, 82) map to this helix and the proximal portions of the four-helix bundle. Deletion of this helix resulted in a strong gain-of-function phenotype in which cells showed a smooth-swimming bias compared to wild-type cells. The carboxyl-terminal 14 amino acids of CheZ constitute a CheY-binding motif (12) and are found in close contact with CheY in the CheZ-CheY co-crystal (125). Deletion of the CheY-binding peptide or the entire carboxyl-terminal region to the base of the four-helix bundle resulted in strongly tumbly, non-chemotactic cells. However, overexpression of these truncated proteins restored smooth swimming, indicating that CheZ can interact, with lower affinity, with CheY~P in the absence of the CheY-binding peptide.

The CheA protein in *E. coli* is produced in two forms in the cell: the full-length form and a truncated form (CheA short, or $CheA_S$) initiating from an internal start site at Met-98 of the full length protein (43, 96). Elimination of $CheA_S$ has no effect on chemotaxis in soft-agar motility plates, but $CheA_S$ coimmunoprecipitates with CheZ using anti-CheZ antibody and forms complexes with CheZ *in vitro* (117), making it the likely target for CheZ interaction at the receptor patch. Using strains expressing various deleted versions of CheA, the portion of the CheA P1 domain remaining in $CheA_S$ was determined to be the binding site of CheZ-GFP at the receptor patch. This region makes

up the end of helix 4 and all of helix 5 of the P1 structure. Hydrophobic residues in helix 5 make contacts with helix 4 in full length P1, but are exposed in $P1_S$.

Involvement of these residues in CheZ localization was tested by substituting residues in helix 5 with Ser or Ala residues. Substitutions at amino acids on the hydrophobic face of helix 5 (I119A L123, L126) strongly reduced localization of CheZ-GFP to receptor patches, while substitutions at other positions on helix 5, including aromatic residues F116 and Y118, had limited or no effect. Even the L126A substitution had no obvious effect on swarm formation in soft-agar motility plates, and has normal kinase activity (71).

Computer-assisted motion analysis of swimming cells expressing non-localizing variants of CheA or CheZ was used to measure swimming behavior. The L126A substitution in CheA caused in a tumble bias, whereas the F98S substitution of CheZ did not, indicating that the two mutations do not have equivalent effects on motility.

CheZ overexpression in cells producing the normal complement of chemoreceptors resulted in the appearance of large numbers of lateral receptor patches. In some cases, the patches were arrayed in helical patterns whose pitch varying widely from cell to cell. Formation of lateral receptor patches was largely abolished in cells expressing only Tar, the less abundant of the high abundance chemoreceptors Tar and Tsr.

**Model of CheZ interaction with $CheA_S$**

The model presented here for $CheA_S$-CheZ interaction proposes that the P1 domain of $CheA_S$ dimerizes through interaction of the hydrophobic face of helix 5 of P1 to

generate the binding site for CheZ at the receptor patch. The $P1_S$ domain has been shown to contribute to the stability of $CheA_S$ homodimers (45), and interaction of $P1_S$ domains on nascent $CheA_S$ molecules could increase the likelihood of formation of $CheA_S$ homodimers. $CheA_S$ homodimers should be catalytically inert, since the phosphoacceptor His-48 is absent. Thus $CheA_S$ homodimers may function exclusively as binding sites for CheZ.

Introduction of the L123A or L126A substitution into CheA probably disrupts dimerization of the P1S domain so that the CheZ binding site is not formed. The residual CheZ-GFP localization seen in the $CheA^{L123A}$ and $CheA^{L126A}$ mutants, which is not seen with $CheZ^{F98S}$, could be the result of a residual level of $P1_S$ dimerization or a weak interaction with the monomeric $P1_S$. The defect in CheZ binding when $CheA_S$ is exposed to oxidizing conditions is due to formation of disulfide-linked dimers of $CheA_S$ P1 via Cys-120. These abnormal dimers presumably do not interact with CheZ. If this model is correct, the L126A substitution should allow more $CheA_L$/$CheA_S$ heterodimers to form, which might lead to more catalytically active CheA, resulting in the tumble bias of seen with the $CheA^{L126A}$ substitution. The ratio of $CheA_S$ to $CheA_L$ has been determined, but the ratio of homodimers to heterodimers *in vivo* is known. This model predicts more $CheA_S$/$CheA_L$ heterodimer will be seen after non-denaturing polyacrylamide gel electrophoresis in cells expressing $CheA_{L126A}$ compared to wild-type CheA.

Interaction of CheZ with $CheA_S$ or the $P1_S$ fragment enhances the phosphatase activity of CheZ. Phosphatase activity can also be enhanced by deletion of the amino-

terminal helix of CheZ, by point mutations in the amino-terminal helix, or in the portion of the four-helix bundle proximal to it. The enhancement of CheZ activity by $CheA_S$ seems likely to involve the regulatory region at the base of the four-helix bundle. The carboxyl-terminal portion of the protein is very mobile and this region is believe to act as a snare to increase CheY~P concentration at the active site. One model for regulating CheZ would be to control mobility of this region by sequestering the flexible linker and CheY-binding peptide through contact with the regulatory domain of CheZ. Binding of $CheA_S$ could enhance CheZ activity by releasing the flexible CheY-binding domain and increasing the amount of CheY~P bound to the receptor site. Chemotaxis defects caused by deletion of the carboxyl-terminal CheY-binding peptide can be partially overcome by high levels of expression of the mutant protein. However, if the model is correct the carboxyl-terminal deletions should be insensitive to gain-of-function mutations. Because cells with too much CheZ activity are smooth swimming and therefore non-chemotactic in soft-agar motility plates, the existing gain of function mutants can be used to isolate suppressing mutations in other parts of the protein and to identify sites of interaction between the regulatory domain and the linker if they exist.

**The role of CheZ localization**

Recent experiments using the *cheZ*$^{F98S}$ mutant have shed light on the role that localization of CheZ plays in chemotaxis. Vaknin and Berg (113) monitored CheY~P concentrations by CheY~P/CheZ FRET in single cells. Wild-type cells have a high concentration of CheY~P at the receptor patch, which rapidly declines away from the

receptor patch and then remains relatively constant over the rest of the cell. In contrast, cells expressing CheZ$^{F98S}$ had a more gradual decline in CheY~P concentration as a function of distance from the receptor patch. Thus, a peritrichiously flagellated wild-type cell has approximately the same concentration of CheY~P at all of the motors, whereas a non-localizing CheZ mutant will have a higher CheY~P concentration at motors near the patch than at motors farther from the patch. Using computational models, Lipkow *et al.* examined diffusion of CheY~P from receptor patches to flagellar motors and observed a similar effect of CheZ localization on gradients of CheY~P (50). A uniform distribution of CheY~P is not required in cells that produce only a single flagellum. Comparison of CheZ sequence alignments with patterns of flagellar distribution among a number of members of the Proteobacteria reveals that those organisms with peritrichous flagellation have Trp and Phe at positions corresponding to Trp-97 and Phe-98 of *E. coli* CheZ (Fig. 25). Thus, among the Proteobacteria, localization of CheZ to the receptor patch appears to be an adaptation to peritrichous flagellation. It is not known whether all peritrichiously flagellated enteric bacteria produce CheA$_S$ or if some utilize an alternative binding site for CheZ. Given the conservation of the Trp-Phe motif, the same binding site seems likely, but the binding site on CheA could be exposed by other means than producing CheA$_S$.

A *cheZ* gene has been identified in members of the β-, δ-, and γ-Proteobacteria. Peritrichous flagellation exists in other groups of bacteria, with the best studied example being the gram-positive *Bacillus subtillus*. *B. subtillus* encodes two phosphatases, CheC and FliY (111), and both are specifically localized: CheC at the receptor patch (42), and

| | | | | |
|---|---|---|---|---|
| *Escherichia. coli* | (86 | SAKALTQRWDD**WF**ADPIDLADAR | ▲ | γ |
| *Salmonella enterica* | (86 | EAKALTQRWDE**WF**DNPIELSDAR | ▲ | γ |
| *Enterobacter cloacae* | (87 | GAKALSKRWDE**WF**ENPIELADAR | ▲ | γ |
| *Shigella flexneri* | (86 | SAKALTQRWDD**WF**ADPIDLADAR | | γ |
| *Yersinia pestis* | (86 | SAKALKIRWDE**WF**ANPIELSDAR | | γ |
| *Photorhabdus luminiscens* | (87 | SAISLKKRWDE**WF**ENPVEMPVAR | ▲ | γ |
| *Azotobacter vinelandii* | (86 | GAKALDERWQA**WF**ADPMELEQAK | ▲ | γ |
| *Chromohalobacter salexigens* | (88 | GAEQLDRRWEE**WF**AAPVELDDAK | ▲ | γ |
| *Pseudomonas aeruginosa* | (12 | DSRELHQEWQRFMRREIDADGFR | ■ | γ |
| *Pseudomonas putida* | (12 | EAKALSTDWQRFMRREVAAPEFR | ■ | γ |
| *Vibrio cholera* | (10 | SLLLIRPEWNGLMNGRIELMHFK | ■ | γ |
| *Vibrio fischeri* | (10 | GLLQVRPQWNSLMKGRIELAQFK | ■ | γ |
| *Photobacterium profundum* | (10 | TLLQVHPQWKRLMAGKIELSEFK | ■ | γ |
| *Idiomarina lohiensis* | (11 | RVEKVMPAWNRLMSDNIQLNEFK | ■ | γ |
| *Shewanella oneidensis* | (11 | NIQQVMPSWEKLMRREIALTDFK | | γ |
| *Xanthomonas campestris* | (11 | G----------GLNQDQGA | | γ |
| *Desulfovibrio vulgaris* | (10 | DIMDIVERHFELQPEAAVILDNL | | δ |
| *Nitrosomonas europaea* | (80 | DAANLHKLWCQIPETTAAIIANQ | ■ | β |
| *Methylobacillus flagellatus* | (94 | QAVSLEERWKSILAAPSLKRDYD | | β |
| *Burkholderia cenocepacia* | (99 | EAEALDARWAQWYAAPIEHAEVR | ■ | β |
| *Ralstonia solanacearium* | (91 | EAEALVRRWQAWMDRRLSDEEIR | ■ | β |
| *Bordetella pertussis* | (84 | GAQALDERWQQWYDQPLELPQAR | | β |

FIG. 25. Peritrichous flagellation is correlated with presence of CheZ Trp-Phe motif. CheZ sequences of represetatives γ-, δ-, and β-Proteobacteria were aligned using the AlignX program of the Vector NTI suite. The residues aligned with those surrounding the $CheA_S$ binding region of *E. coli* CheZ are shown. Highlighted residues are similar in the majority of sequences aligned. The bold residues are identical to Trp-97 and Phe-98 of *E. coli* CheZ. All proteobacteria examined with peritrichous flagellation (▲) have the Trp-Phe motif whereas the organisms with polar flagella (■) do not.

FliY, which has 10-fold greater phosphatase activity (111), at the flagellar motors (110). Rao *et al.* analyzed the localization of *B. subtilis* phosphatases by computational modeling and reached the same conclusion seen with *E. coli*, that localization of phosphatase activity allows randomly distributed motors to experience uniform CheY-P concentrations (76).

These studies have demonstrated that the intracellular distribution of CheY~P can be affected by phosphatase localization, but whether these changes are sufficiently large alter the switching frequency of motors has yet to be determined experimentally. Cells expressing $CheZ^{F98S}$ do not show any differences swarm-ring formation in soft agar plates or as free swimming cells. The identification of the minimal localizing CheZ-GFP fragment will allow direct assessment of the effects of CheZ localization on motors. The $CheZ^{70-134}$-GFP protein can be expressed as a marker for receptor patch location without affecting the activities of the normal complement of chemotaxis proteins. The rotational bias of tethered cells can be analyzed for cells expressing either normal or non-localizing CheZ, and the rotational bias can be determined as a function of the distance from the receptor patch to the motor of the tethering flagella. Also, the highly sensitive microfluidic chemotaxis assay (59) can be used to monitor the subtle differences in the chemotactic response to both attractants and repellents.

A peritrichous pattern of flagellation must offer some selective advantage to cells sufficient to drive evolution of phosphatase localization. Cells with peritrichous distribution of flagella reorient by tumbling, whereas cells with polar flagella typically reorient using reversals, stops, or changes in swimming speed. These modes of

reorientation produce smaller net changes in direction than tumbling. Thus peritrichous flagellation produces the largest random excursions and the best search pattern. Tumbling is likely to be especially important for the detection of gradients formed by a point source, where the cells will need to search effectively in three dimensions in order to move up the gradient and avoid moving through the gradient and away from the source of an attractant. In contrast, detection of uniform gradients might be as easily detected by cells with polar flagellation, since movement perpendicular to the gradient does not cause the cell to move out of the gradient. Thus cells such as *E. coli* which have receptors which detect amino acids and sugars will gain sufficiently from peritrichous flagellation to warrant the added cost to the cell. Cells that primarily detect uniform gradients such as oxygen tension or light intensity would be expected to utilize a polar flagellar arrangement.

## REFERENCES


1. **Adler, J.** 1969. Chemoreceptors in bacteria. Science **166:**1588-1597.

2. **Ames, P., and J. S. Parkinson.** 2006. Conformational suppression of inter-receptor signaling defects. Proc. Natl. Acad. Sci. U. S. A. **103:**9292-9297.

3. **Ames, P., C. A. Studdert, R. H. Relser, and J. S. Parkinson.** 2002. Collaborative signaling by mixed chemoreceptor teams in *Escherichia coli*. Proc. Natl. Acad. Sci. U. S. A. **99:**7060-7065.

4. **Amsler, C. D., M. Cho, and P. Matsumura.** 1993. Multiple factors underlying the maximum motility of Escherichia coli as cultures enter post-exponential growth J. Bacteriol. **175:**6238-6244.

5. **Aravind, L., and C. P. Ponting.** 1999. The cytoplasmic helical linker domain of receptor histidine kinase and methyl-accepting proteins is common to many prokaryotic signalling proteins. FEMS Microbiol. Lett. **176:**111-116.

6. **Banno, S., D. Shiomi, M. Homma, and I. Kawagishi.** 2004. Targeting of the chemotaxis methylesterase/deamidase CheB to the polar receptor-kinase cluster in an *Escherichia coli* cell. Mol. Microbiol. **53:**1051-1063.

7. **Berg, H. C.** 1975. Chemotaxis in bacteria. Annual Reviews of Biophysics and Bioengineering **4:**119-136.

8. **Berg, H. C., and D. A. Brown.** 1972. Chemotaxis in *Escherichia coli* analyzed by three-dimensional tracking. Nat. Biotechnol. **239:**500-504.

9. **Berg, H. C., and E. M. Purcell.** 1977. Physics of chemoreception. Biophysical Journal **20:**193-219.

10. **Bibikov, S. I., R. Biran, K. E. Rudd, and J. S. Parkinson.** 1997. A signal transducer for aerotaxis in *Escherichia coli*. J. Bacteriol. **179:**4075-4079.

11. **Bilwes, A. M., L. A. Alex, B. R. Crane, and M. I. Simon.** 1999. Structure of CheA, a signal transducing histidine kinase. Cell **96:**131-141.

12. **Blat, Y., and M. Eisenbach.** 1996. Conserved C-terminus of the phosphatase CheZ is a binding domain for the chemotactic response regulator CheY. Biochemistry (Mosc). **35:**5679-5683.

13. **Blat, Y., and M. Eisenbach.** 1996. Mutants with defective phosphatase activity show no phosphorylation-dependent oligomerization of CheZ. J. Biol. Chem. **271:**1232-1236.

14. **Blat, Y., and M. Eisenbach.** 1996. Oligomerization of the phosphatase CheZ upon interaction with the phosphorylated form of CheY J. Biol. Chem. **271:**1226-1231.

15. **Blat, Y., and M. Eisenbach.** 1994. Phosphorylation-dependent binding of the chemotaxis signal molecule CheY to its phosphatase, CheZ. Biochemistry (Mosc). **33:**902-906.

16. **Boesch, K. C., R. E. Silversmith, and R. B. Bourret.** 2000. Isolation and characterizationof nonchemotactic CheZ mutants of *Escherichia coli*. J. Bacteriol. **182:**3544-3552.

17. **Borkovich, K. A., L. A. Alex, and M. I. Simon.** 1992. Attenuation of sensory receptor signaling by covalent modification. Proc. Natl. Acad. Sci. U. S. A. **89:**6756-6760.

18. **Borkovich, K. A., N. Kaplan, J. F. Hess, and M. I. Simon.** 1989. Transmembrane signal transduction in bacterial chemotaxis involves ligand-dependent activation of phosphate group transfer. Proc. Natl. Acad. Sci. U. S. A. **86:**1208-1212.

19. **Bourret, R. B., J. Davagnino, and M. I. Simon.** 1993. The carboxy-terminal portion of the CheA kinase mediates regulation of autophosphorylation by transducer and CheW. J. Bacteriol. **175:**2097-2101.

20. **Boyd, D., D. S. Weiss, J. C. Chen, and J. Beckwith.** 2000. Towards single-copy gene expression systems making gene cloning physiologically relevant: Lambda InCh, a simple *Escherichia coli* plasmid-chromosome shuttle system. J. Bacteriol. **182:**842-847.

21. **Bren, A., M. Welch, Y. Blat, and M. Eisenbach.** 1996. Signal termination in bacterial chemotaxi: CheZ mediates dephosphorylation of free rather than switch-bound CheY. Proc. Natl. Acad. Sci. U. S. A. **93:**10090-10093.

22. **Cantwell, B. J., R. R. Draheim, R. B. Weart, C. Nguyen, R. C. Stewart, and M. D. Manson.** 2003. CheZ phosphatase localizes to chemoreceptor patches via CheA-short. J. Bacteriol. **185:**2354-2361.

23. **Carbadillido-Lopez, R.** 2006. Orchestrating bacterial cell morphogenesis. Mol. Microbiol. **60:**815-819.

24. **Cluzel, P., M. Surette, and S. Leibler.** 2000. An ultrasensitive bacterial motor revealed by monitoring signaling proteins in single cells. Science **287:**1652-1655.

25. **Cormack, B. P., R. H. Valdivia, and S. Falkow.** 1996. FACS-optimized mutants of the green fluorescent protein (GFP). Gene **173:**33-38.

26. **DeFranco, A. L., and D. E. Koshland Jr.** 1981. Molecular cloning of chemotaxis genes and overproduction of gene products in the bacterial sensing system. J. Bacteriol. **147:**390-400.

27. **DePamphilis, M. L., and J. Adler.** 1971. Attachment of flagellar basal bodies to the cell envelope: specific attachment to the outer, lipopolysaccharide membrane and the cytoplasmic membrane. J. Bacteriol. **105:**396-407.

28. **DePamphilis, M. L., and J. Adler.** 1971. Fine structure and ioslation of the hook-basal body complex of flagella from *Escherichia coli* and *Bacillus subtilis*. J. Bacteriol. **105:**384-395.

29. **Dye, N. A., Z. Pincus, J. A. Theriot, L. Shapiro, and Z. Gitai.** 2005. Two independent spiral structures control cell shape in *Caulobacter*. Proc. Natl. Acad. Sci. U. S. A. **102:**18608-18613.

30. **Francis, N. R., M. N. Levit, T. R. Shaikh, L. A. Melanson, J. B. Stock, and D. J. DeRosier.** 2002. Subunit organization in a soluble complex of Tar, CheW, and CheA by electron microscopy. J. Biol. Chem. **277:**36755-36759.

31. **Francis, N. R., P. M. Wolanin, J. B. Stock, D. J. DeRosier, and D. R. Thomas.** 2004. Three-dimensional structure and organization of a receptor/signaling complex. Proc. Natl. Acad. Sci. U. S. A. **101:**17480-17485.

32. **Gardina, P. J., C. Conway, M. Kossman, and M. D. Manson.** 1992. Aspartate and maltose-binding protein interact with adjacent sites in the Tar chemotactic signal transducer of *Escherichia coli*. J. Bacteriol. **174:**1528-1536.

33. **Garzon, A., and J. S. Parkinson.** 1996. Chemotactic signaling by the phosphorylation domain liberated from the CheA histidine kinase of *Escherichia coli* J. Bacteriol. **178:**6752-6758.

34. **Gegner, J. A., D. R. Graham, A. F. Roth, and F. W. Dahlquist.** 1992. Assembly of an MCP receptor, CheW, and kinase CheA complex in the bacterial chemotaxis signal transduction pathway. Cell **70:**975-982.

35. **Guzman, L.-M., D. Belin, M. J. Carson, and J. Beckwith.** 1995. Tight regulation, modulation, and high-level expression by vectors containing the arabinose $P_{BAD}$ promoter J. Bacteriol. **177:**4121-4130.

36. **Hess, J. F., R. B. Bourret, and M. I. Simon.** 1988. Histidine phosphorylation and phosphoryl group transfer in bacterial chemotaxis. Nature **336:**139-143.

37. **Hess, J. F., K. Oosawa, N. Kaplan, and M. I. Simon.** 1988. Phosphorylation of three proteins in the signaling pathway of bacterial chemotaxis. Cell **53:**79-87.

38. **Jones, L. J. F., R. Carballido-Lopez, and J. Errington.** 2001. Control of cell shape in bacteria: helical, actin-like filaments in *Bacillus subtilis*. Cell **104:**913-922.

39. **Kentner, D., S. Thiem, M. Hildenbeutel, and V. Sourjik.** 2006. Determinants of chemoreceptor cluster formation in *Escherichia coli*. Mol. Microbiol. **61:**407-417.

40. **Kim, K. K., H. Yokota, and S.-H. Kim.** 1999. Four-helical-bundle structure of the cytoplasmic domain of a serine chemotaxis receptor. Nature **400:**787-792.

41. **Kim, S. Y., Z. Gitai, A. Kinkhabwala, L. Shapiro, and W. E. Moerner.** 2006. Single molecules of the bacterial actin MreB undergo directed treadmilling motion in *Caulobacter crescentus*. Proc. Natl. Acad. Sci. U. S. A. **103:**10929-10934.

42. **Kirby, J. R., C. J. Kristich, M. M. Saulmon, M. A. Zimmer, L. F. Garrity, I. B. Zhulin, and G. W. Ordal.** 2001. CheC is related to the family of flagellar switch proteins and acts independently from CheD to control chemotaxis in *Bacillus subtilis*. Mol. Microbiol. **42:**573-585.

43. **Kofoid, E. C., and J. S. Parkinson.** 1991. Tandem translation starts in the *cheA* locus of *Escherichia coli*. J. Bacteriol. **173:**2116-2119.

44. **Kondoh, H., and H. Hotani.** 1974. Flagellin from *Escherichia coli* K12: polymerization and molecular weight in comparison with *Salmonella* flagellins. . Biochimica et Biophysica Acta **336:**117-139.

45. **Kott, L., E. H. Braswell, A. L. Shrout, and R. M. Weis.** 2004. Distributed subunit interactions in CheA contribute to dimer stability: a sedimentation equilibrium study. Biochimica et Biophysica Acta **1696:**131-140.

46. **Lai, R.-Z., J. M. B. Manson, A. F. Bormans, R. R. Draheim, N. T. Nguyen, and M. D. Manson.** 2005. Cooperative signaling among bacterial chemoreceptors. Biochemistry (Mosc). **44:**14298-14307.

47. **Lee, S.-Y., H. S. Cho, J. G. Pelton, D. Yan, E. A. Berry, and D. E. Wemmer.** 2001. Crystal structure of activated CheY: Comparison with other activated receiver domains J. Biol. Chem. **276:**16425-16431.

48. **Levit, M. N., Y. Liu, M. Surette, and J. B. Stock.** 1996. Active site interference and asymmetric activation in the chemotaxis protein histidine kinase CheA. J. Biol. Chem. **271:**32057-32063.

49. **Li, M., and G. L. Hazelbauer.** 2004. Cellular stoichiometry of the components of the chemotaxis signaling complex J. Bacteriol. **186:**3687-3694.

50. **Lipkow, K., S. S. Andrewss, and D. Bray.** 2005. Simulated diffusion of phosphorylated CheY through the cytoplasm of *Escherichia coli*. J. Bacteriol. **187:**45-53.

51. **Lupas, A., and J. Stock.** 1989. Phosphorylationod an N-terminal regulatory domain activates the CheB methylesterase in bacterial chemotaxis. J. Biol. Chem. **264:**17337-17342.

52. **Lybarger, S. R., and J. R. Maddock.** 2000. Differences in the polar clustering of the high- and low-abundance chemoreceptors of *Escherichia coli*. Proc. Natl. Acad. Sci. U. S. A. **97:**8057-8062.

53. **Lybarger, S. R., and J. R. Maddock.** 1999. Clustering of the chemorecpetor complex in *Escherichia coli* is independent of the methyltransferase CheR and the methylesterase CheB. J. Bacteriol. **181:**5527-5529.

54. **Lynch, B. A., and D. E. Koshland Jr.** 1991. Disulfide cross-linking studies of the transmembrane regions of the aspartate sensory receptor of *Escherichia coli*. Proc. Natl. Acad. Sci. U. S. A. **88:**10402-10406.

55. **Macnab, R. M.** 1977. Bacterial flagella rotating in bundles: a study in helical geometry. Proc. Natl. Acad. Sci. U. S. A. **74:**221-225.

56. **Macnab, R. M., and M. K. Ornston.** 1977. Normal-to-curly flagellar transitions and their role in bacterial tumbling. Stabilization of an alternative structure by mechanical force. J. Mol. Biol. **112:**1-30.

57. **Maddock, J. R., and L. Shapiro.** 1993. Polar localization of the chemoreceptor complex in the *Escherichia coli* cell. Science **259:**1717-1723.

58. **Manson, M. D., P. Tedesco, H. C. Berg, F. M. Harold, and C. van der Drift.** 1977. A protonmotive force drives bacterial flagella. Proc. Natl. Acad. Sci. U. S. A. **74:**3060-3064.

59. **Mao, H., P. S. Cremer, and M. D. Manson.** 2003. A sensitive, versatile microfluidic assay for bacterial chemotaxis. Proc. Natl. Acad. Sci. U. S. A. **100:**5449-5454.

60. **Margolin, W.** 2005. Bacterial mitosis: actin in a new role at the origin. Curr. Biol. **15:**259-261.

61. **McAndrew, R. S., E. A. Ellis, R.-Z. Lai, M. D. Manson, and A. Holzenburg.** 2005. Identification of Tsr and Tar chemoreceptor arrays in *E. coli* inner membranes. Microsopy and Microanalysis **11:**1190-1191.

62. **McAndrew, R. S., E. A. Ellis, M. D. Manson, and A. Holzenburg.** 2004. TEM analysis of chemoreceptor arrays in native membranes of *E. coli*. Microsopy and Microanalysis **10:**416.

63. **McEvoy, M. M., A. Bren, M. Eisenbach, and F. W. Dahlquist.** 1999. Identification of the binding interfaces on CheY for two of its targets, the phosphatase CheZ and the flagellar switch protein FliM. J. Mol. Biol. **289:**1423-1433.

64. **McNamara, B. P., and A. J. Wolfe.** 1997. Coexpression of the long and short forms of CheA, the chemotaxis histidine kinase, by members of the family *Enterobacteriaceae*. J. Bacteriol. **179:**1813-1818.

65. **Milburn, M., G. Prive, D. Milligan, W. Scott, J. Yeh, J. Jancarik, D. E. Koshland Jr., and S. Kim.** 1991. Three-dimensional structures of the ligand-binding domain of the bacterial aspartate receptor with and without a ligand. Science **254:**1342-1347.

66. **Miller, J. H.** 1972. Experiments in Molecular Genetics. Cold Spring Harbor Laboratories, Cold Spring Harbor, NY.

67. **Moller-Jensen, J., and J. Lowe.** 2005. Increasing complexity of the bacterial cytoskeleton. Current Opinion in Cell Biology **17:**75-81.

68. **Morrison, T. B., and J. S. Parkinson.** 1994. Liberation of an interaction domain from the phosphotransfer region of CheA, a signaling kinase of *Escherichia coli*. Proc. Natl. Acad. Sci. U. S. A. **91:**5485-5489.

69. **Mourey, L., S. Da Res, J.-D. Pedelacq, T. Tolstykh, C. Faurie, V. Guillet, J. B. Stock, and J.-P. Samama.** 2001. Crystal structure of the CheA histidine phosphotransfer domain that mediates response regulator phosphorylation in bacterial chemotaxis. J. Biol. Chem. **276:**31074-31082.

70. **Ninfa, E. G., A. Stock, S. Mowbray, and J. Stock.** 1991. Reconstitution of the bacterial chemotaxis signal transduction system from the purified components. J. Biol. Chem. **266:**9764-9770.

71. **O'Connor, C., B. J. Cantwell, M. D. Manson, and P. Matsumura.** 2006. Swimming Behavior of *Escherichia coli* is altered by $CheA_S$ ability to bind CheZ. J. Bacteriol.**:**manuscript in preparation.

72. **O'Connor, C., and P. Matsumura.** 2004. The accessibility of Cys-120 in $CheA_S$ is important for the binding of CheZ and enhancement of CheZ phosphatase activity. Biochemistry (Mosc). **43:**6909-6916.

73. **Park, S. Y., B. Lowder, A. M. Bilwes, D. F. Blair, and B. R. Crane.** 2006. Structure of FliM provides insight into assembly of the switch complex in the bacterial flagella motor. Proc. Natl. Acad. Sci. U. S. A. **103:**11886-11891.

74. **Parkinson, J. S.** 1978. Complementation analysis and deletion mapping of *Escherichia coli* mutants defective in chemotaxis. J. Bacteriol. **135:**45-53.

75. **Parkinson, J. S., and S. E. Houts.** 1982. Isolation and behavior of *Escherichia coli* deletion mutants lacking chemotaxis functions. J. Bacteriol. **151:**106-113.

76. **Rao, C. V., J. R. Kirby, and A. P. Arkin.** 2005. Phosphatase localization in bacterial chemotaxis: divergent mechanisms, convergent principles. Physical Biology **2:**148-158.

77. **Russo, A. F., and D. E. Koshland Jr.** 1983. Separation of signal transduction and adaptation functions of the aspartate receptor in bacterial sensing. Science **220:**1016-1020.

78. **Sager, B. M., J. J. Sekelsky, P. Matsumura, and J. Adler.** 1988. Use of a computer to assay motility in bacteria. Analyytical Biochemistry **173:**271-277.

79. **Sanatinia, H., E. C. Kofoid, T. B. Morrison, and J. S. Parkinson.** 1995. The smaller of two overlapping *cheA* gene products is not essential for chemotaxis in *Escherichia coli*. J. Bacteriol. **177:**2713-2720.

80. **Sanders, D. A., B. L. Gillece-Castro, A. M. Stock, A. L. Burlingame, and D. E. Koshland Jr.** 1989. Identification of the site of phosphorylation of the chemotaxis response regulator protein, CheY. J. Biol. Chem. **264:**21770-21778.

81. **Sanna, M. G., and M. I. Simon.** 1996. *In vivo* and *in vitro* characterization of *Escherichia coli* protein CheZ gain- and loss-of-function mutants. J. Bacteriol. **178:**6275-6280.

82. **Sanna, M. G., and M. I. Simon.** 1996. Isolation and *in vitro* characterization of CheZ suppressors for the *Escherichia coli* chemotactic response regulator mutnat CheYN23D* J. Biol. Chem. **271:**7357-7361.

83. **Scharf, B. E., K. A. Fahrner, L. Turner, and H. C. Berg.** 1998. Control of direction of flagellar rotation in bacterial chemotaxis. Proc. Natl. Acad. Sci. U. S. A. **95:**201-206.

84. **Schuster, M., R. Zhao, R. B. Bourret, and E. J. Collins.** 2000. Correlated switch binding and signaling in bacterial chemotaxis. J. Biol. Chem. **275:**19752-19758.

85. **Segall, J. E., S. M. Block, and H. C. Berg.** 1986. Temporal comparisons in bacterial chemotaxis. Proc. Natl. Acad. Sci. U. S. A. **83:**8987-8991.

86. **Segall, J. E., M. D. Manson, and H. C. Berg.** 1982. Signal processing times in bacterial chemotaxis. Nature **296:**855-857.

87. **Shih, Y.-L., I. Kawagishi, and L. Rothfield.** 2005. The MreB and Min cytoskeletal-like systems play independent roles in prokaryotic polar differentiation. Mol. Microbiol. **58:**917-928.

88. **Shih, Y.-L., T. Le, and L. Rothfield.** 2003. Division site selection in *Escherichia coli* involves dynamic redistribution of Min proteins within coiled structures that extend between the cell poles. Proc. Natl. Acad. Sci. U. S. A. **100:**7865-7870.

89. **Shimizu, T. S., N. Le Novere, M. D. Levin, A. J. Beavil, B. J. Sutton, and D. Bray.** 2000. Molecular model of a lattice of signalling proteins involved in bacterial chemotaxis. Nature Cell Biology **2:**792-796.

90. **Shiomi, D., M. Yoshimoto, M. Homma, and I. Kawagishi.** 2006. Helical distribution of the bacterial chemoreceptor via colocalization with the Sec protein translocation machinery. Mol. Microbiol. **60:**894-906.

91. **Silverman, M., and M. I. Simon.** 1977. Identification of polypeptides necessary for chemotaxis in *Escherichia coli*. J. Bacteriol. **130:**1317-1325.

92. **Silverman, M., and M. I. Simon.** 1974. Flagellar rotation and the mechanism of bacterial motility. Nature **249:**73-74.

93. **Silversmith, R. E.** 2005. High mobility of carboxy-terminal region of bacterial chemotaxis phosphatase CheZ is diminished upon binding divalent cation or CheY-P substrate. Biochemistry (Mosc). **44:**7768-7776.

94. **Silversmith, R. E., J. G. Smith, G. P. Guanga, J. T. Les, and R. B. Bourret.** 2001. Alteration of a nonconserved active site residue in the chemotaxis response regulator CheY affects phosphorylation and interaction with CheZ. J. Biol. Chem. **276:**18478-18484.

95. **Skidmore, J. M., D. D. Ellefson, B. P. McNamara, M. M. P. Couto, A. J. Wolfe, and J. R. Maddock.** 2000. Polar clustering of the chemoreceptor complex in *Escherichia coli* occurs in the absence of complete CheA function. J. Bacteriol. **182:**967-973.

96. **Smith, R. A., and J. S. Parkinson.** 1980. Overlapping genes at the *cheA* locus of *Escherichia coli*. Proc. Natl. Acad. Sci. U. S. A. **77:**5370-5374.

97. **Sockett, H., S. Yamaguchi, M. Kihara, V. M. Irikura, and R. M. MacNab.** 1992. Molecular analysis of the flagellar switch protein FliM of *Salmonella typhimurium*. J. Bacteriol. **174:**793-806.

98. **Sourjik, V., and H. C. Berg.** 2004. Functional interactions between receptors in bacterial chemotaxis. Nature **428:**437-441.

99. **Sourjik, V., and H. C. Berg.** 2000. Localization of components of the chemotaxis machinery of *Escherichia coli* using fluorescent protein fusions. Mol. Microbiol. **37:**740-751.

100. **Springer, W. R., and D. E. Koshland Jr.** 1977. Identification of a protein methyltransferase as the *cheR* gene product in the bacterial sensing system. Proc. Natl. Acad. Sci. U. S. A. **74:**533-537.

101. **Stewart, G. C.** 2005. Taking Shape: control of bacterial cell wall biosynthesis. Mol. Microbiol. **57:**1177-1181.

102. **Stewart, R. C.** 1997. Kinetic characterization of phosphotransfer between CheA and CheY in the bacterial chemotaxis signal transduction pathway. Biochemistry (Mosc). **36:**2030-2040.

103. **Stewart, R. C., R. VanBruggen, D. D. Ellefson, and A. J. Wolfe.** 1998. TNP-ATP and TNP-ADP as probes of the nucleotide binding site of CheA, the histidine protein kinase in the chemotaxis signal transduction pathway of *Escherichia coli*. Biochemistry (Mosc). **37:**12269-12279.

104. **Stock, A., T. Chen, D. Welsh, and J. Stock.** 1988. CheA protein, a central regulator of bacterial chemotaxis, belongs to a family of proteins that control gene expression in response to changing environmental conditions. Proc. Natl. Acad. Sci. U. S. A. **85:**1403-1407.

105. **Stock, A., D. E. Koshland Jr., and J. Stock.** 1985. Homologies between the *Salmonella typhimurium* CheY protein and proteins involved in the regulation of chemotaxis, membrane protein synthesis, and sporulation. Proc. Natl. Acad. Sci. U. S. A. **82:**7989-7993.

106. **Stock, J. B., and D. E. Koshland Jr.** 1978. A protein methylesterase involved in bacterial sensing. Proc. Natl. Acad. Sci. U. S. A. **75:**3659-3663.

107. **Studdert, C. A., and J. S. Parkinson.** 2004. Crosslinking snapshots of bacterial chemoreceptor squads. Proc. Natl. Acad. Sci. U. S. A. **101:**2117-2122.

108. **Swanson, R. V., R. B. Bourret, and M. I. Simon.** 1993. Intermolecular complementation of the kinase activity of CheA. Mol. Microbiol. **8:**435-441.

109. **Swanson, R. V., S. C. Schuster, and M. I. Simon.** 1993. Expression of CheA fragments which define domains encoding kinase, phosphotransfer, and CheY binding activities. Biochemistry (Mosc). **32:**7623-7629.

110. **Szurmant, H., M. W. Bunn, V. J. Cannistraro, and G. W. Ordal.** 2003. *Bacillus subtilis* hydrolyzes CheY-P at the location of its action, the flagellar switch. J. Biol. Chem. **278:**48611-48616.

111. **Szurmant, H., T. J. Muff, and G. W. Ordal.** 2004. *Bacillus subtilis* CheC and FliY are members of a novel class of CheY-P-hydrolyzing proteins in the chemotaxis signal transduction cascade. J. Biol. Chem. **279:**21787-21792.

112. **Turner, L., W. S. Ryu, and H. C. Berg.** 2000. Real-time imaging of fluorescent flagellar filaments. J. Bacteriol. **182:**2793-2801.

113. **Vaknin, A., and H. C. Berg.** 2004. Single-cell FRET imaging of phosphatase activity in the *Escherichia coli* chemotaxis system. Proc. Natl. Acad. Sci. U. S. A. **101:**17072-17077.

114. **van den Ent, F., L. A. Amos, and J. Lowe.** 2001. Prokaryotic origins of the actin cytoskeleton. Nature **413:**39-44.

115. **van den Ent, F., J. Moller-Jensen, L. A. Amos, K. Gerdes, and J. Lowe.** 2002. F-actin-like filaments formed by plasmid segregation protein ParM. EMBO J. **21:**6935-6943.

116. **Wang, H., and P. Matsumura.** 1997. Phosphorylating and dephosphorylating protein complexes in bacterial chemotaxis. J. Bacteriol. **179:**287-289.

117. **Wang, H., and P. Matsumura.** 1996. Characterization of the $CheA_S$/CheZ complex: a specific interaction resulting in enhanced dephosphorylation activity on CheY-phosphate. Mol. Microbiol. **19:**695-703.

118. **Ward, S. M., A. Delgado, R. P. Gunsalus, and M. D. Manson.** 2002. A NarX-Tar chimera mediates repellent chemotaxis to nitrate and nitrite. Mol. Microbiol. **44:**709-719.

119. **Welch, M., N. Chinardet, L. Mourey, C. Birck, and J.-P. Samama.** 1998. Structure of the CheY-binding domain of histidine kinase CheA in complex with CheY. Nat. Struct. Biol. **5:**25-29.

120. **Welch, M., K. Oosawa, S.-I. Aizawa, and M. Eisenbach.** 1993. Phosphorylation-dependent binding of a signal molecule to the flagellar switch of bacteria. Proc. Natl. Acad. Sci. U. S. A. **90:**8787-8791.

121. **Williams, S. B., and R. C. Stewart.** 1999. Functional similarities among two-component sensors and methyl-accepting chemotaxis proteins suggest a role for linker region amphipathic helices in transmembrane signal transduction. Mol. Microbiol. **33:**1093-1102.

122. **Wolfe, A. J., B. P. McNamara, and R. C. Stewart.** 1994. The short form of CheA couples chemoreception to CheA phosphorylation. J. Bacteriol. **176:**4483-4491.

123. **Yeh, J. I., H.-P. Biemann, J. Pandit, D. E. Koshland Jr., and S.-H. Kim.** 1993. The three-dimensional structure of the ligand-binding domain of a wild-type bacterial chemotaxis receptor. J. Biol. Chem. **268:**9787-9792.

124. **Zhang, Y., P. J. Gardina, A. S. Kuebler, H. S. Kang, J. A. Christopher, and M. D. Manson.** 1999. Model of maltose-binding protein/chemoreceptor complex supports intrasubunit signaling mechanism. Proc. Natl. Acad. Sci. U. S. A. **96:**939-944.

125. **Zhao, R., E. J. Collins, R. B. Bourret, and R. E. Silversmith.** 2002. Structure and catalytic mechanism of the *E. coli* chemotaxis phosphatase CheZ. Nat. Struct. Biol. **9:**570-575.

126. **Zhou, H., D. F. Lowry, R. V. Swanson, M. I. Simon, and F. W. Dahlquist.** 1995. NMR studies of the phosphotransfer domain of the histidine kinase CheA from *Escherichia coli*: assignments, secondary structure, general fold, and backbone dynamics. Biochemistry (Mosc). **34:**13585-13570.

127. **Zhou, Y., X. Zhang, and R. H. Ebright.** 1991. Random mutagenesis of gene-sized DNA molecules by use of PCR with Taq DNA polymerase. Nucleic Acids Research **19:**6052.

# VITA

Name: Brian Jay Cantwell

Address: M409 WLS
University of Tennessee
Knoxville, TN 37996-0845

Email: bcantwe1@utk.edu

Education: B.S., Microbiology, Texas A&M University, 1991

M.S., Microbiology, University of Washington, 1995